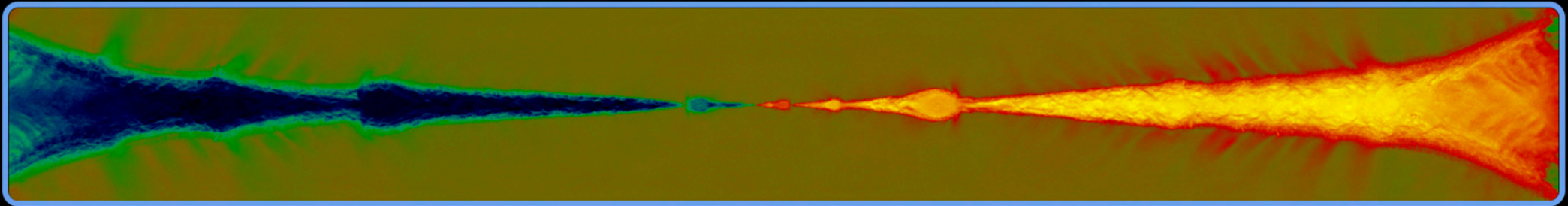


Magnetic dissipation in collisionless accretion flows

Michael Rowan

Adviser: Ramesh Narayan; Co-adviser: Lorenzo Sironi

8-26-2019



Outline

- Introduction
- Magnetic reconnection
- Kelvin-Helmholtz instability

Outline

- Introduction
- Magnetic reconnection
- Kelvin-Helmholtz instability

Black hole distance scales \gg plasma scales

Sgr A* (black hole at the center of our galaxy) has Schwarzschild radius $R_G \sim 10^{12}$ cm

For the corona of Sgr A*, plasma scale is: $c/\omega_{pe} \sim 1$ cm

This is a challenge for numerical (MHD) simulations of black hole environments, which resolve only the macroscopic scales

Plasma physics controls energy dissipation at small scales:

- Reconnection
- Shocks
- Turbulence

Can turbulence or other instabilities induce reconnection?

Black hole distance scales \gg plasma scales

Sgr A* (black hole at the center of our galaxy) has Schwarzschild radius $R_G \sim 10^{12}$ cm

For the corona of Sgr A*, plasma scale is: $c/\omega_{pe} \sim 1$ cm

This is a challenge for numerical (MHD) simulations of black hole environments, which resolve only the macroscopic scales

Plasma physics controls energy dissipation at small scales:

- Reconnection
- Shocks
- Turbulence

Can turbulence or other instabilities induce reconnection?

Black hole distance scales \gg plasma scales

Sgr A* (black hole at the center of our galaxy) has Schwarzschild radius $R_G \sim 10^{12}$ cm

For the corona of Sgr A*, plasma scale is: $c/\omega_{pe} \sim 1$ cm

This is a challenge for numerical (MHD) simulations of black hole environments, which resolve only the macroscopic scales

Plasma physics controls energy dissipation at small scales:

- Reconnection
- Shocks
- Turbulence

Can turbulence or other instabilities induce reconnection?

Structure of black hole accretion flows

Reconnection is well-studied in *non-relativistic*

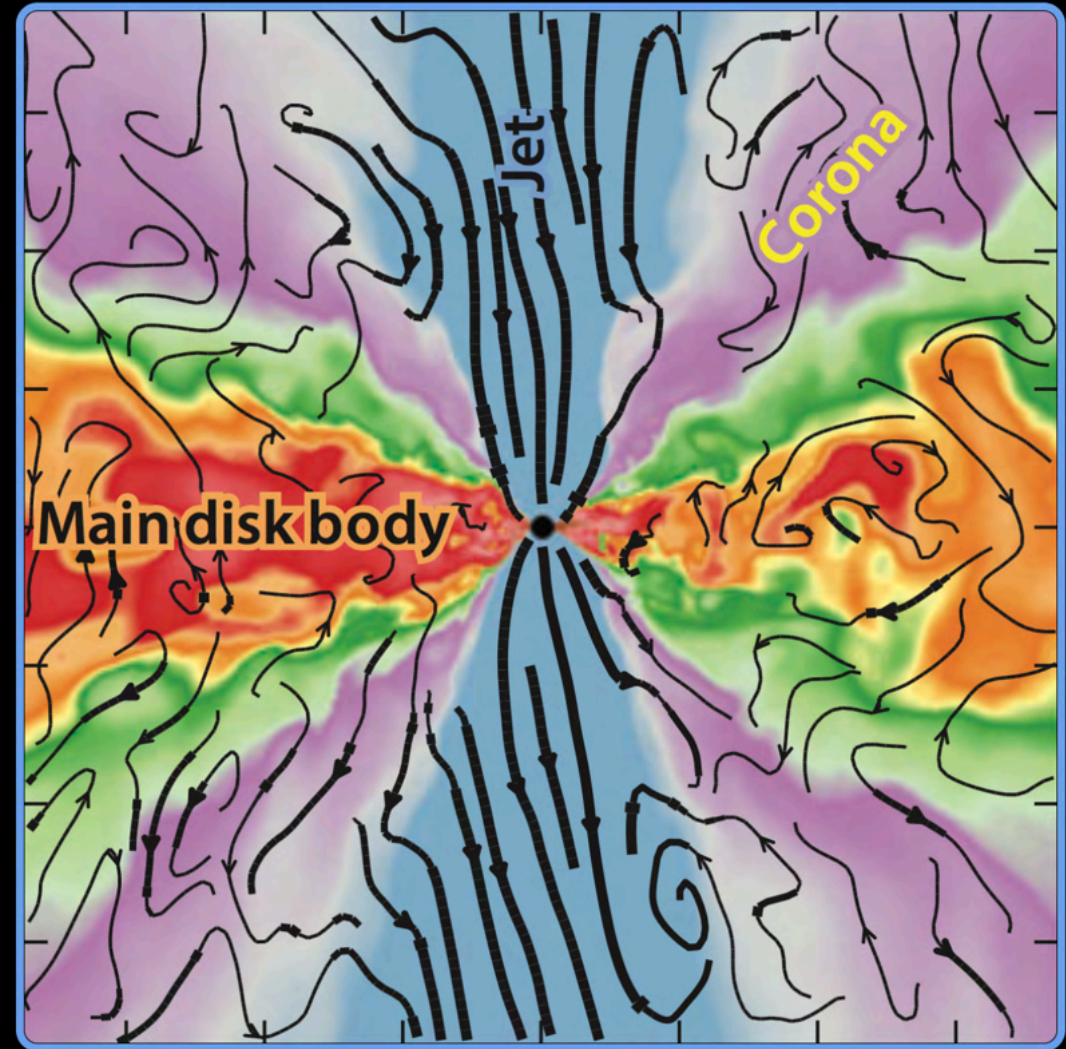
- Solar corona
- Earth's magnetosphere

and *relativistic* systems

- Jets (AGN, GRB)

BH coronae expected to be inbetween these two limits:

⇒ **'transrelativistic'**

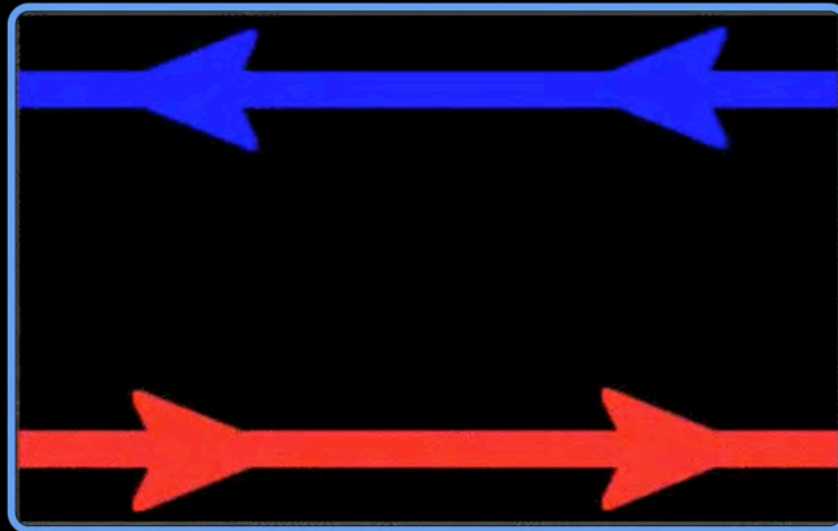


Outline

- Introduction
- **Magnetic reconnection**
- Kelvin-Helmholtz instability

'Cartoon' picture of reconnection

Magnetic energy \Rightarrow kinetic (heating, acceleration, bulk motion)



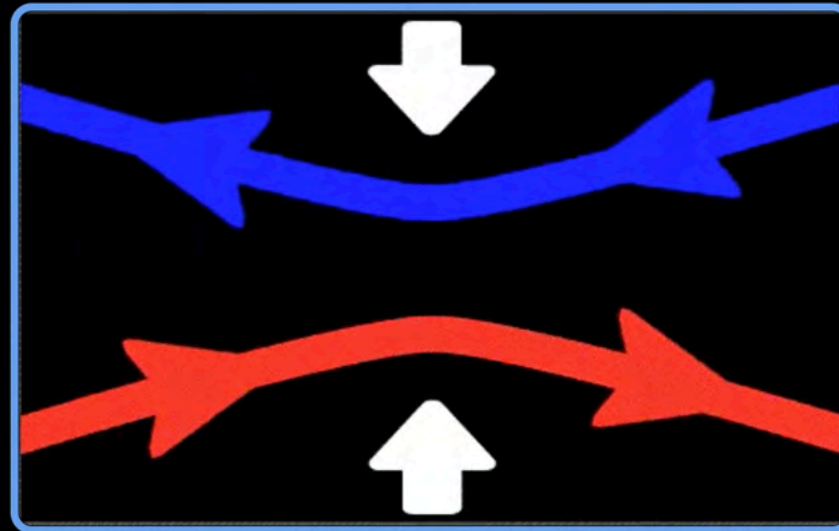
Center for Visual computing, University of California Riverside

Magnetic tension drags away field lines at the *Alfvén speed*:

$$\frac{v_A}{c} = \sqrt{\frac{\sigma_w}{1 + \sigma_w}}, \text{ where } \sigma_w \propto \frac{\text{magnetic pressure}}{\text{enthalpy density}}$$

'Cartoon' picture of reconnection

Magnetic energy \Rightarrow kinetic (heating, acceleration, bulk motion)



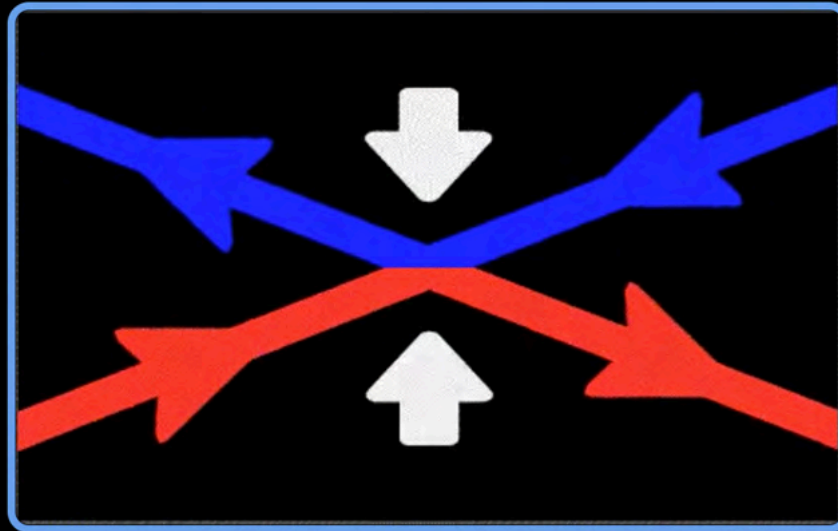
Center for Visual computing, University of California Riverside

Magnetic tension drags away field lines at the *Alfvén speed*:

$$\frac{v_A}{c} = \sqrt{\frac{\sigma_w}{1 + \sigma_w}}, \text{ where } \sigma_w \propto \frac{\text{magnetic pressure}}{\text{enthalpy density}}$$

'Cartoon' picture of reconnection

Magnetic energy \Rightarrow kinetic (heating, acceleration, bulk motion)



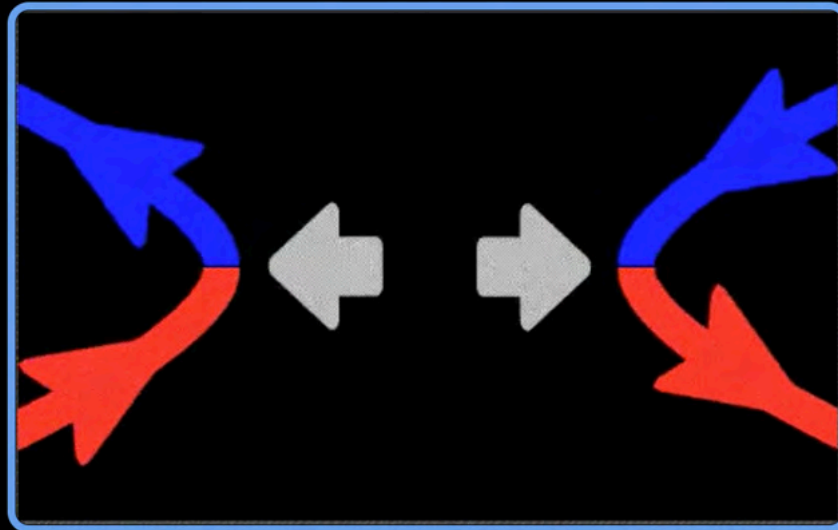
Center for Visual computing, University of California Riverside

Magnetic tension drags away field lines at the *Alfvén speed*:

$$\frac{v_A}{c} = \sqrt{\frac{\sigma_w}{1 + \sigma_w}}, \text{ where } \sigma_w \propto \frac{\text{magnetic pressure}}{\text{enthalpy density}}$$

'Cartoon' picture of reconnection

Magnetic energy \Rightarrow kinetic (heating, acceleration, bulk motion)



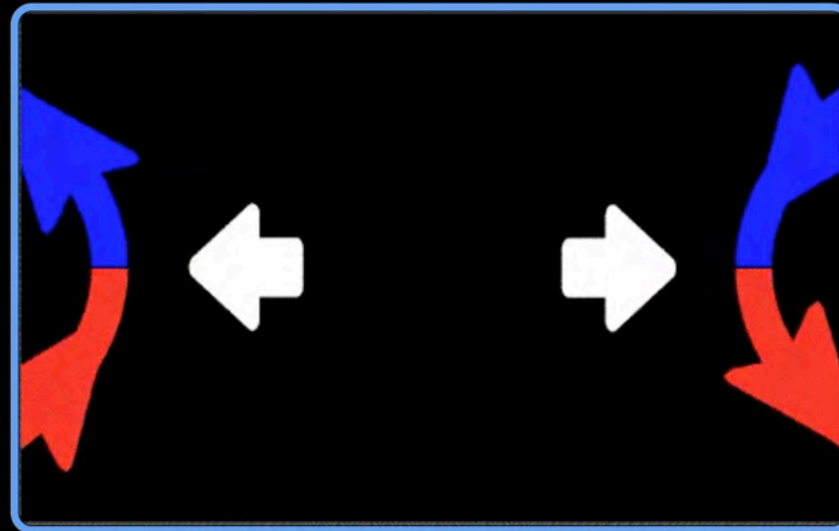
Center for Visual computing, University of California Riverside

Magnetic tension drags away field lines at the *Alfvén speed*:

$$\frac{v_A}{c} = \sqrt{\frac{\sigma_w}{1 + \sigma_w}}, \text{ where } \sigma_w \propto \frac{\text{magnetic pressure}}{\text{enthalpy density}}$$

'Cartoon' picture of reconnection

Magnetic energy \Rightarrow kinetic (heating, acceleration, bulk motion)



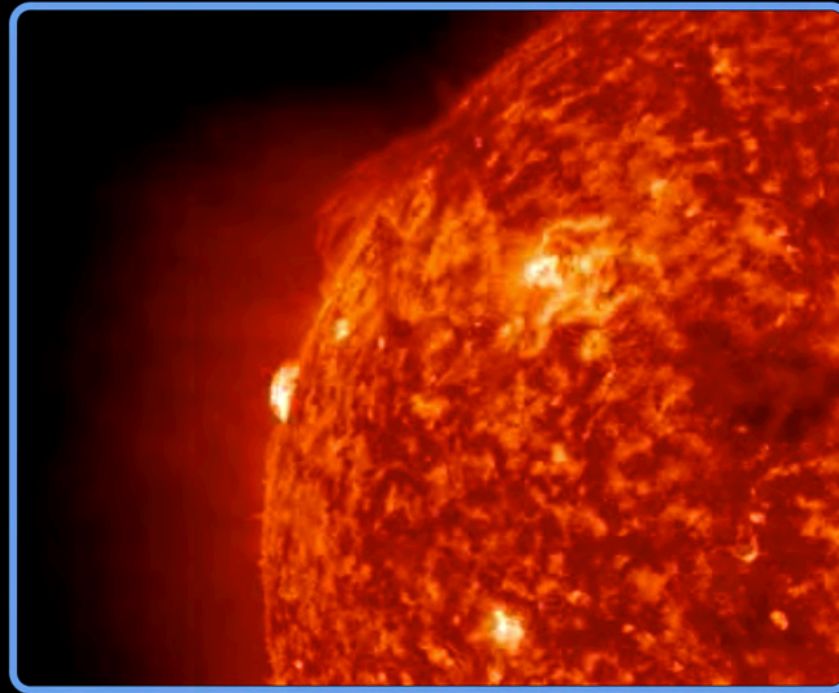
Center for Visual computing, University of California Riverside

Magnetic tension drags away field lines at the *Alfvén speed*:

$$\frac{v_A}{c} = \sqrt{\frac{\sigma_w}{1 + \sigma_w}}, \text{ where } \sigma_w \propto \frac{\text{magnetic pressure}}{\text{enthalpy density}}$$

Reconnection occurs in all sorts of plasmas

Occurs in magnetized plasmas, like the solar corona:

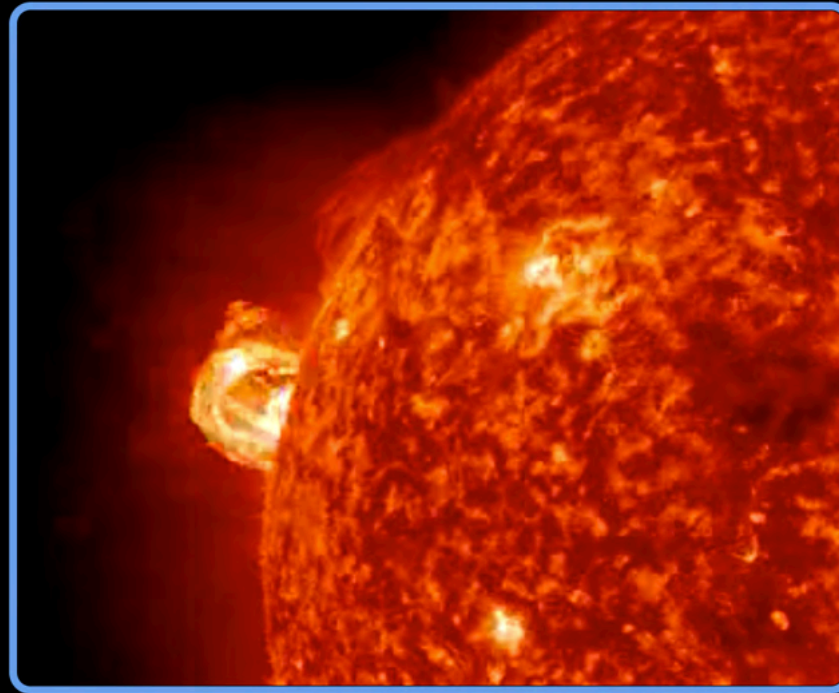


NASA SDO

What would reconnection look like in *black hole coronae*?

Reconnection occurs in all sorts of plasmas

Occurs in magnetized plasmas, like the solar corona:

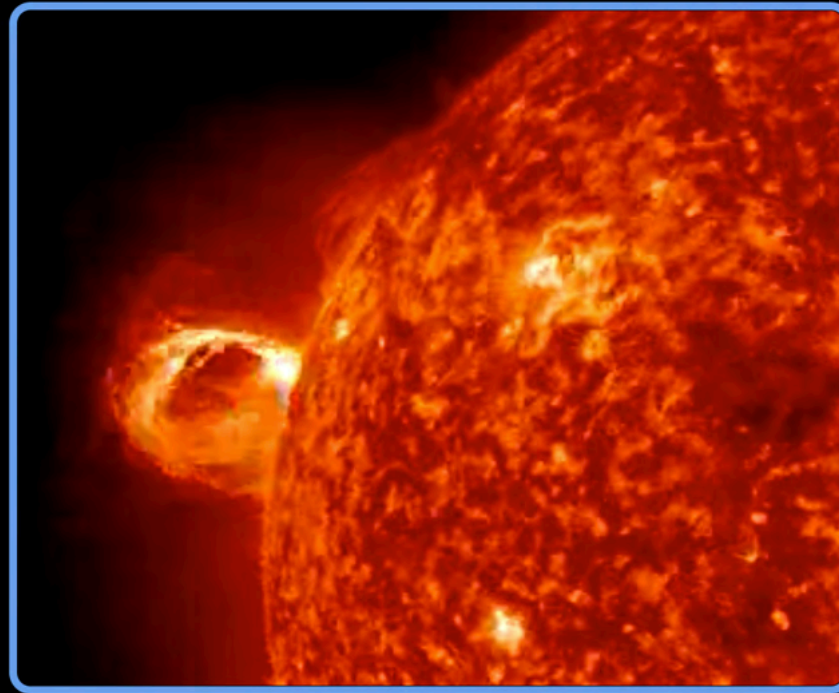


NASA SDO

What would reconnection look like in *black hole coronae*?

Reconnection occurs in all sorts of plasmas

Occurs in magnetized plasmas, like the solar corona:

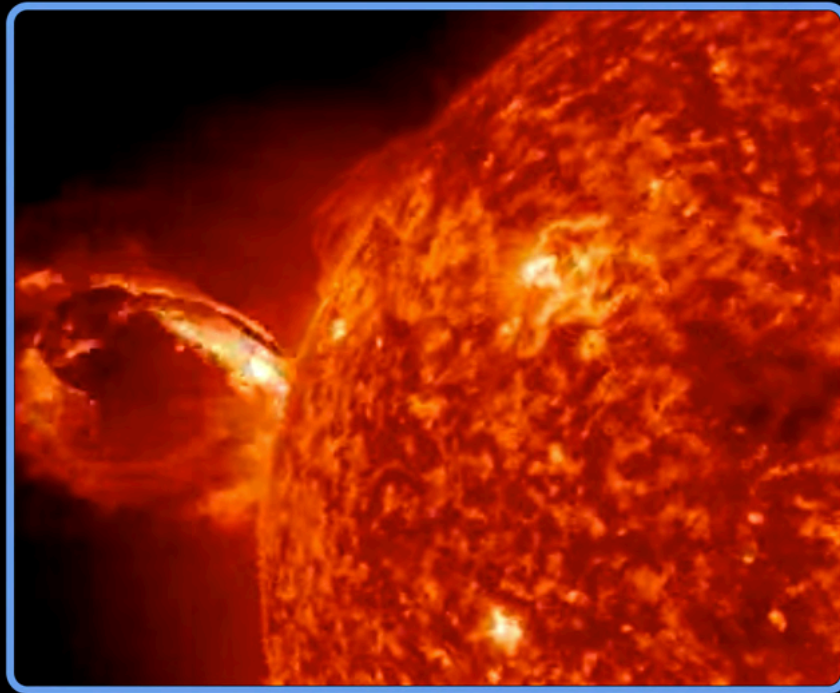


NASA SDO

What would reconnection look like in *black hole coronae*?

Reconnection occurs in all sorts of plasmas

Occurs in magnetized plasmas, like the solar corona:

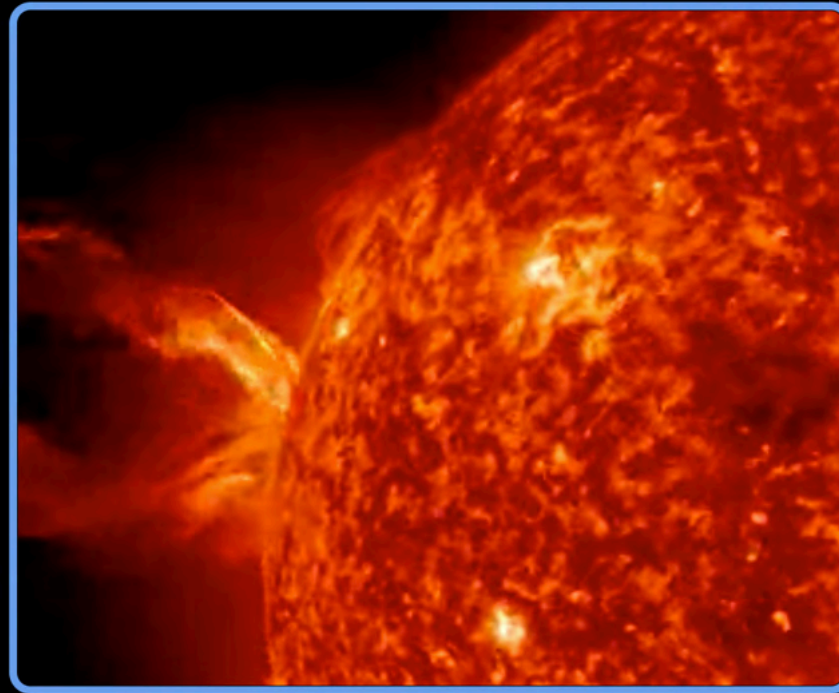


NASA SDO

What would reconnection look like in *black hole coronae*?

Reconnection occurs in all sorts of plasmas

Occurs in magnetized plasmas, like the solar corona:

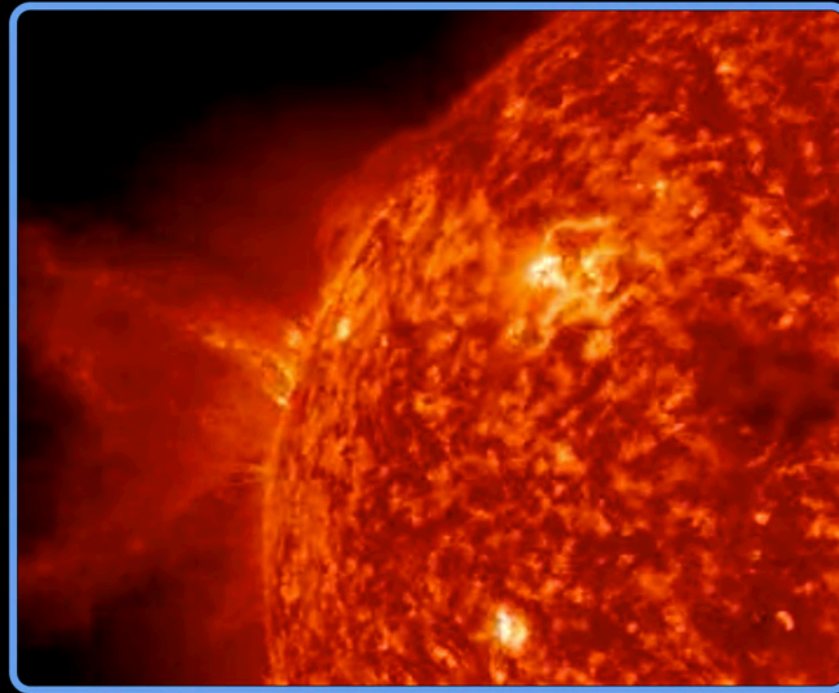


NASA SDO

What would reconnection look like in *black hole coronae*?

Reconnection occurs in all sorts of plasmas

Occurs in magnetized plasmas, like the solar corona:

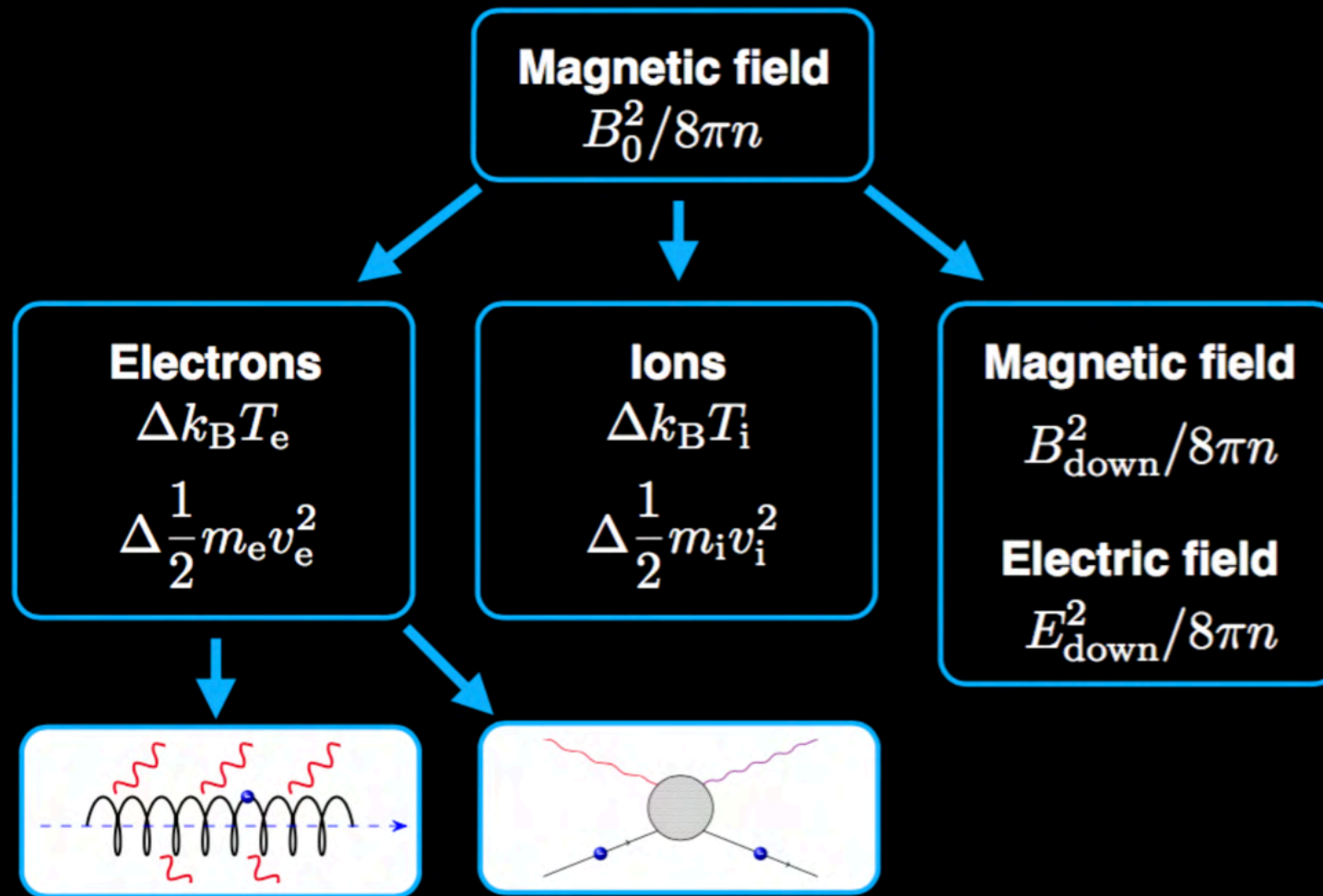


NASA SDO

What would reconnection look like in *black hole coronae*?

Key questions in reconnection physics

How much magnetic energy is dissipated to electrons, ions?





PiC: Particle in Cell

- Lorentz force law
- Maxwell equations (Ampère's law, Faraday's law)
- Divergence Eqs. satisfied at initialization
⇒ satisfied throughout time evolution

TRISTAN-MP

2D in space, but track all 3 components of momentum

Describe plasma with a few parameters

"Plasma-beta," "magnetization," and "guide field strength" describe the initial state of the upstream plasma:

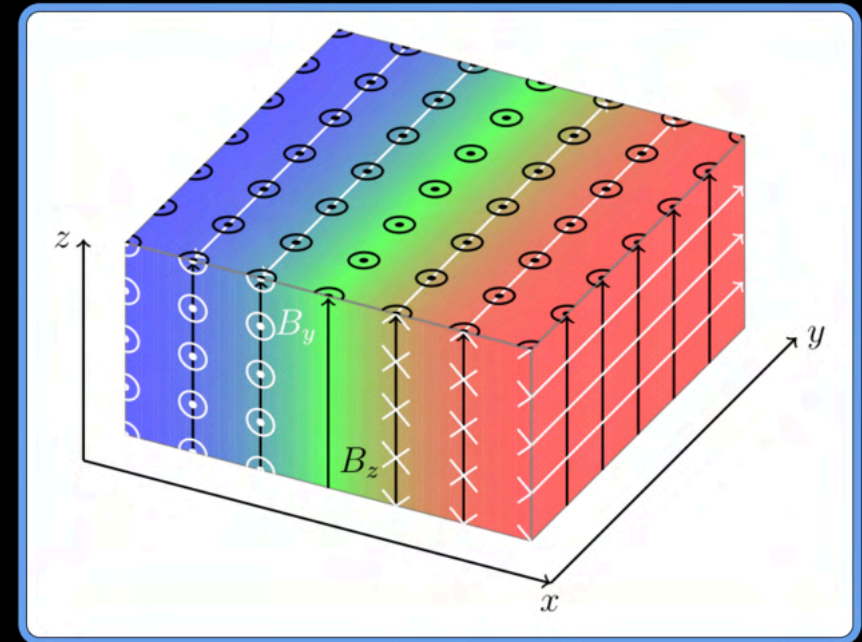
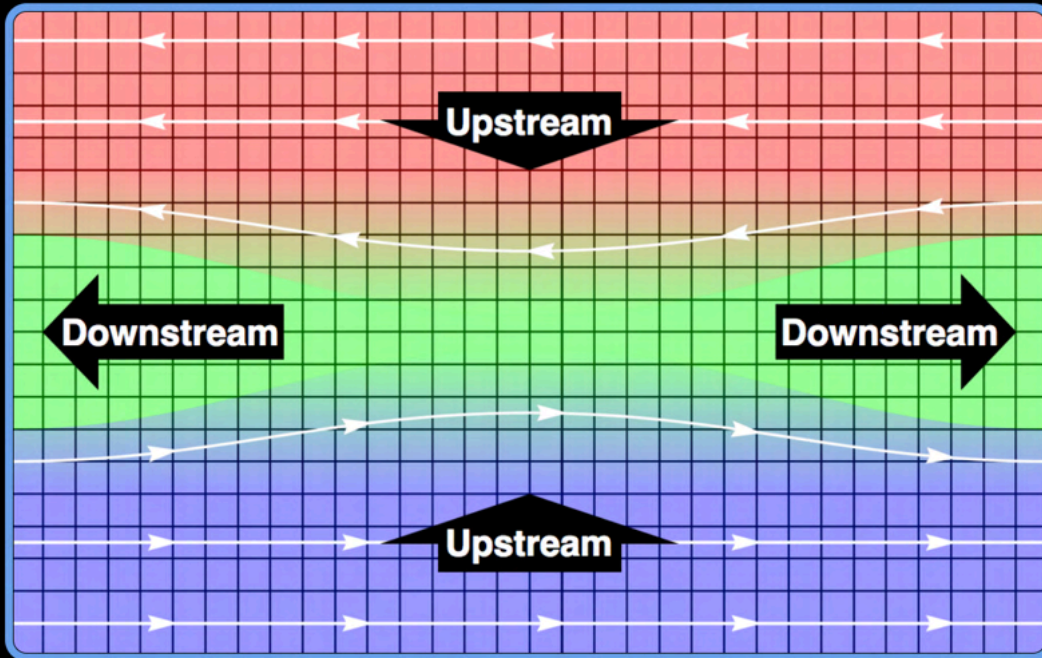
$$\beta_i = \frac{n_i k_B T_i}{B_0^2 / 8\pi} = \frac{\text{thermal pressure}}{\text{magnetic pressure}}$$
$$\sigma_w = \frac{B_0^2 / 4\pi}{w} = \frac{\text{magnetic pressure} (\times 2)}{\text{enthalpy density}}$$
$$b_g = B_z / B_0 = \frac{\text{Strength of out-of-plane } B}{\text{Strength of in-plane } B}$$

Tune these in the *upstream*, measure heating in the *downstream*

How to describe heating efficiency?

How much are particles heated? Define heating fractions for e^- , p^+ :

$$M_{Te} = \frac{\theta_{e,\text{down}} - \theta_{e,\text{up}}}{\frac{m_i}{m_e} \sigma_i}, \quad M_{Ti} = \frac{\theta_{i,\text{down}} - \theta_{i,\text{up}}}{\sigma_i}$$



Electron heating in non-rel. regime

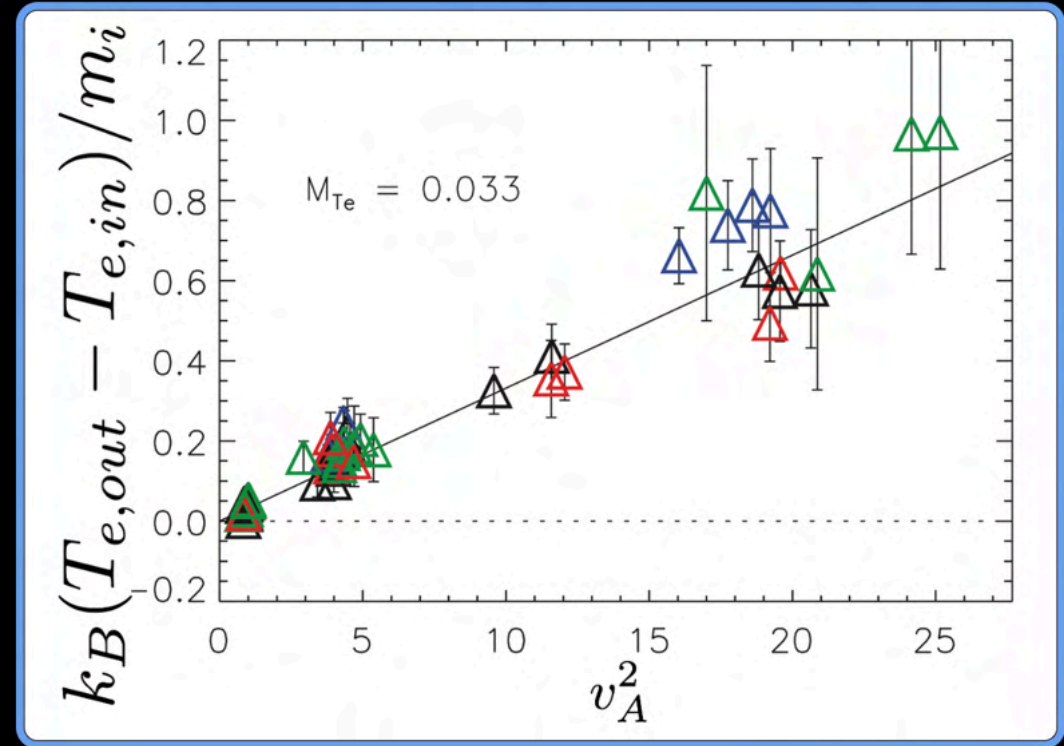
Heating fraction can be written as:

$$M_{Te} = \frac{k_B T_{e,out} - k_B T_{e,in}}{m_i v_A^2}$$

(slope of black line in this plot →)

For wide range of inflow parameters, M_{Te} is constant

$M_{Te} \approx 0.033$ for $m_i/m_e = 25$. When extrapolated to realistic mass ratio $m_i/m_e = 1836$, $M_{Te} \approx 0.017$



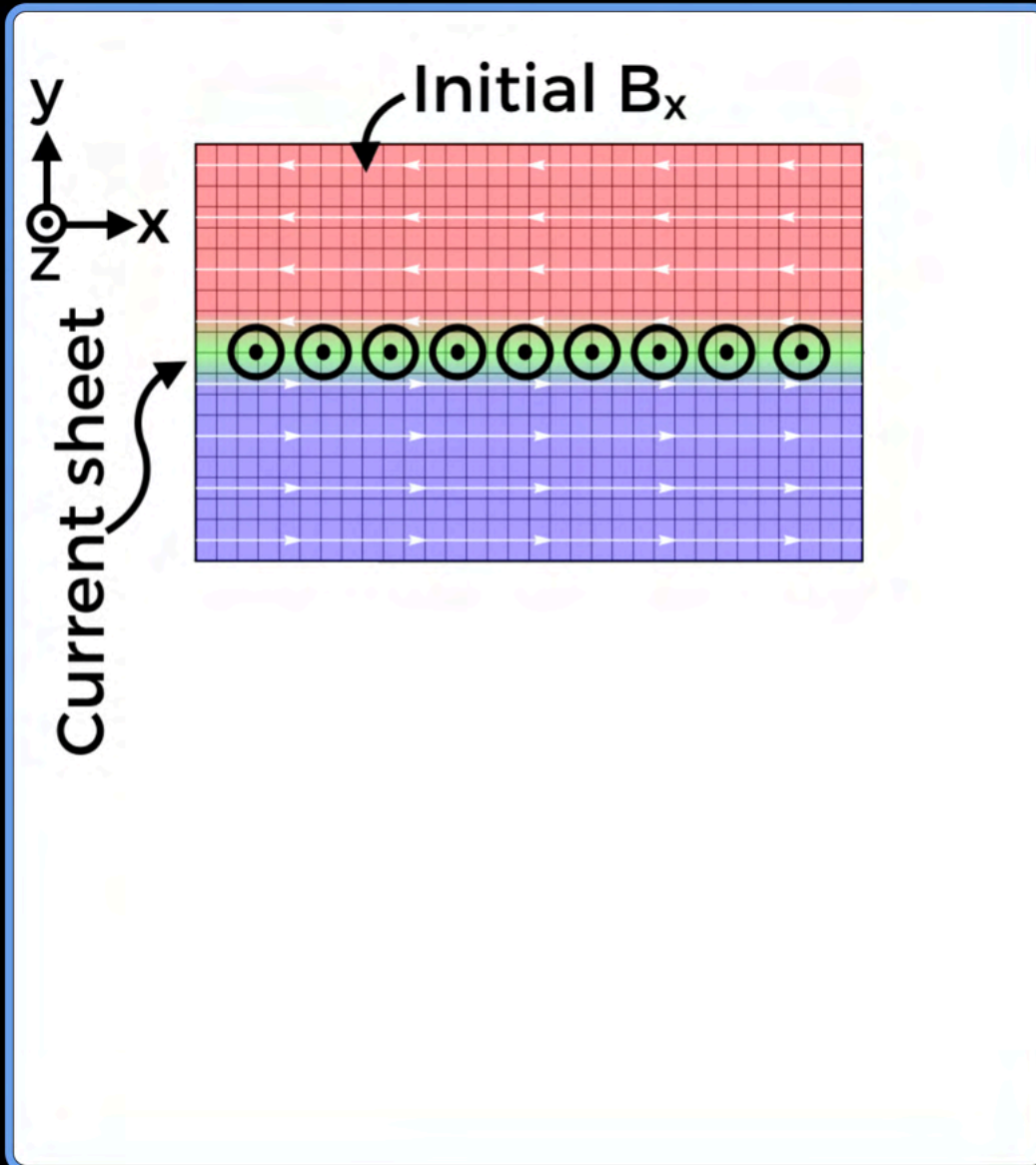
Drake+ (2014)

Simulation setup: inflow parameters

β_i	σ_i	θ_e	θ_i
4.9×10^{-4}	0.10	0.010	2.4×10^{-5}
0.031	0.10	0.041	0.0016
0.50	0.12	0.77	0.031
2.0	0.38	9.9	0.39

- For each case, vary guide field from $b_g = 0$ (antiparallel) to 6
- Electron temperature ranges from non-rel. to ultra-rel.
- Ions remain sub-relativistic
- Realistic mass ratio: $m_i/m_e = 1836$, and $T_e/T_i = 1$
- $\sigma_w = 0.1$ for each row in the table; σ_i changes
- For a few cases, vary σ_w and T_e/T_i

Simulation setup: trigger reconnection

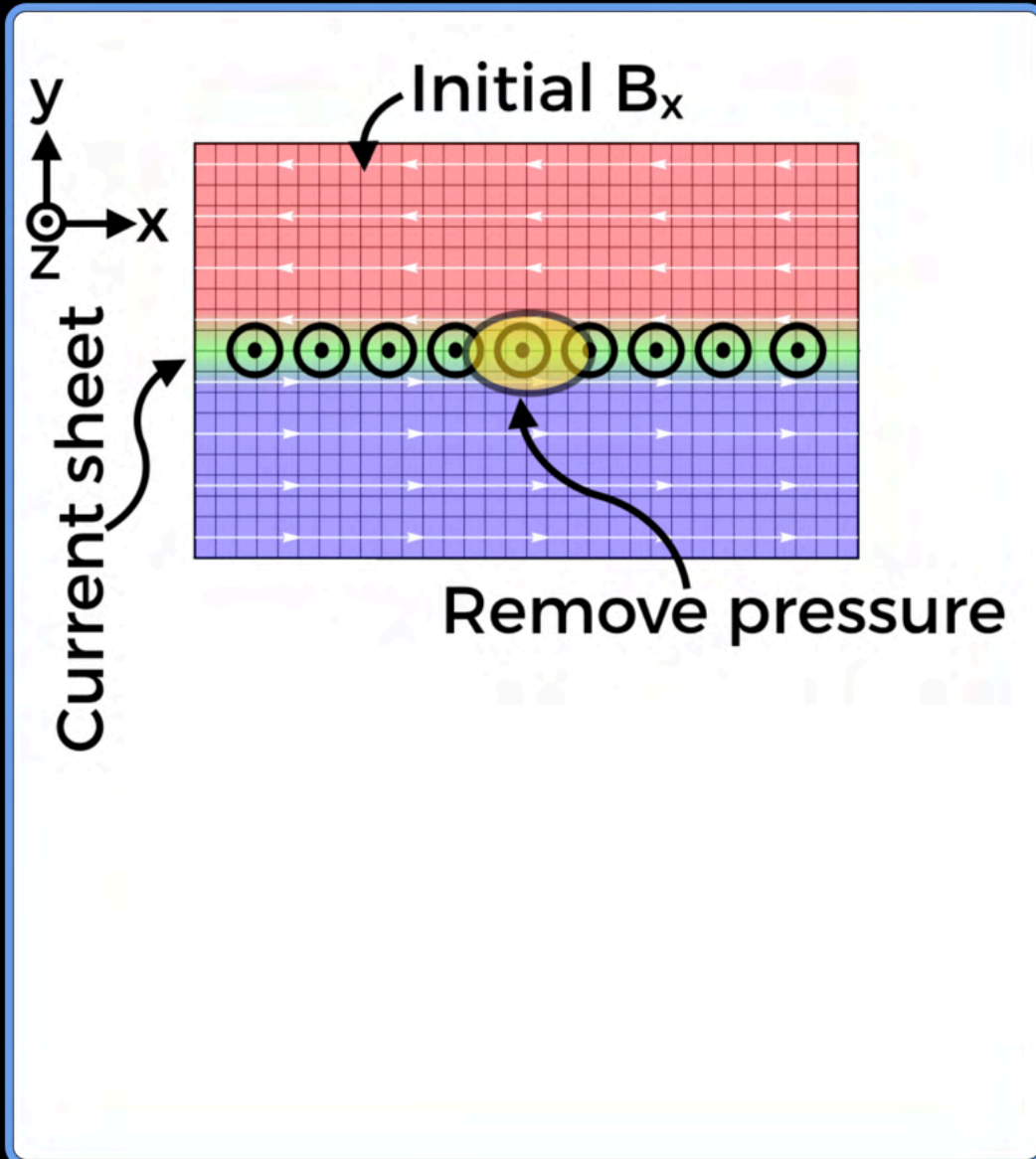


B-field initialized in Harris equilibrium:

$$\mathbf{B} = B_0 \tanh(y/\Delta) \hat{\mathbf{x}}$$

- Hot, overdense strip of particles (green)
- Remove particle pressure in center to drive reconnection
- System evolves self-consistently

Simulation setup: trigger reconnection

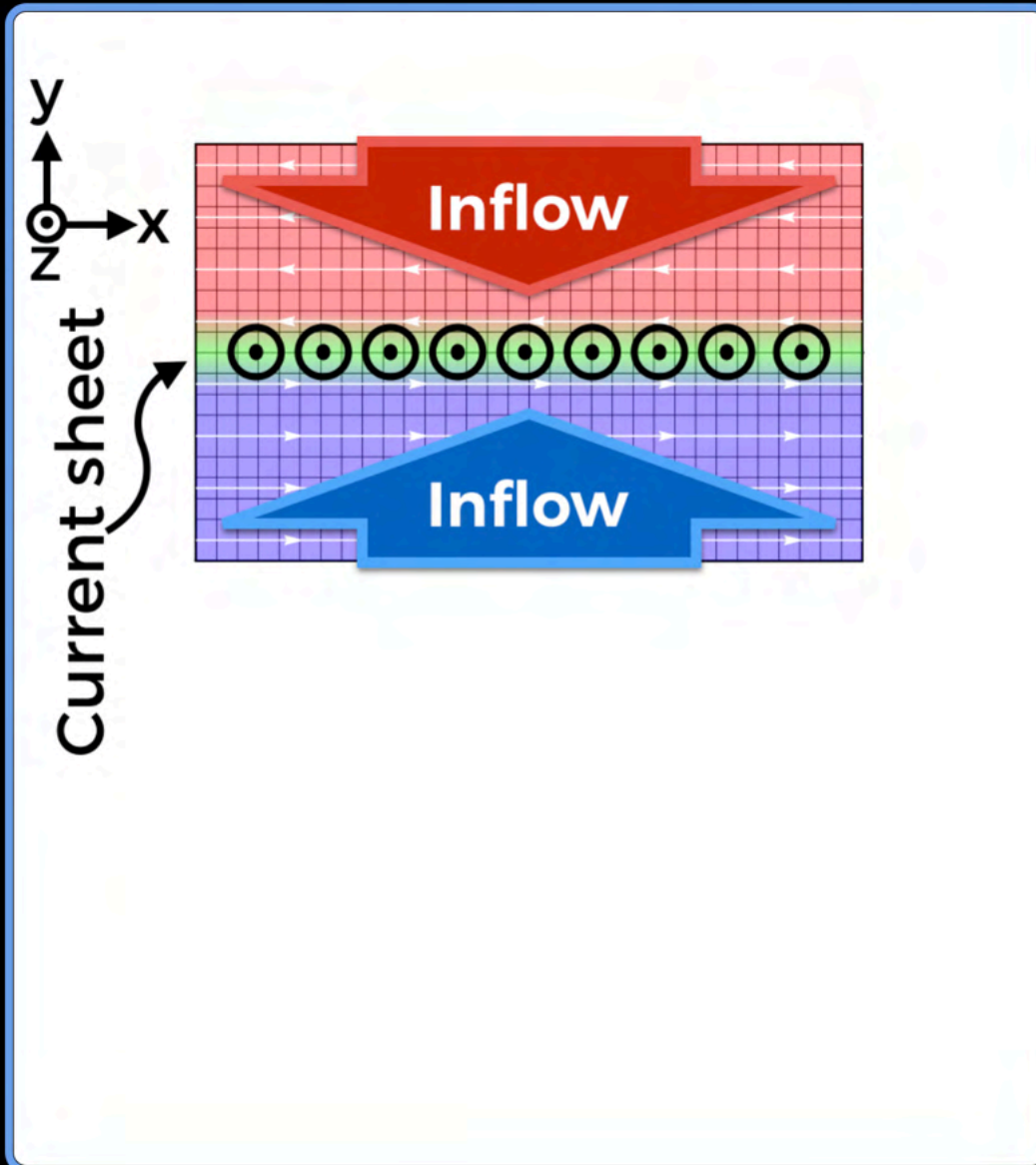


B-field initialized in Harris equilibrium:

$$\mathbf{B} = B_0 \tanh(y/\Delta) \hat{\mathbf{x}}$$

- Hot, overdense strip of particles (green)
- Remove particle pressure in center to drive reconnection
- System evolves self-consistently

Simulation setup: trigger reconnection

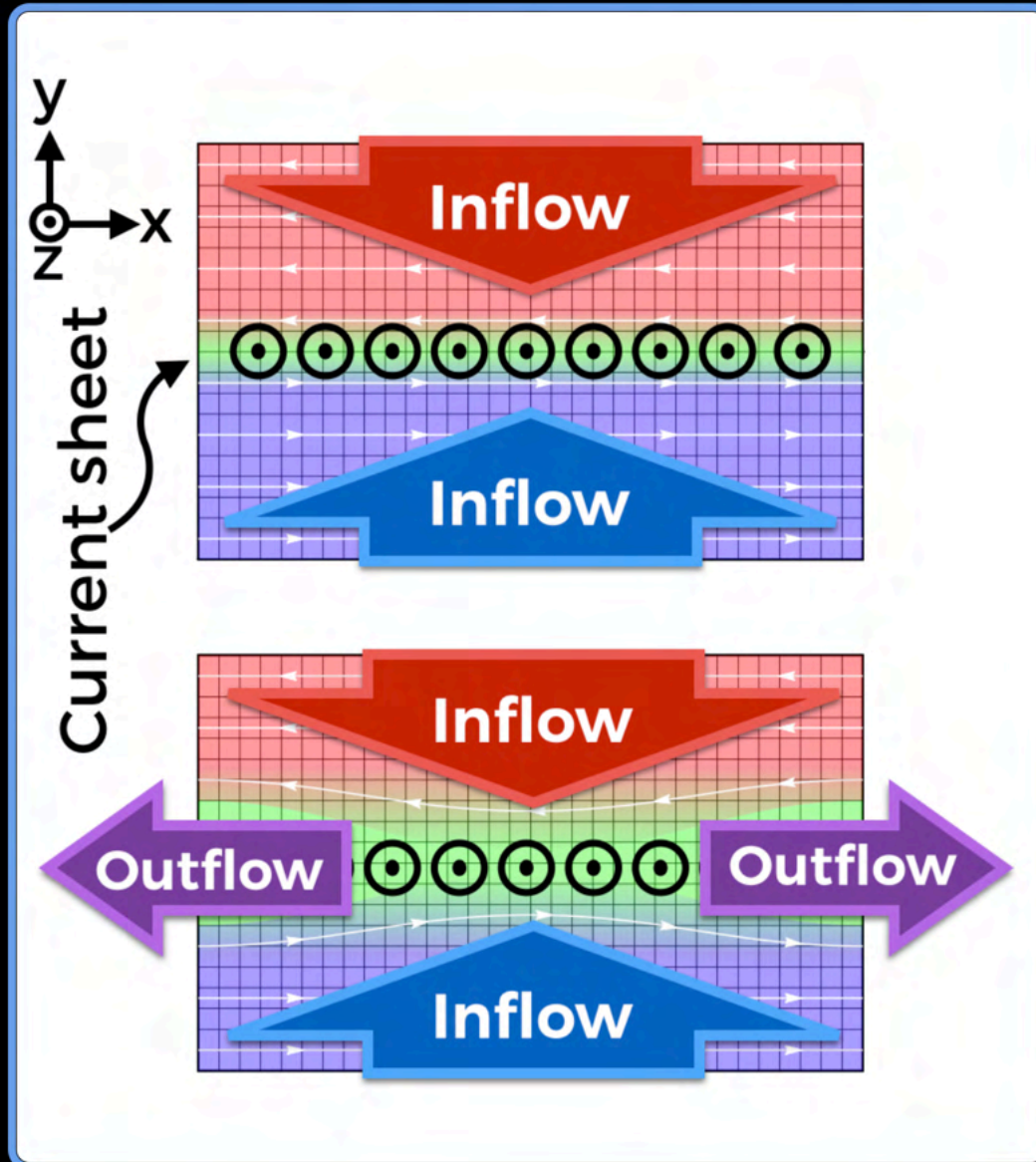


B-field initialized in Harris equilibrium:

$$\mathbf{B} = B_0 \tanh(y/\Delta) \hat{\mathbf{x}}$$

- Hot, overdense strip of particles (green)
- Remove particle pressure in center to drive reconnection
- System evolves self-consistently

Simulation setup: trigger reconnection



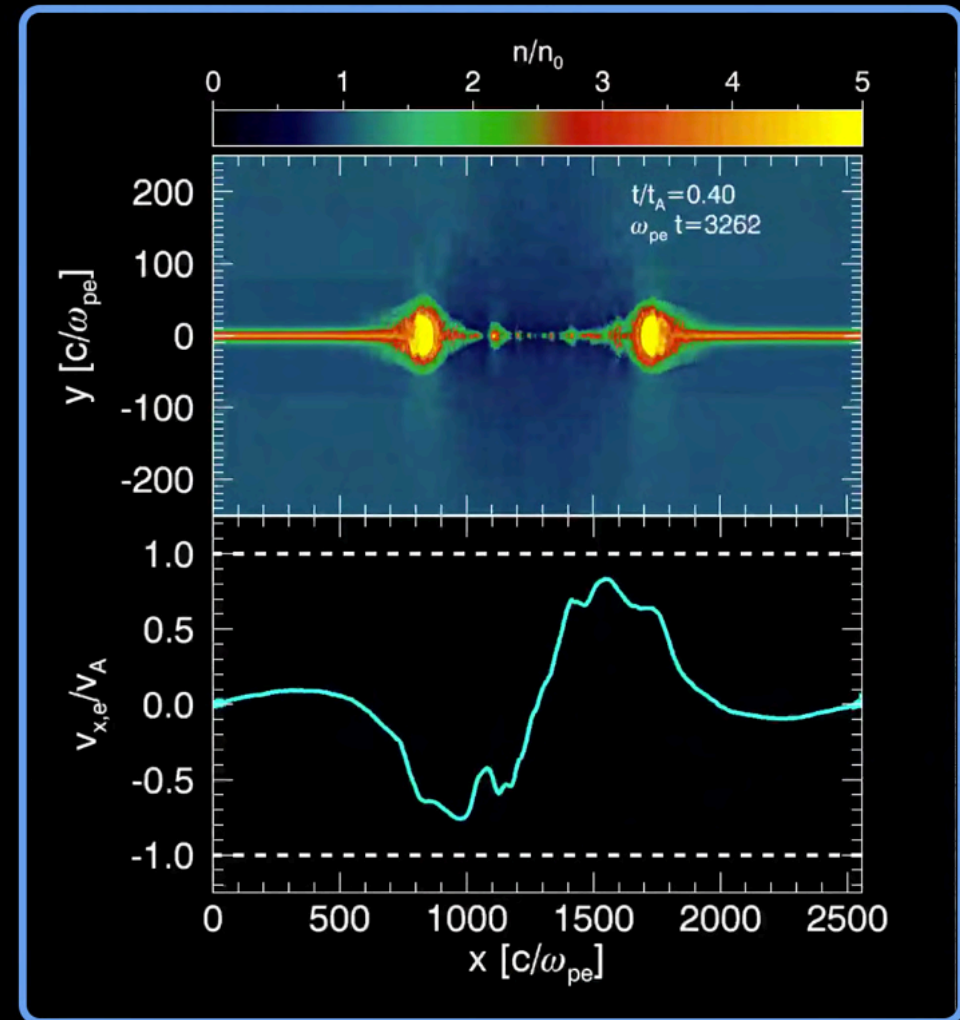
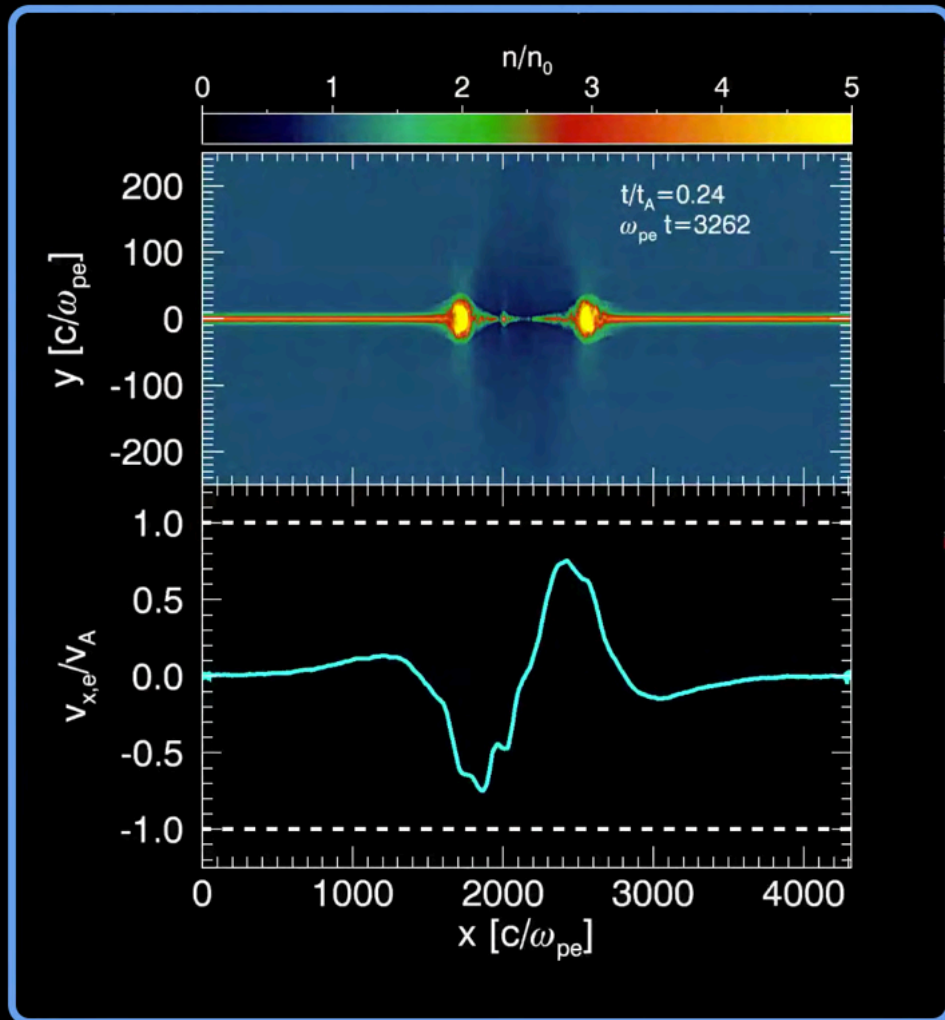
B-field initialized in Harris equilibrium:

$$\mathbf{B} = B_0 \tanh(y/\Delta) \hat{\mathbf{x}}$$

- Hot, overdense strip of particles (green)
- Remove particle pressure in center to drive reconnection
- System evolves self-consistently

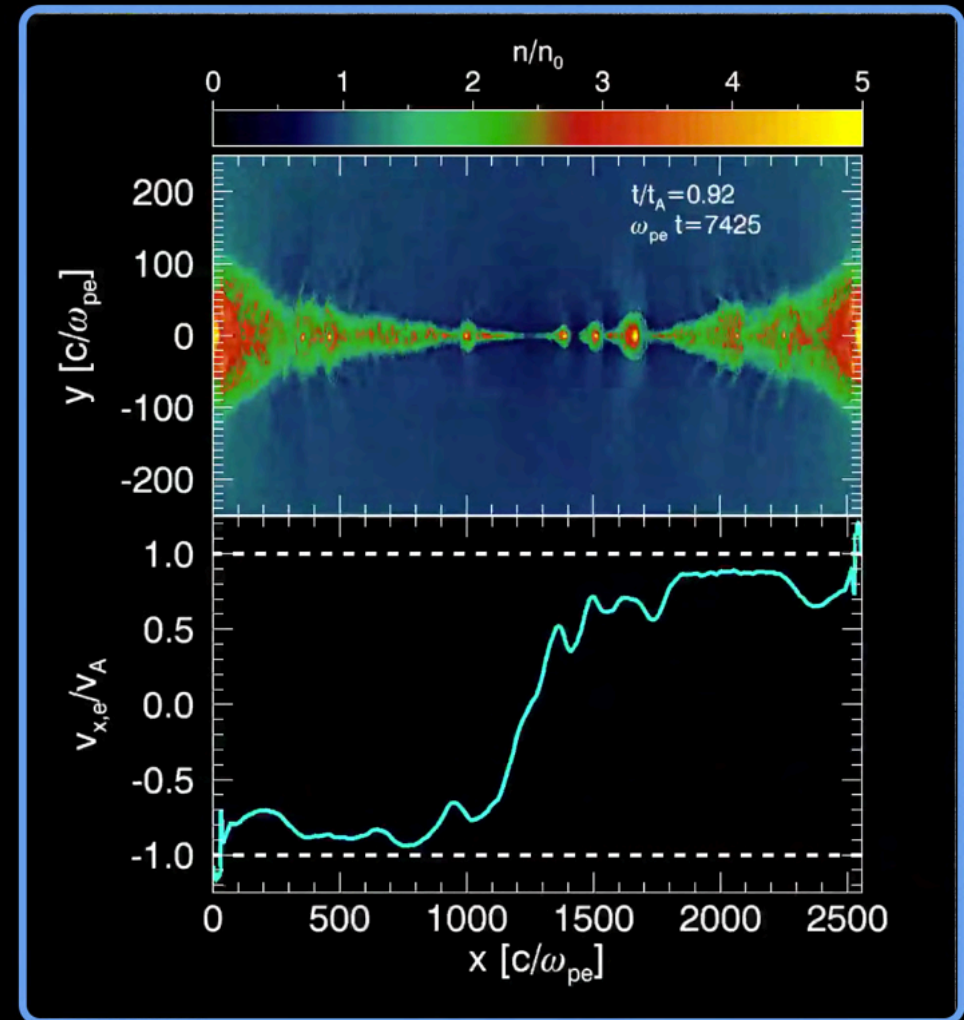
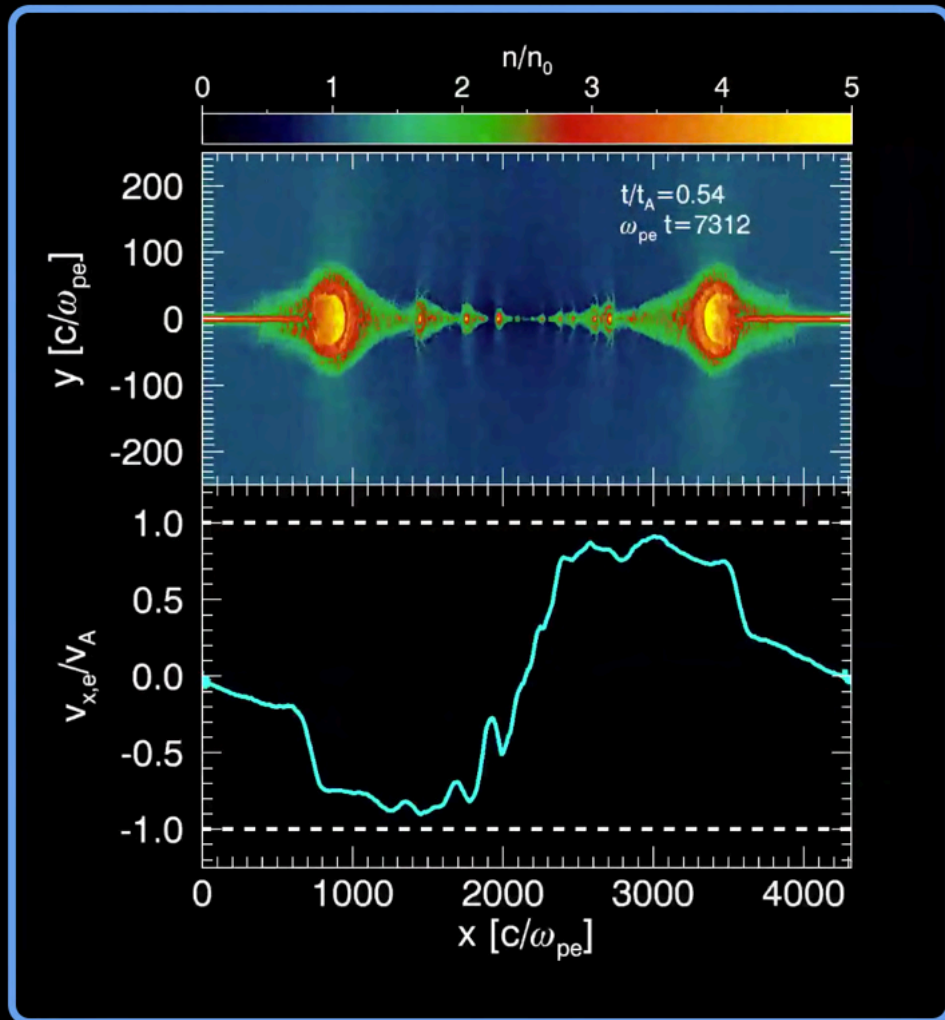
Simulation setup: periodic vs. outflow bc

Outflow simulations allow for evolution of system over multiple Alfvénic crossing times t_A (but converge to results of periodic if measured appropriately)



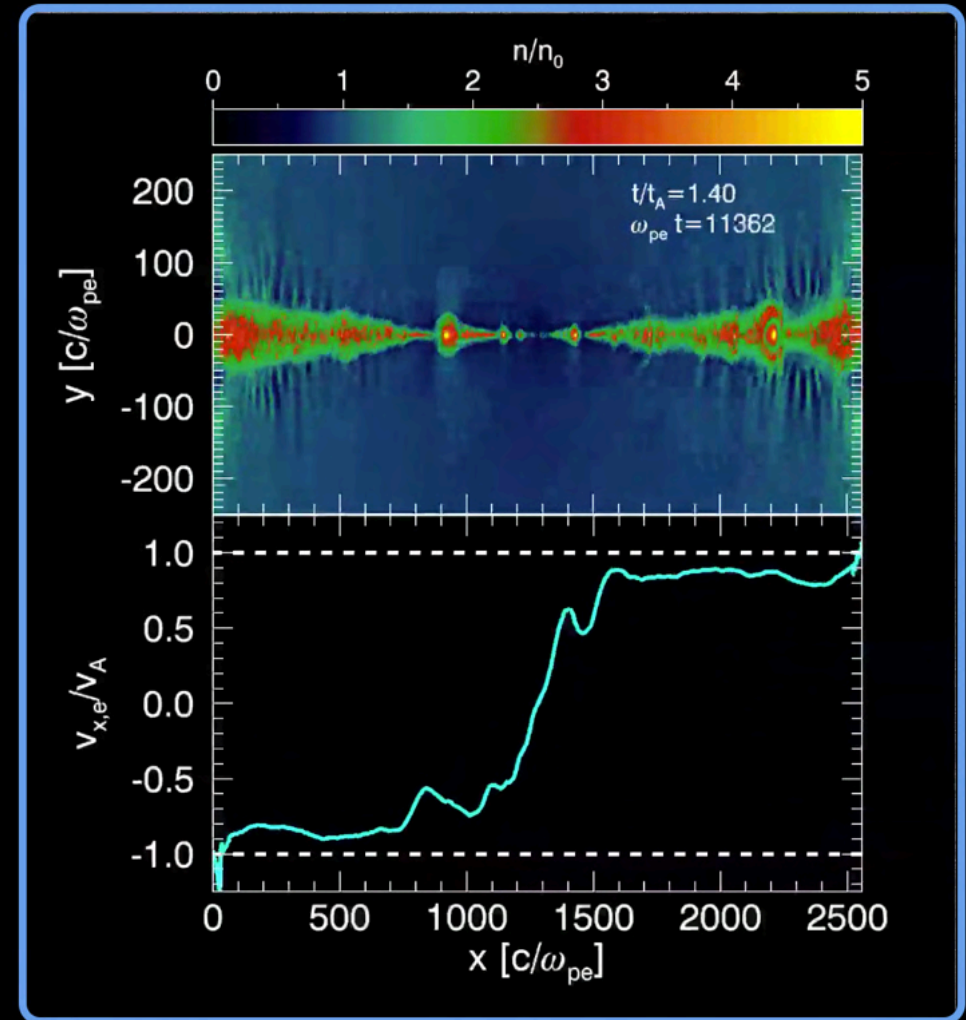
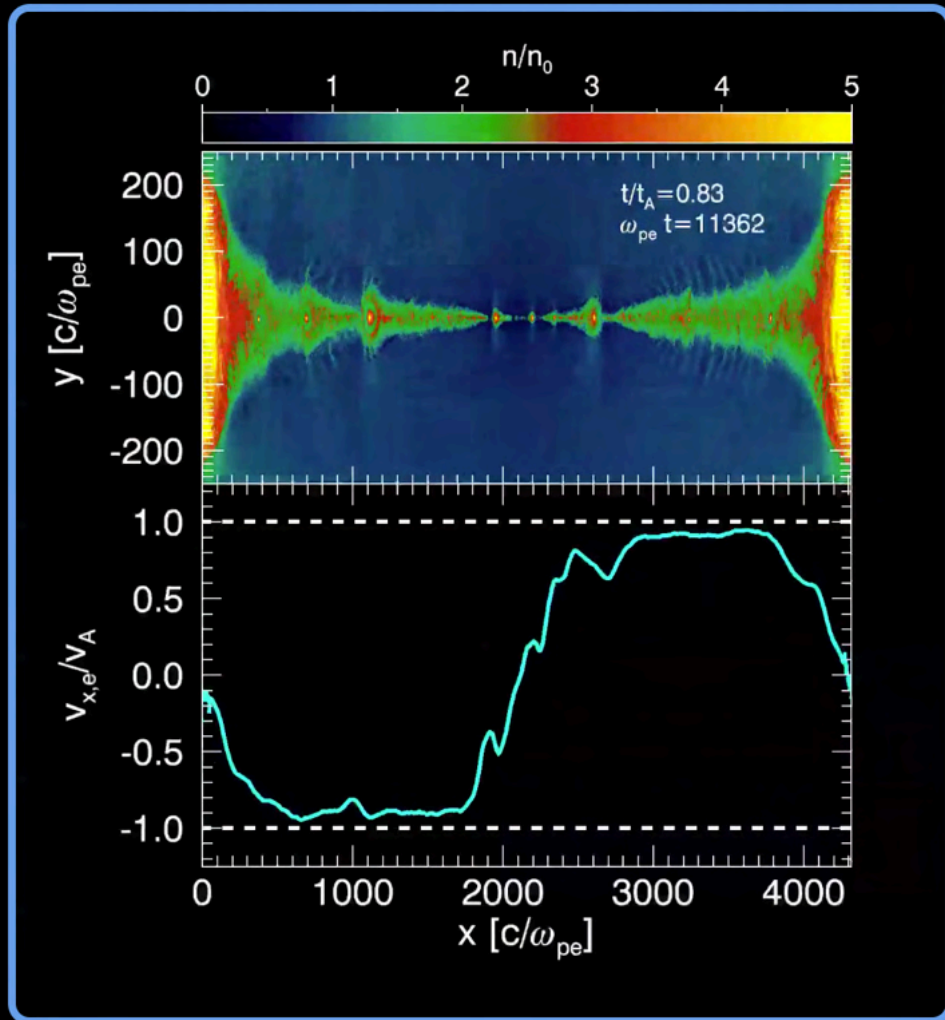
Simulation setup: periodic vs. outflow bc

Outflow simulations allow for evolution of system over multiple Alfvénic crossing times t_A (but converge to results of periodic if measured appropriately)



Simulation setup: periodic vs. outflow bc

Outflow simulations allow for evolution of system over multiple Alfvénic crossing times t_A (but converge to results of periodic if measured appropriately)

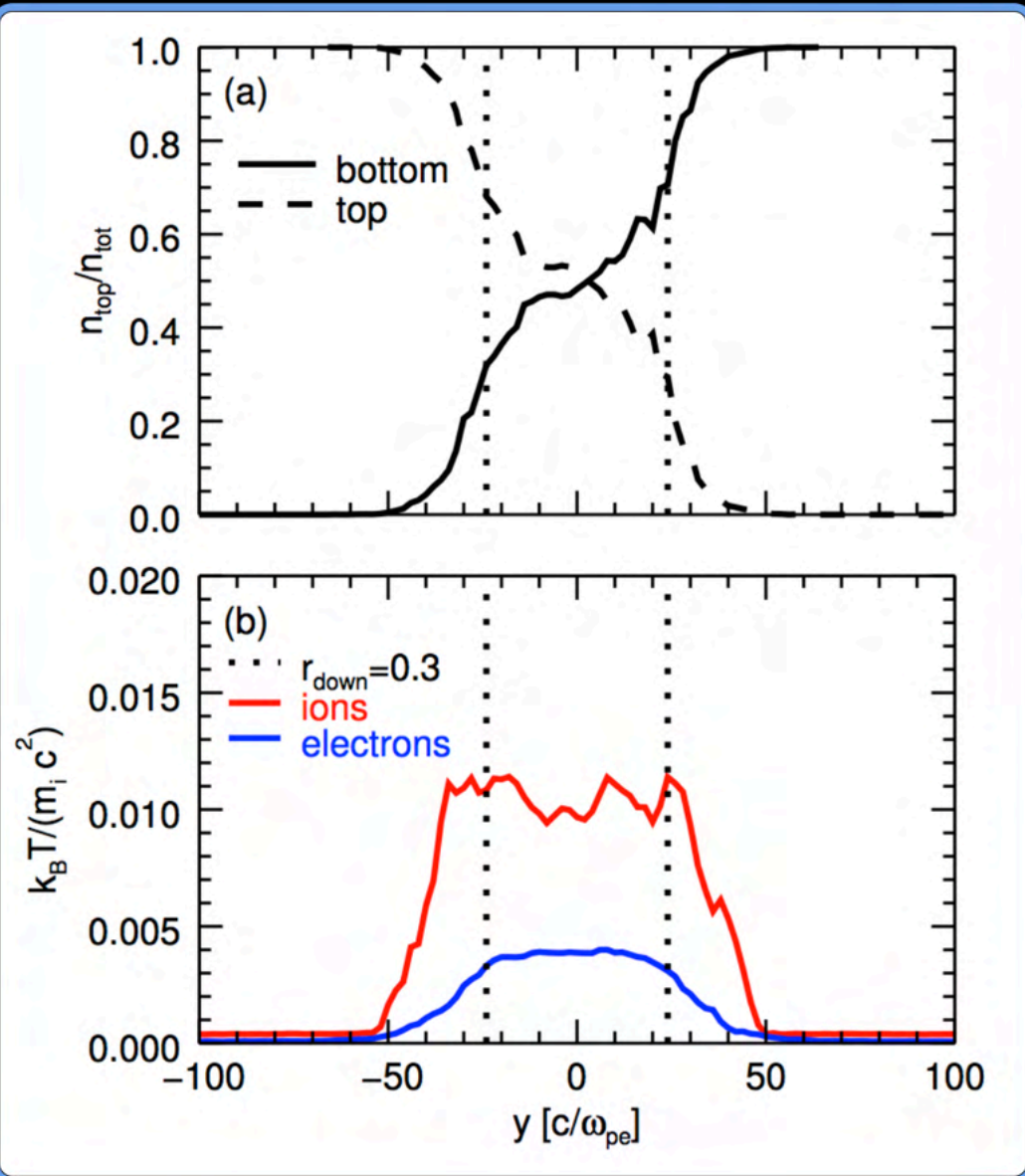


Use particle mixing as a proxy for rec. region

Use mixing as a criterion to ID cells where rec. has occurred:

$$r_{\text{down}} < \frac{n_{\text{top}}}{n_{\text{tot}}} < 1 - r_{\text{down}}$$

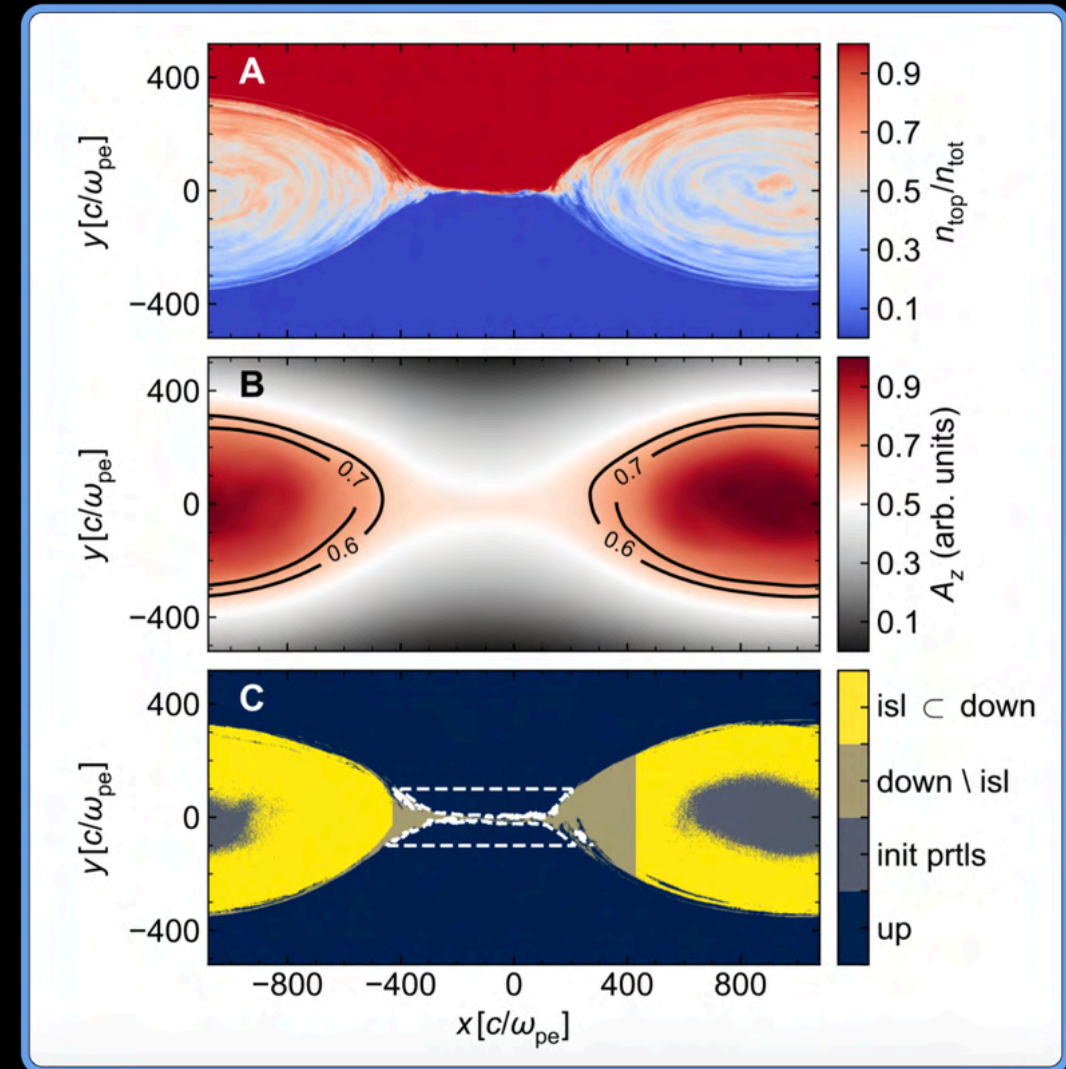
- Measured heating fractions M_{Te}, M_{Ti} somewhat sensitive to choice of r_{down}
- Change of $\sim 15\%$ from $r_{\text{down}} = 0.1$ to 0.3
- Mixing criterion appropriate for nonzero guide field



Focus on particles in 'primary islands'

Focus on 'island' region, where energy of bulk motion from outflows has thermalized:

- Select region within a contour of the vector potential A_z as 'island'
- Threshold value of vector potential is chosen based on mixing at $x = \pm 1000 c/\omega_{pe}$
- Exclude particles leftover from initialization (gray region at cores of island)



Adiabatic-compressive vs. genuine heating

When gas is compressed adiabatically, internal energy increases and entropy per particle remains **constant**

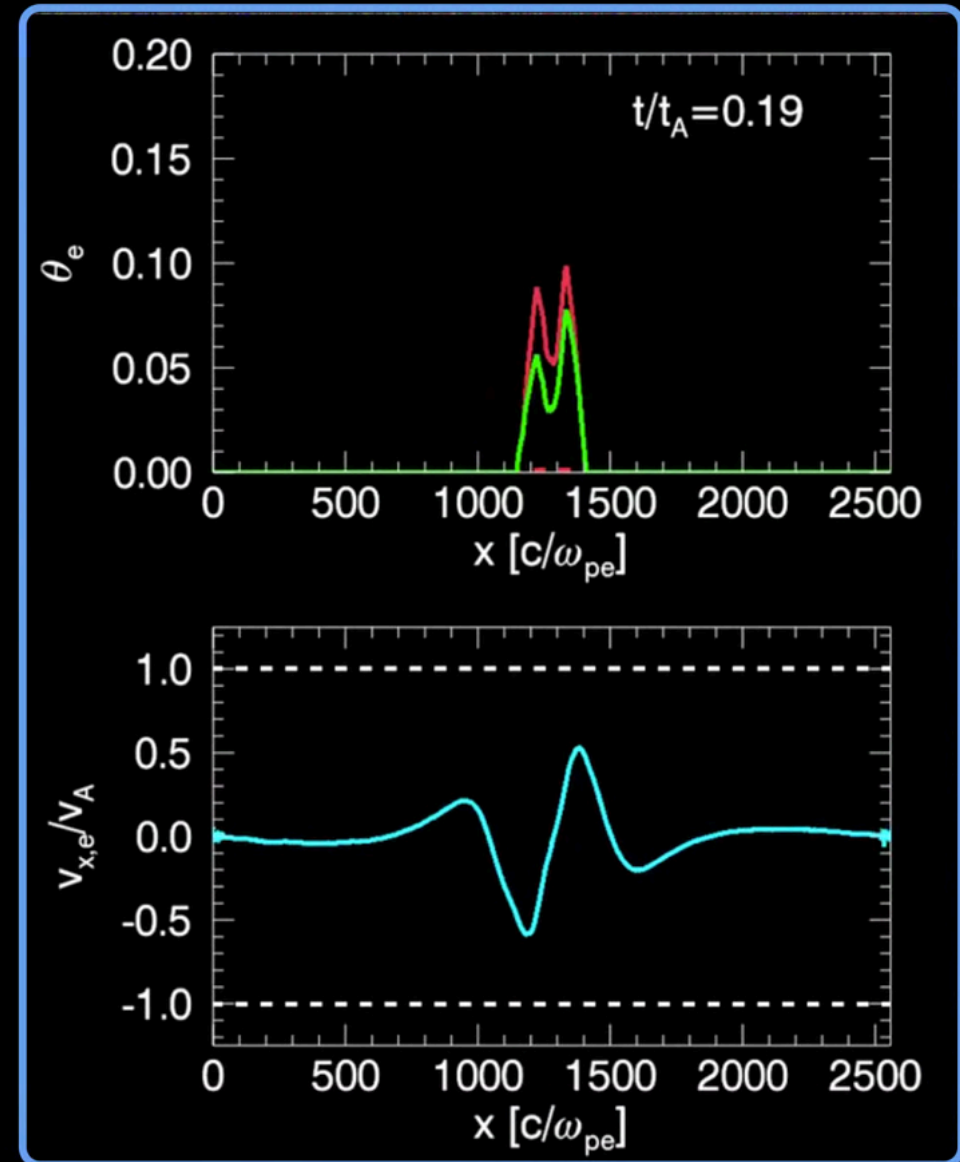
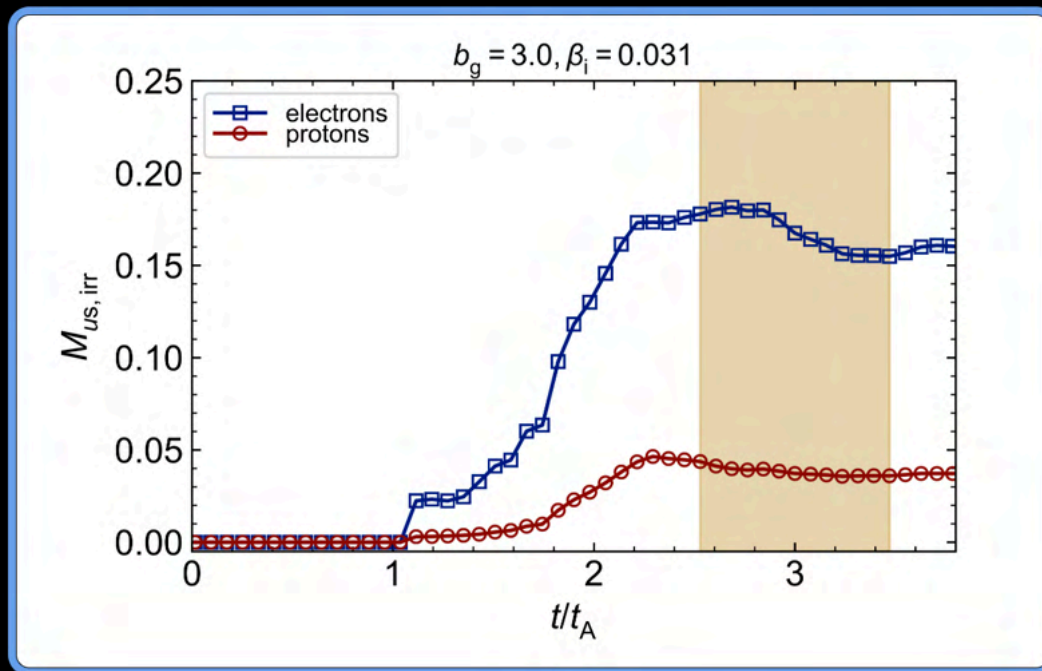
How much heating in the downstream is an effect of adiabatic-compression (no increase in entropy)?

$$\int_{u^{\text{up}}}^{u^{\text{f}}} \frac{1}{(\hat{\gamma}(u) - 1)u} du - \log\left(\frac{n^{\text{f}}}{n^{\text{up}}}\right) = 0$$

- Solve for u_{f} , the predicted dimensionless internal energy
- Take the difference $u_{\text{down}} - u_{\text{f}}$ as the genuine heating

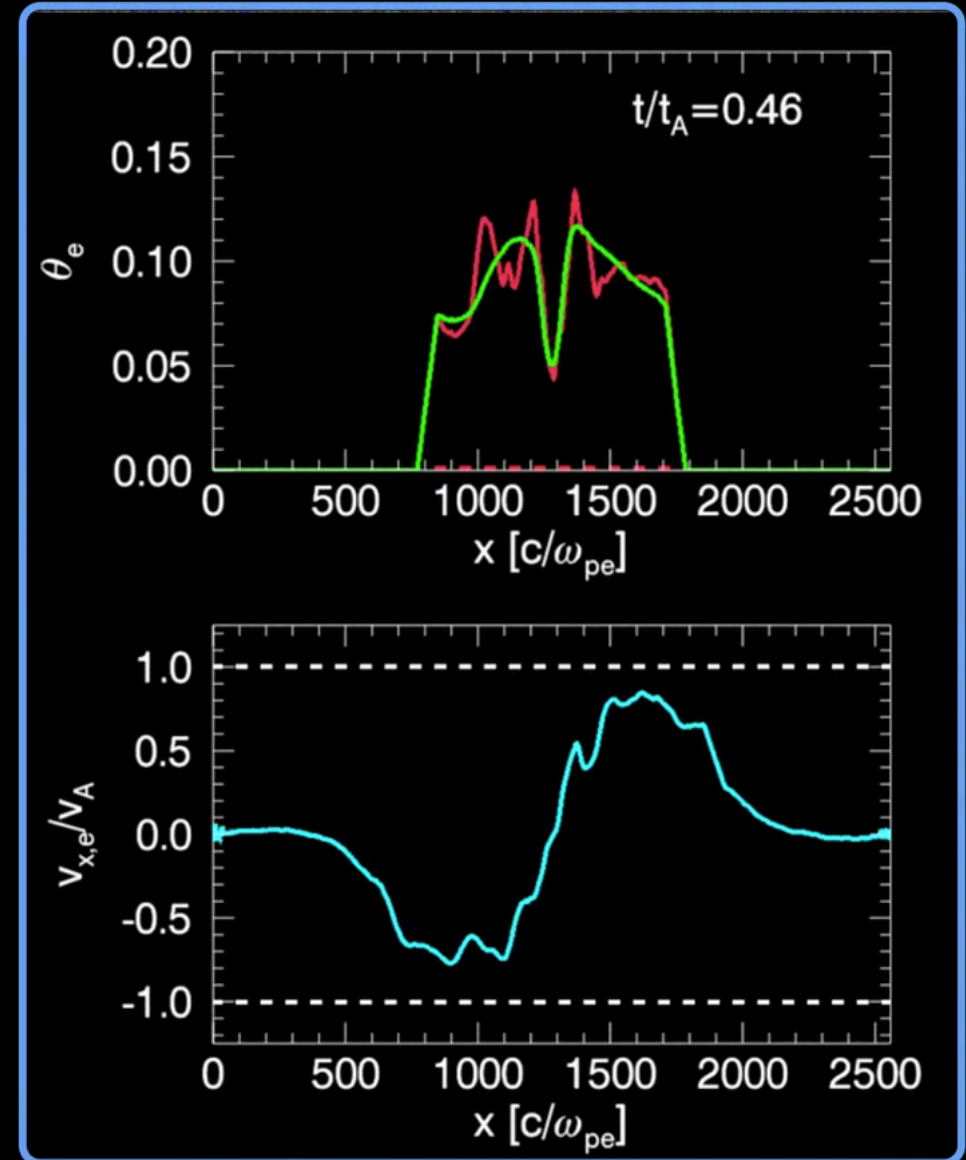
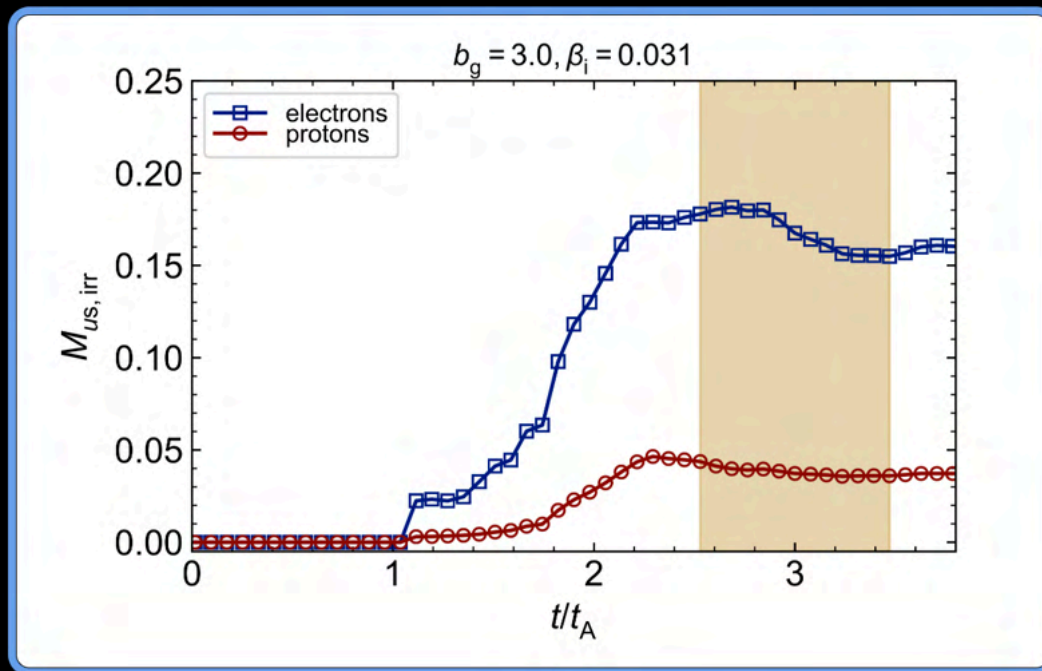
Measure heating when 'quasi-steady'

Extract heating by measuring 'quasi-steady' values in the island region; time average heating over ~ 1 Alfvénic crossing time:



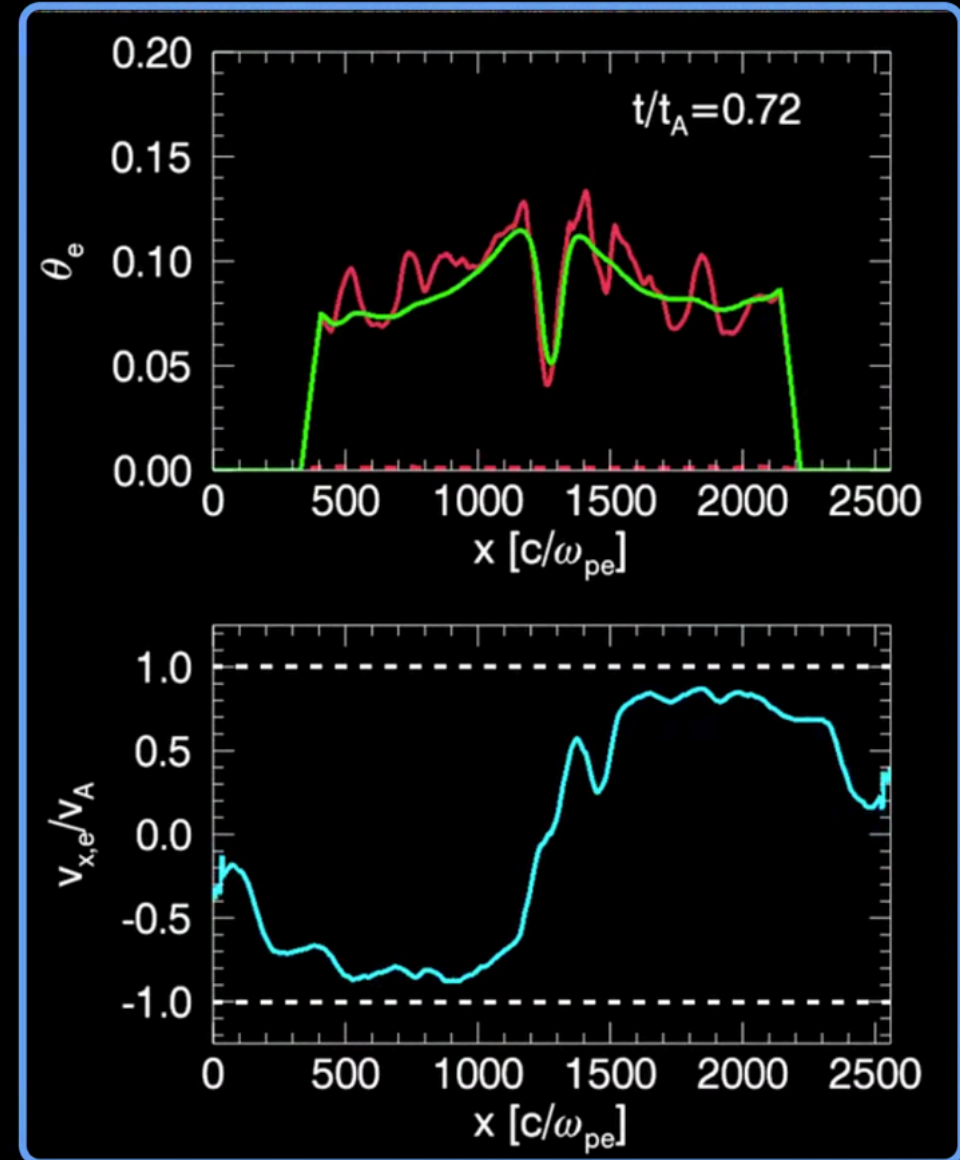
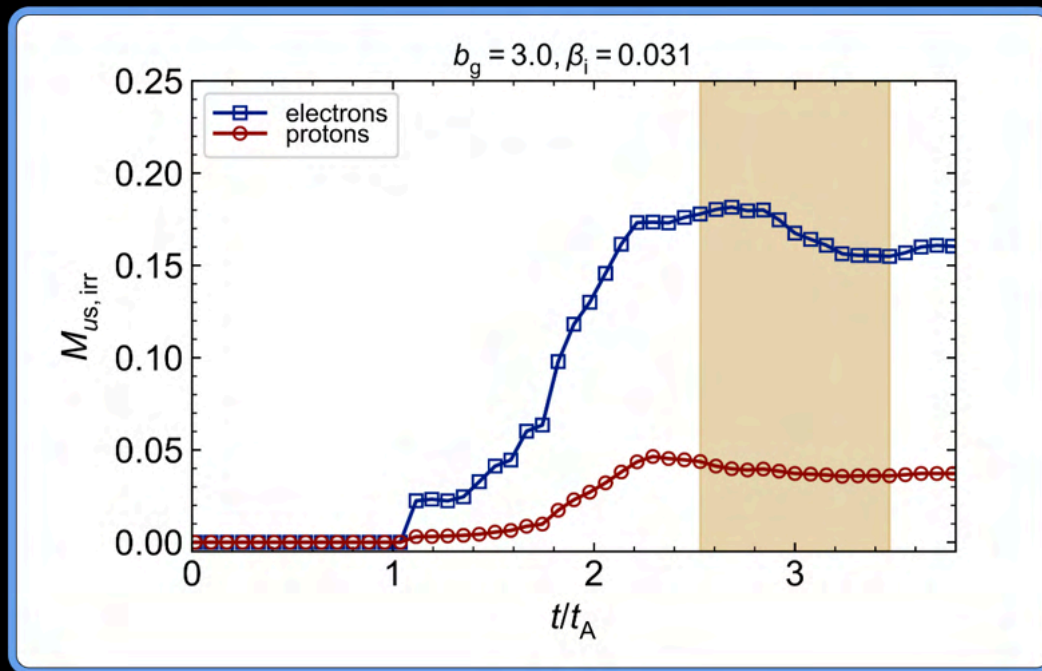
Measure heating when 'quasi-steady'

Extract heating by measuring 'quasi-steady' values in the island region; time average heating over ~ 1 Alfvénic crossing time:



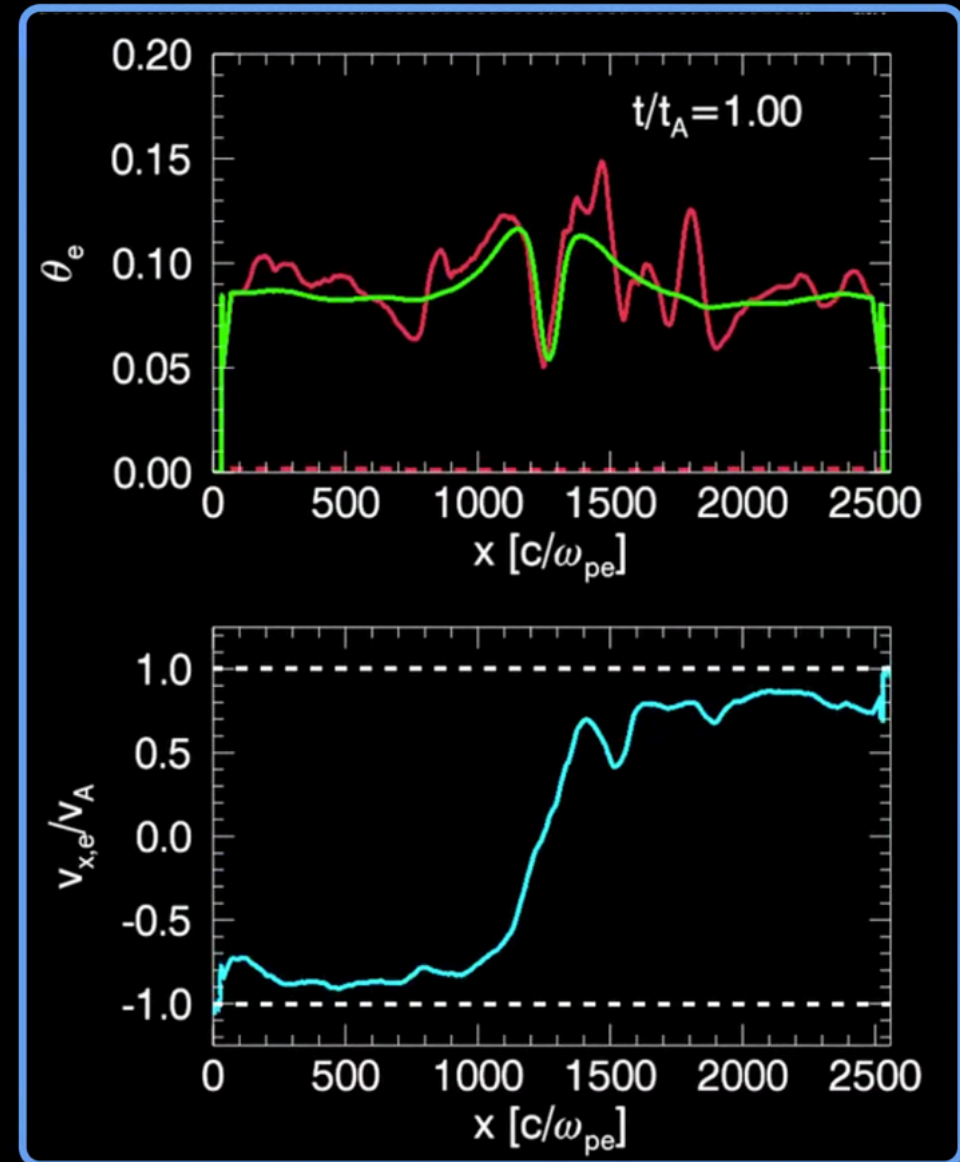
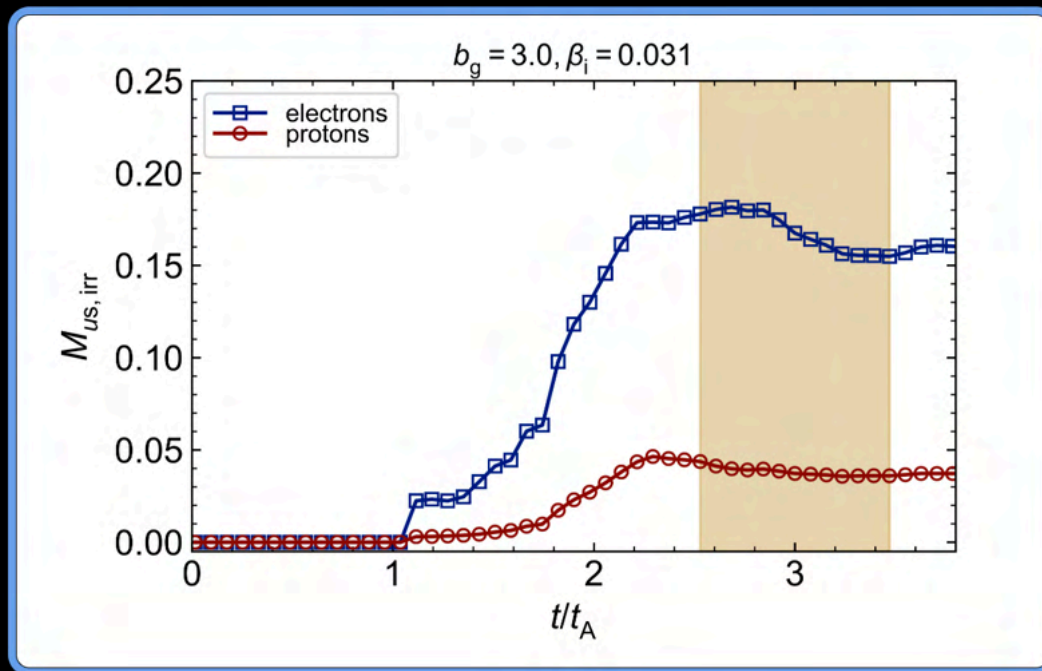
Measure heating when 'quasi-steady'

Extract heating by measuring 'quasi-steady' values in the island region; time average heating over ~ 1 Alfvénic crossing time:



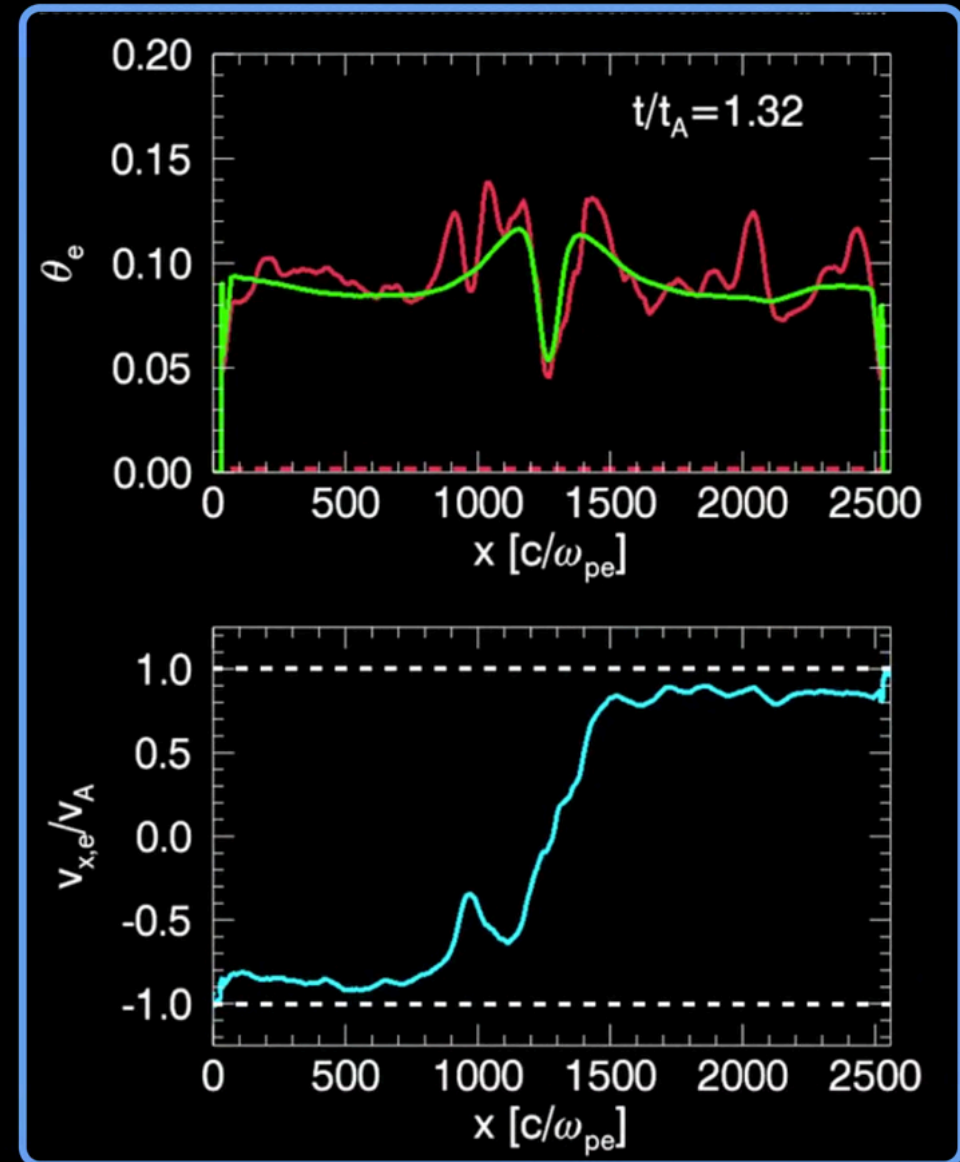
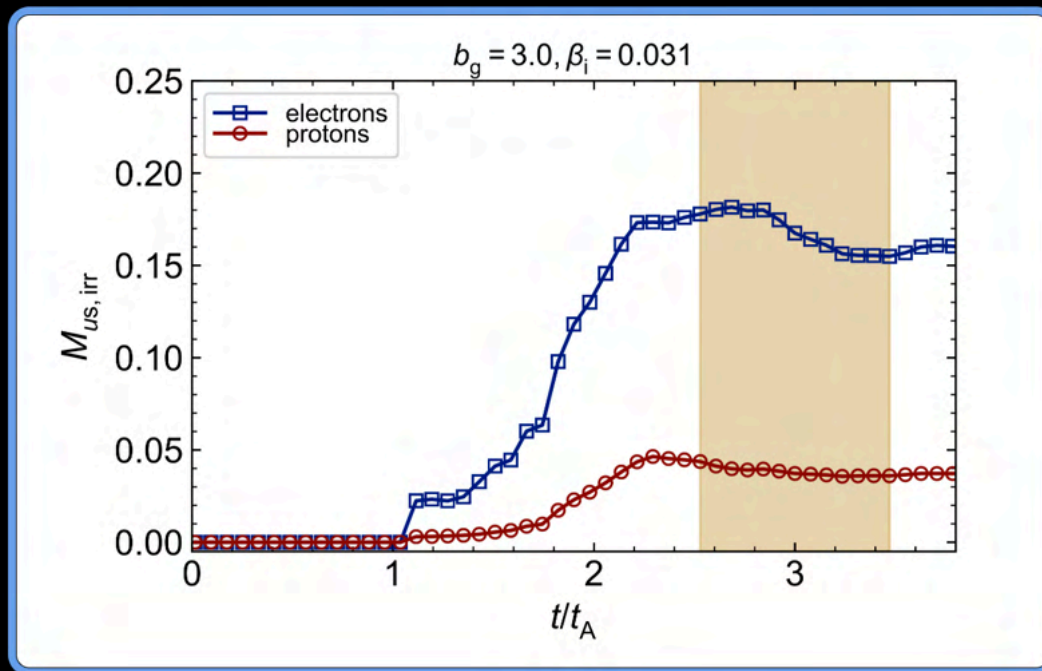
Measure heating when 'quasi-steady'

Extract heating by measuring 'quasi-steady' values in the island region; time average heating over ~ 1 Alfvénic crossing time:



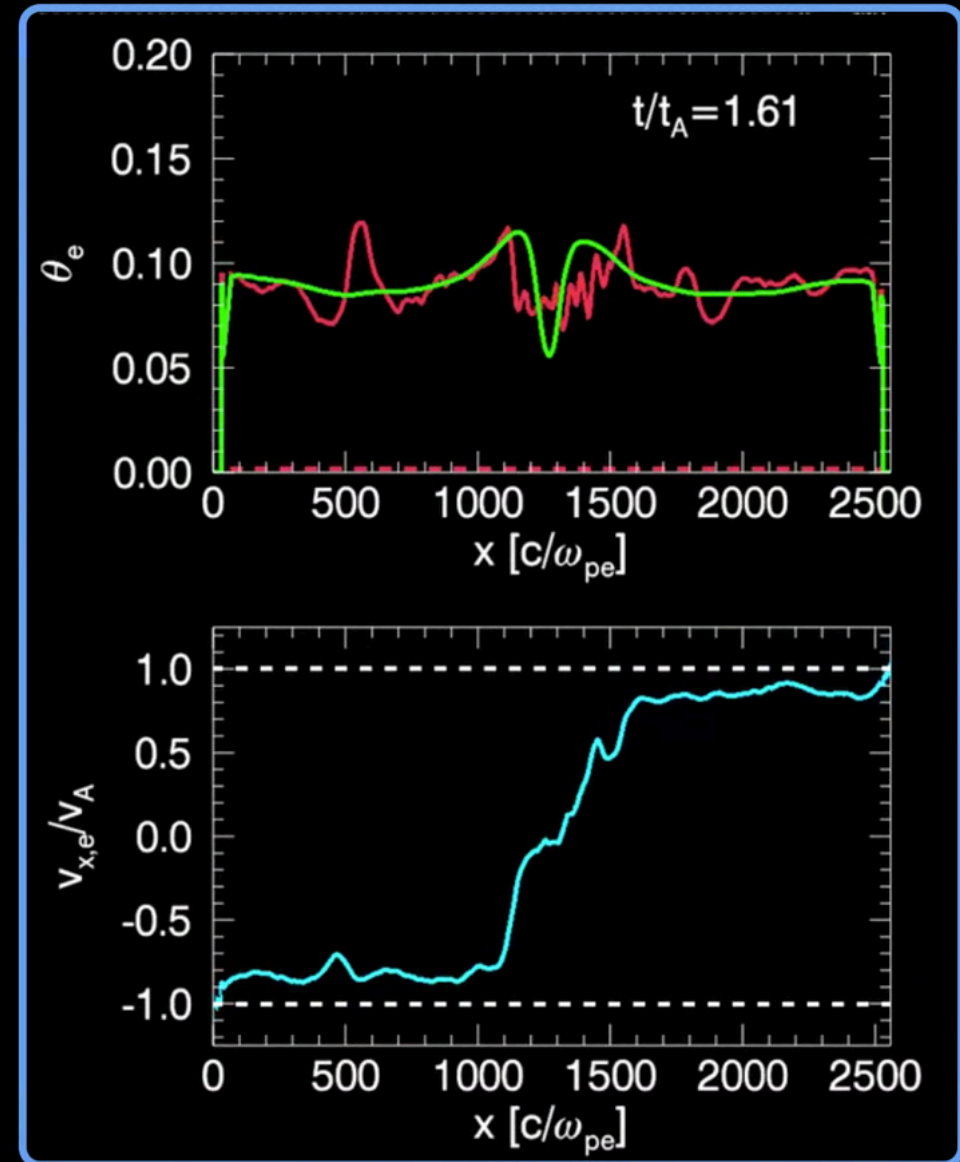
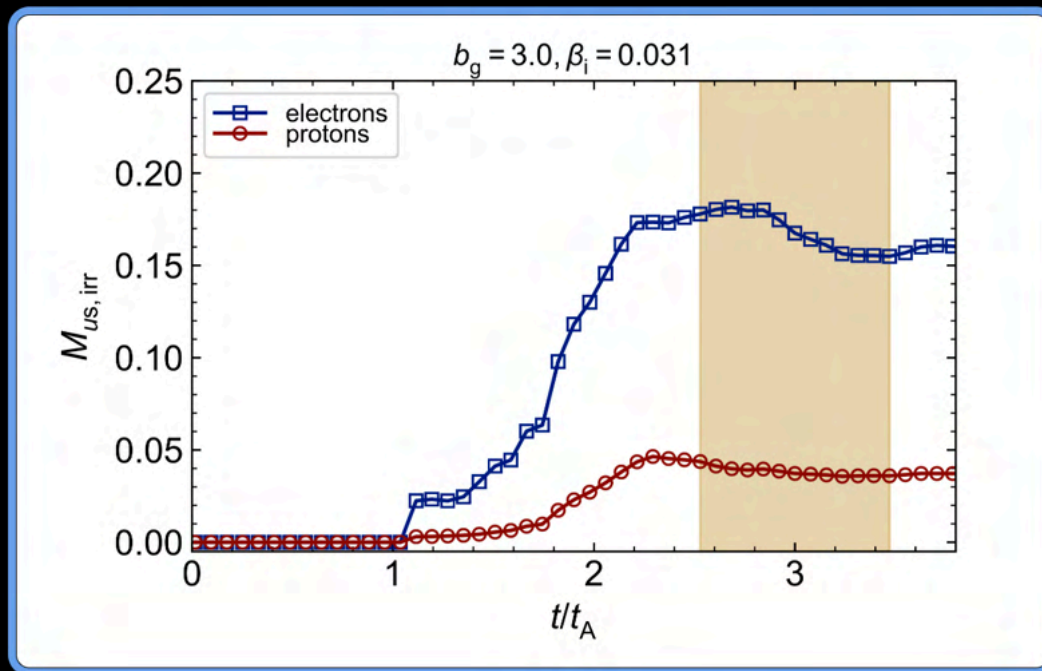
Measure heating when 'quasi-steady'

Extract heating by measuring 'quasi-steady' values in the island region; time average heating over ~ 1 Alfvénic crossing time:



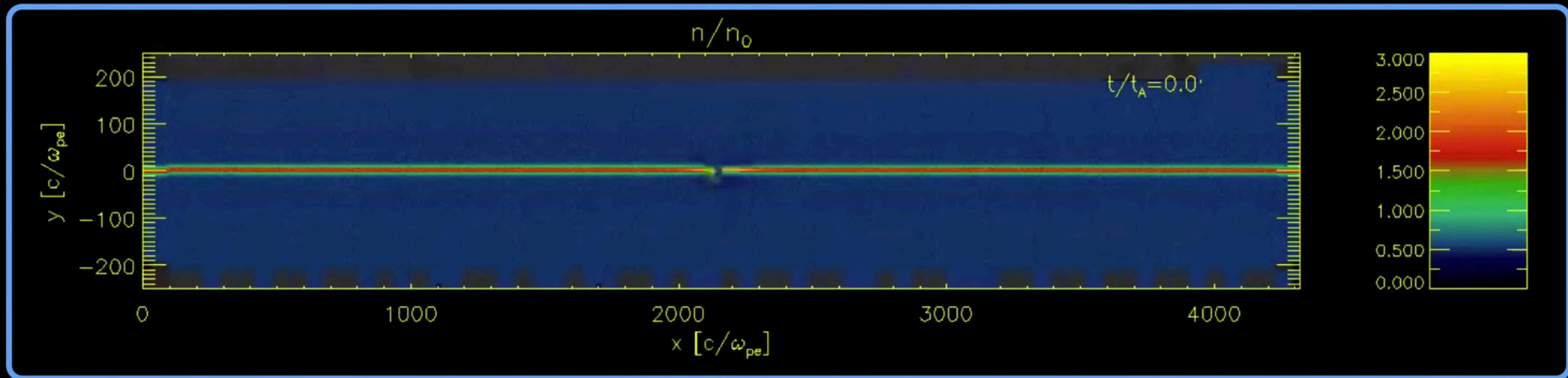
Measure heating when 'quasi-steady'

Extract heating by measuring 'quasi-steady' values in the island region; time average heating over ~ 1 Alfvénic crossing time:



Low- β_i , antiparallel reconnection ($b_g = 0$)

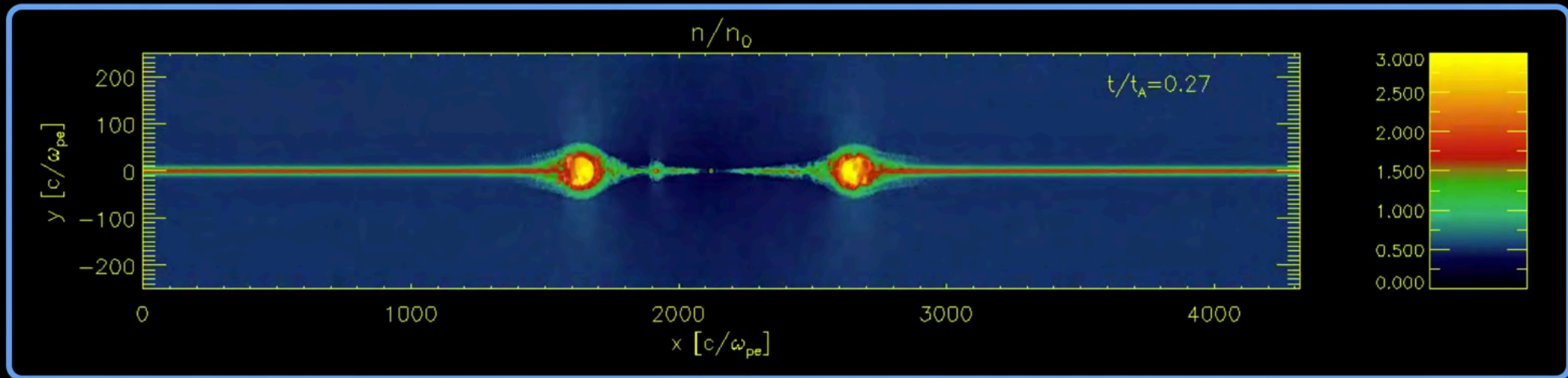
Simulation parameters: $\beta_i = 0.0078$, $\sigma_w = 0.1$, $T_e/T_i = 0.1$



- 'Wavefronts' recede at Alfvén speed (dragged by magnetic tension); plasma starts flowing into the reconnection layer
- Primary islands (the large blobs) contain particles used at initialization; secondary islands form due to tearing instability

Low- β_i , antiparallel reconnection ($b_g = 0$)

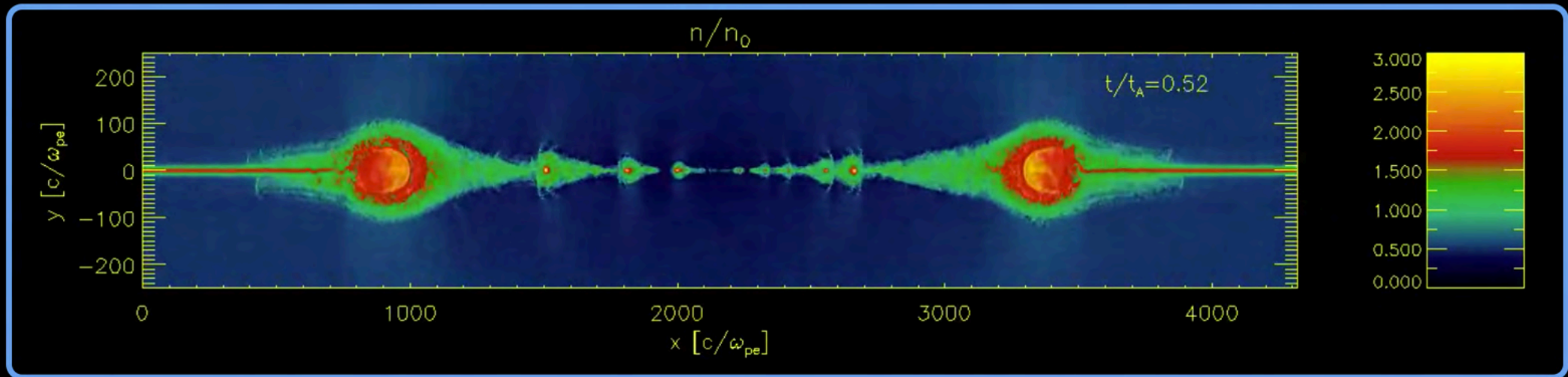
Simulation parameters: $\beta_i = 0.0078$, $\sigma_w = 0.1$, $T_e/T_i = 0.1$



- 'Wavefronts' recede at Alfvén speed (dragged by magnetic tension); plasma starts flowing into the reconnection layer
- Primary islands (the large blobs) contain particles used at initialization; secondary islands form due to tearing instability

Low- β_i , antiparallel reconnection ($b_g = 0$)

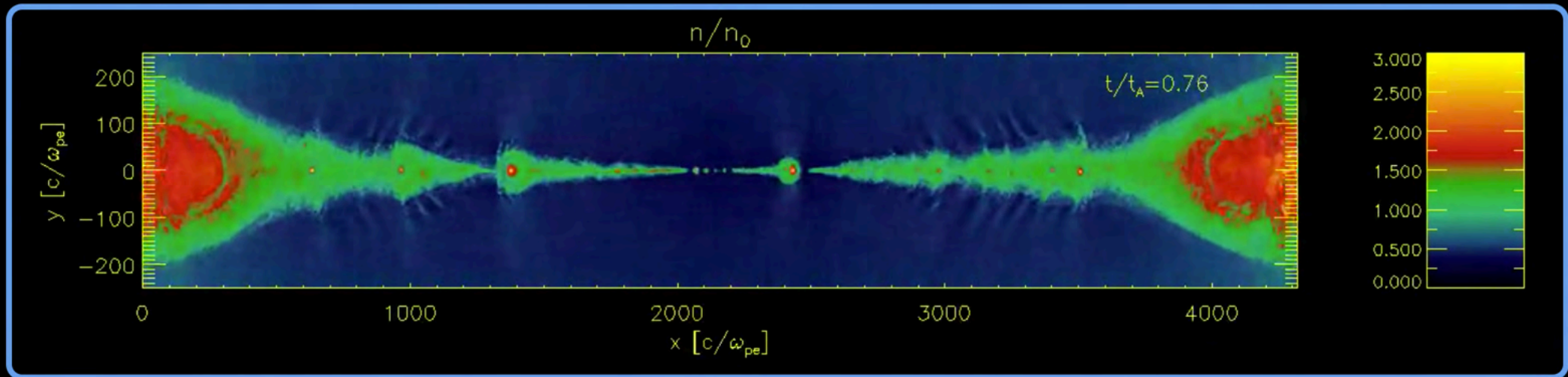
Simulation parameters: $\beta_i = 0.0078$, $\sigma_w = 0.1$, $T_e/T_i = 0.1$



- 'Wavefronts' recede at Alfvén speed (dragged by magnetic tension); plasma starts flowing into the reconnection layer
- Primary islands (the large blobs) contain particles used at initialization; secondary islands form due to tearing instability

Low- β_i , antiparallel reconnection ($b_g = 0$)

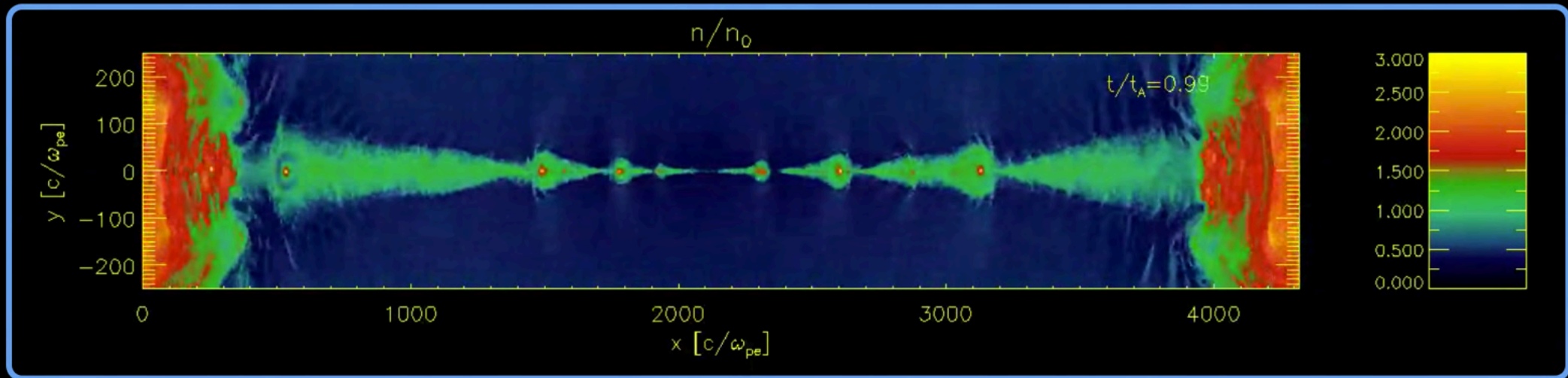
Simulation parameters: $\beta_i = 0.0078$, $\sigma_w = 0.1$, $T_e/T_i = 0.1$



- 'Wavefronts' recede at Alfvén speed (dragged by magnetic tension); plasma starts flowing into the reconnection layer
- Primary islands (the large blobs) contain particles used at initialization; secondary islands form due to tearing instability

Low- β_i , antiparallel reconnection ($b_g = 0$)

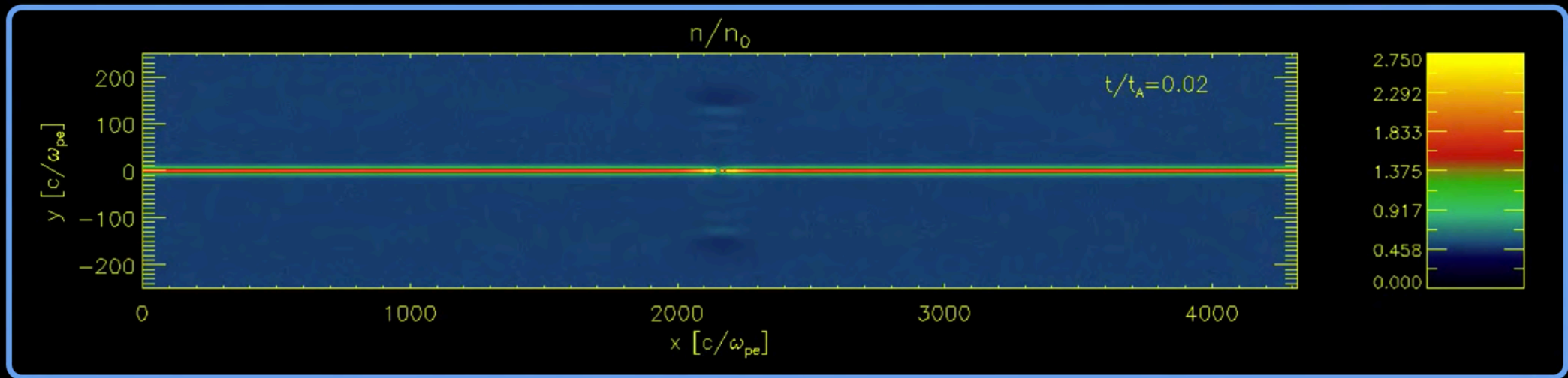
Simulation parameters: $\beta_i = 0.0078$, $\sigma_w = 0.1$, $T_e/T_i = 0.1$



- 'Wavefronts' recede at Alfvén speed (dragged by magnetic tension); plasma starts flowing into the reconnection layer
- Primary islands (the large blobs) contain particles used at initialization; secondary islands form due to tearing instability

High- β_i , antiparallel reconnection ($b_g = 0$)

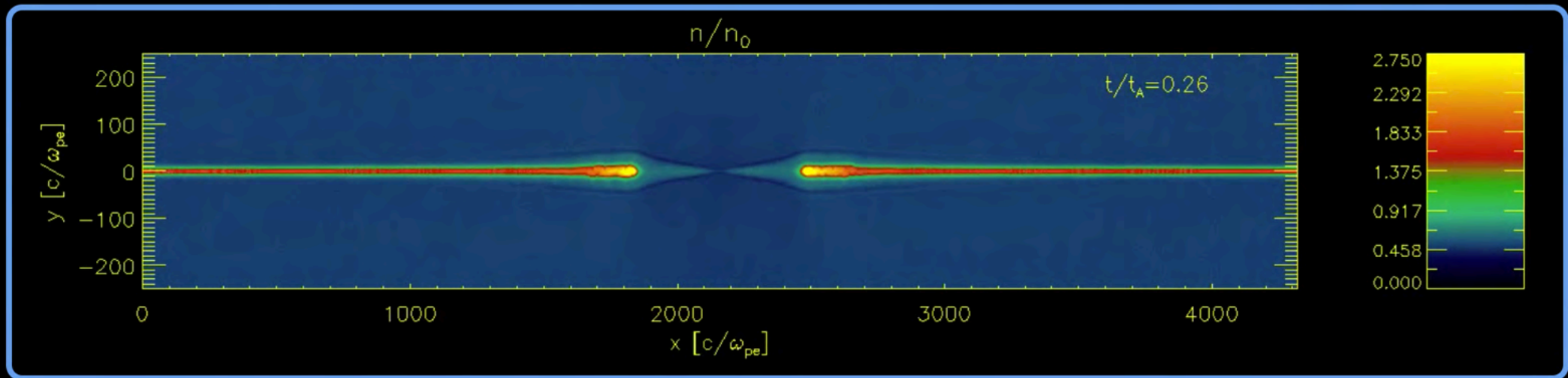
Simulation parameters: $\beta_i = 2$, $\sigma_w = 0.1$, $T_e/T_i = 0.1$, $N_{ppc} = 64$



- No secondary islands
- Outflow is more homogeneous than in low- β_i case
- Fractional increase of quantities in reconnection exhaust is less than at low- β_i (e.g. electron and ion temperatures, density)

High- β_i , antiparallel reconnection ($b_g = 0$)

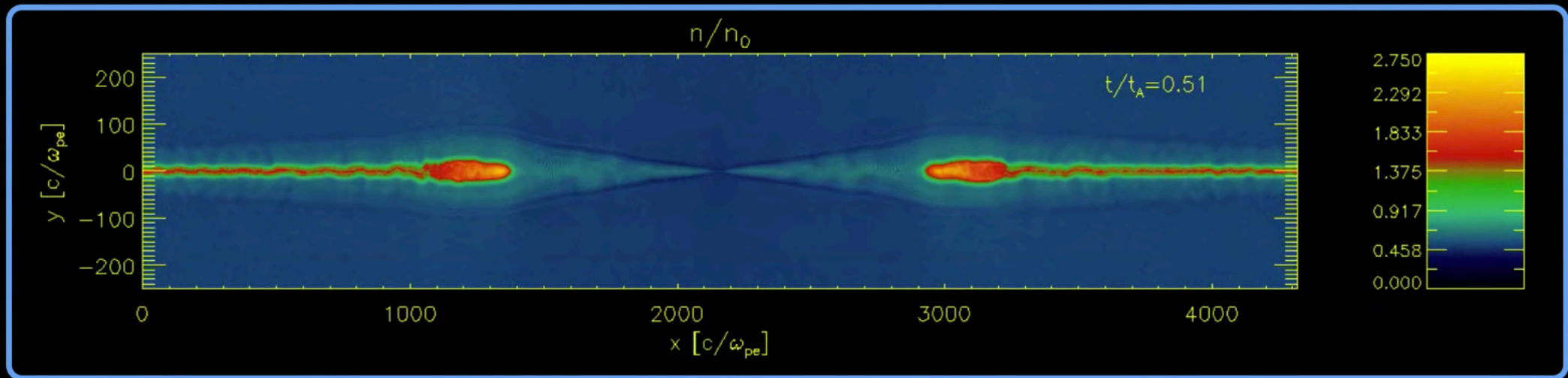
Simulation parameters: $\beta_i = 2$, $\sigma_w = 0.1$, $T_e/T_i = 0.1$, $N_{ppc} = 64$



- No secondary islands
- Outflow is more homogeneous than in low- β_i case
- Fractional increase of quantities in reconnection exhaust is less than at low- β_i (e.g. electron and ion temperatures, density)

High- β_i , antiparallel reconnection ($b_g = 0$)

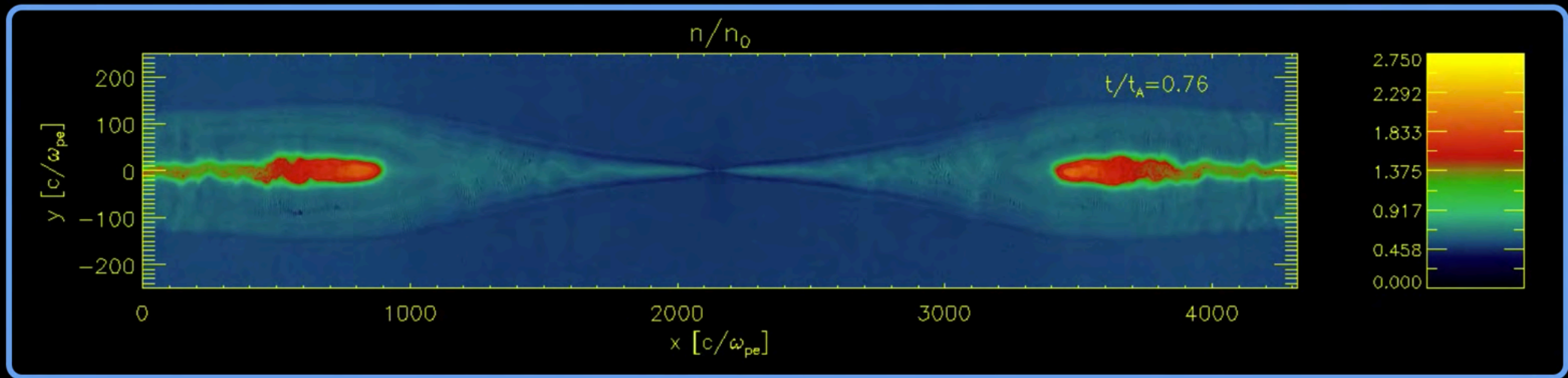
Simulation parameters: $\beta_i = 2$, $\sigma_w = 0.1$, $T_e/T_i = 0.1$, $N_{ppc} = 64$



- No secondary islands
- Outflow is more homogeneous than in low- β_i case
- Fractional increase of quantities in reconnection exhaust is less than at low- β_i (e.g. electron and ion temperatures, density)

High- β_i , antiparallel reconnection ($b_g = 0$)

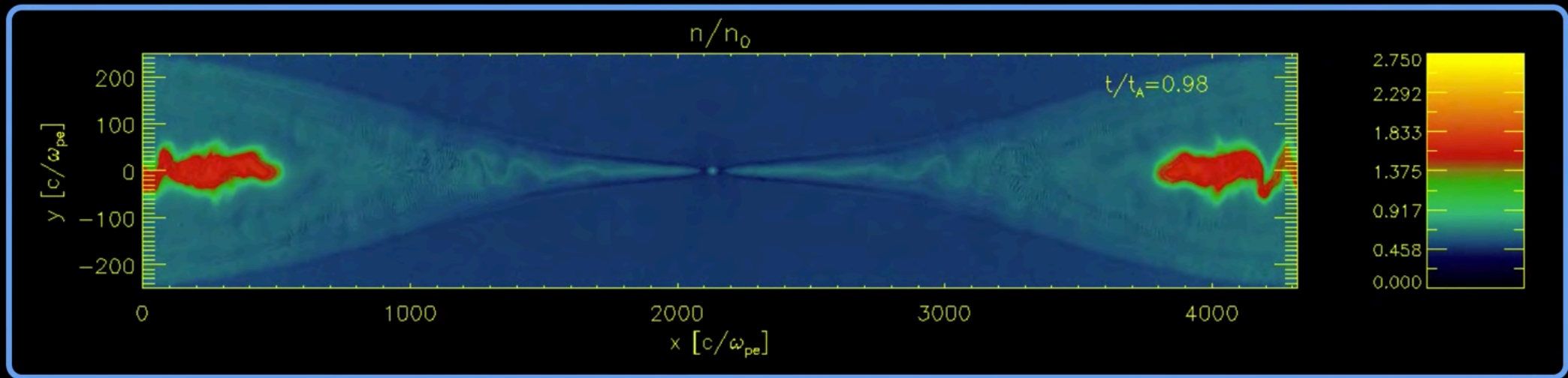
Simulation parameters: $\beta_i = 2$, $\sigma_w = 0.1$, $T_e/T_i = 0.1$, $N_{ppc} = 64$



- No secondary islands
- Outflow is more homogeneous than in low- β_i case
- Fractional increase of quantities in reconnection exhaust is less than at low- β_i (e.g. electron and ion temperatures, density)

High- β_i , antiparallel reconnection ($b_g = 0$)

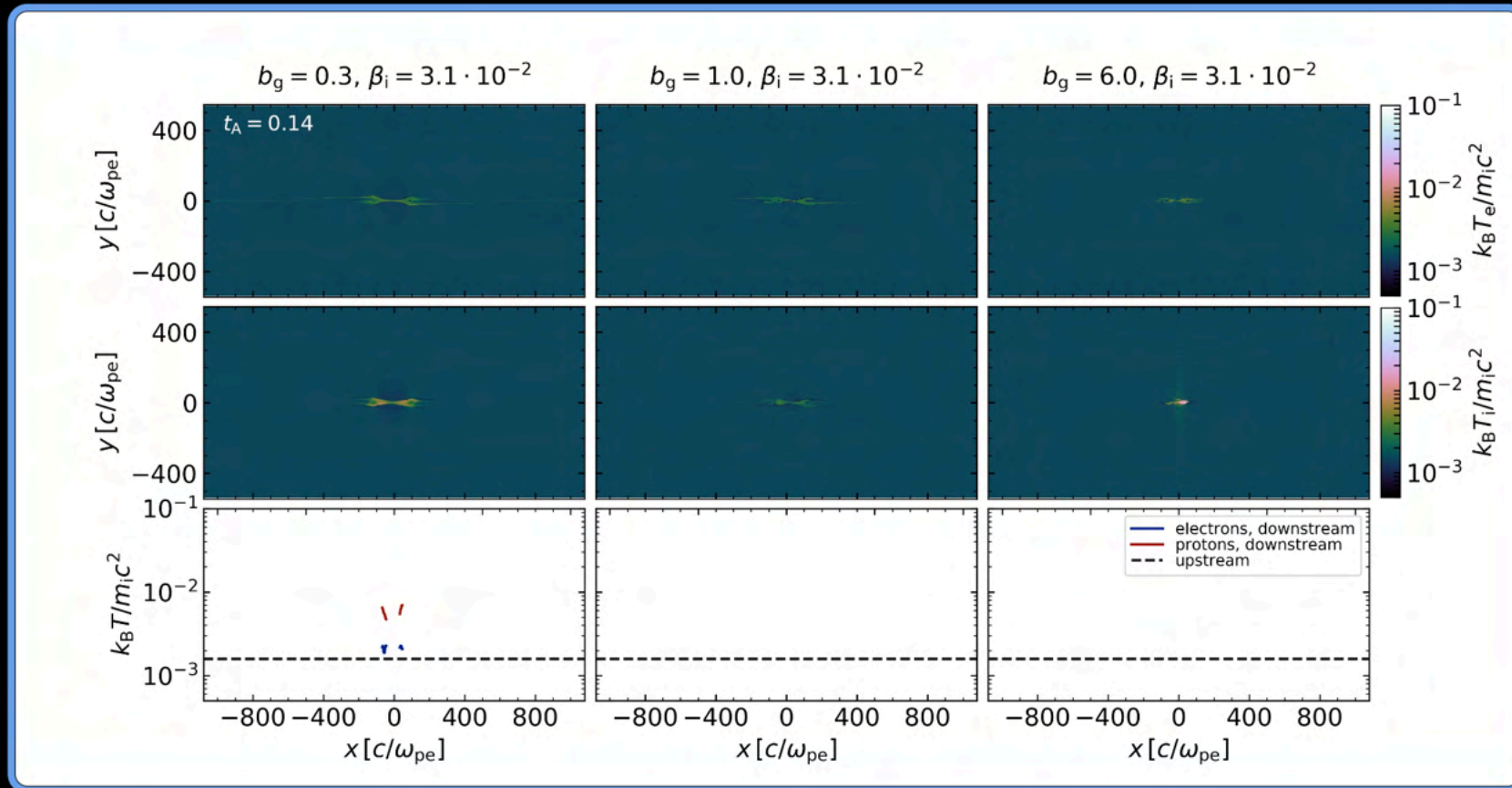
Simulation parameters: $\beta_i = 2$, $\sigma_w = 0.1$, $T_e/T_i = 0.1$, $N_{ppc} = 64$



- No secondary islands
- Outflow is more homogeneous than in low- β_i case
- Fractional increase of quantities in reconnection exhaust is less than at low- β_i (e.g. electron and ion temperatures, density)

Low- β_i , guide field dependence

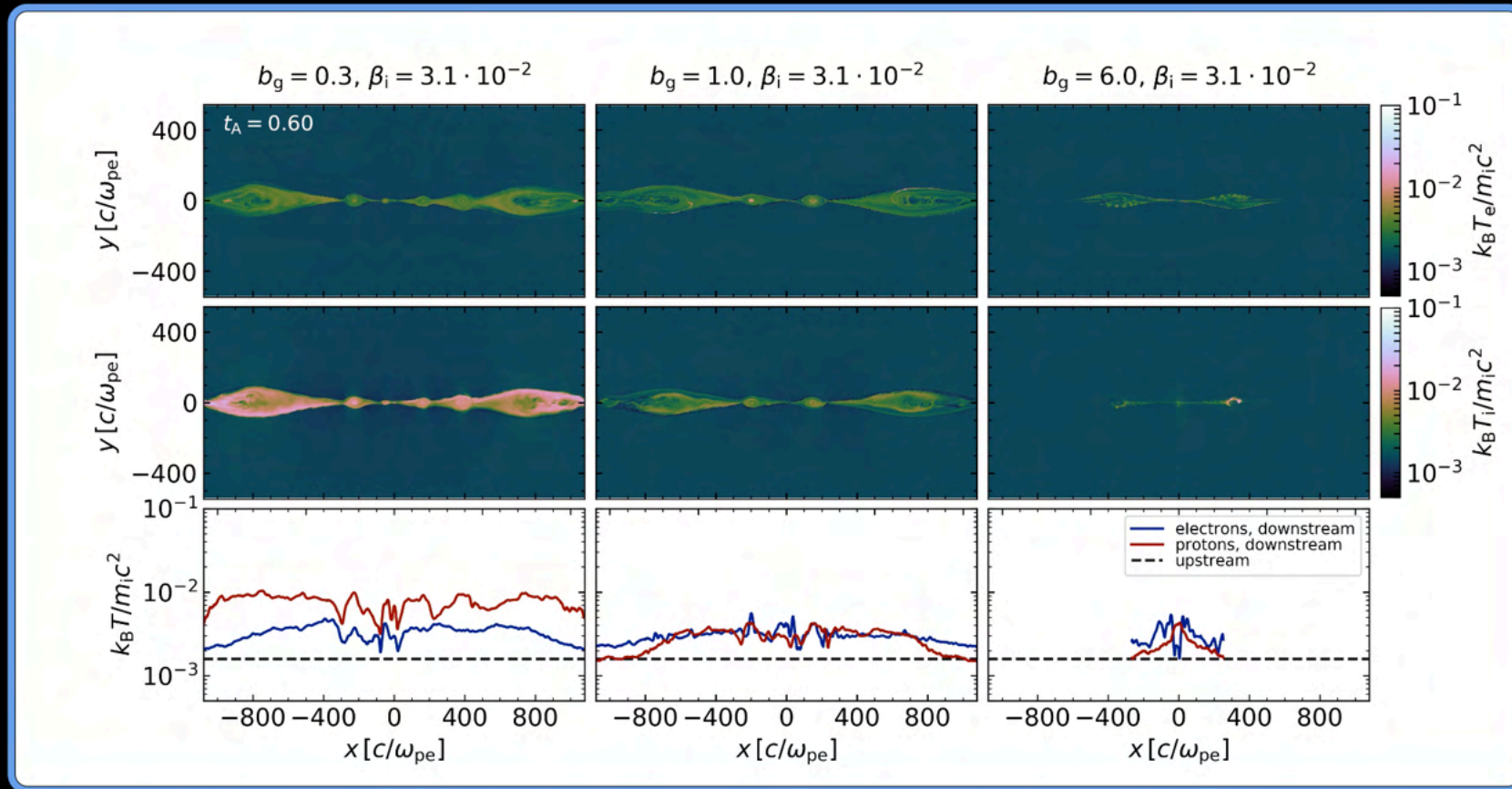
Simulation parameters: $\beta_i = 0.03$, $\sigma_w = 0.1$, $b_g = 0.3, 1, 6$



Guide field radically shifts energy partition between electrons and protons; electrons heated more than protons at high- b_g

Low- β_i , guide field dependence

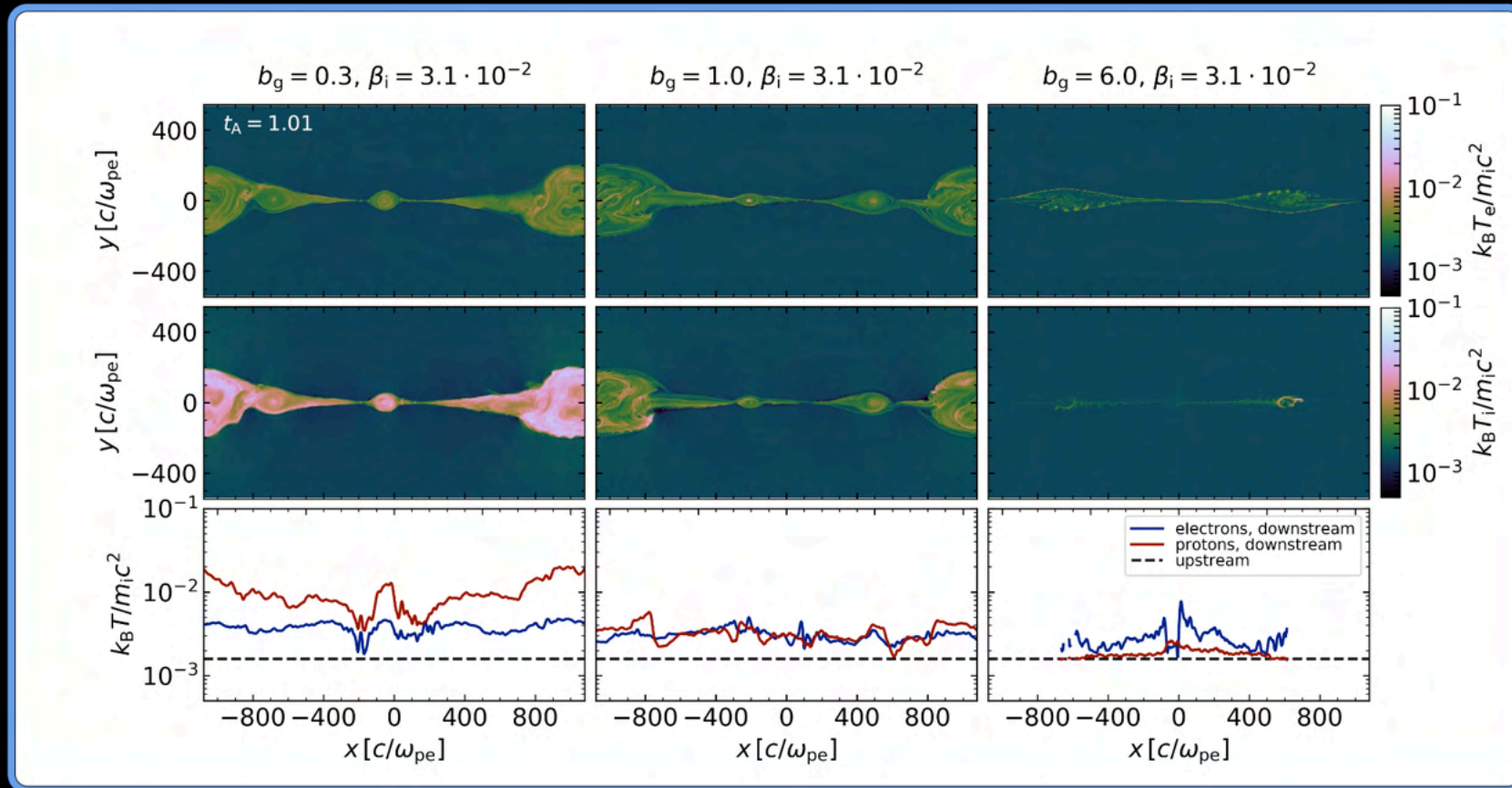
Simulation parameters: $\beta_i = 0.03$, $\sigma_w = 0.1$, $b_g = 0.3, 1, 6$



Guide field radically shifts energy partition between electrons and protons; electrons heated more than protons at high- b_g

Low- β_i , guide field dependence

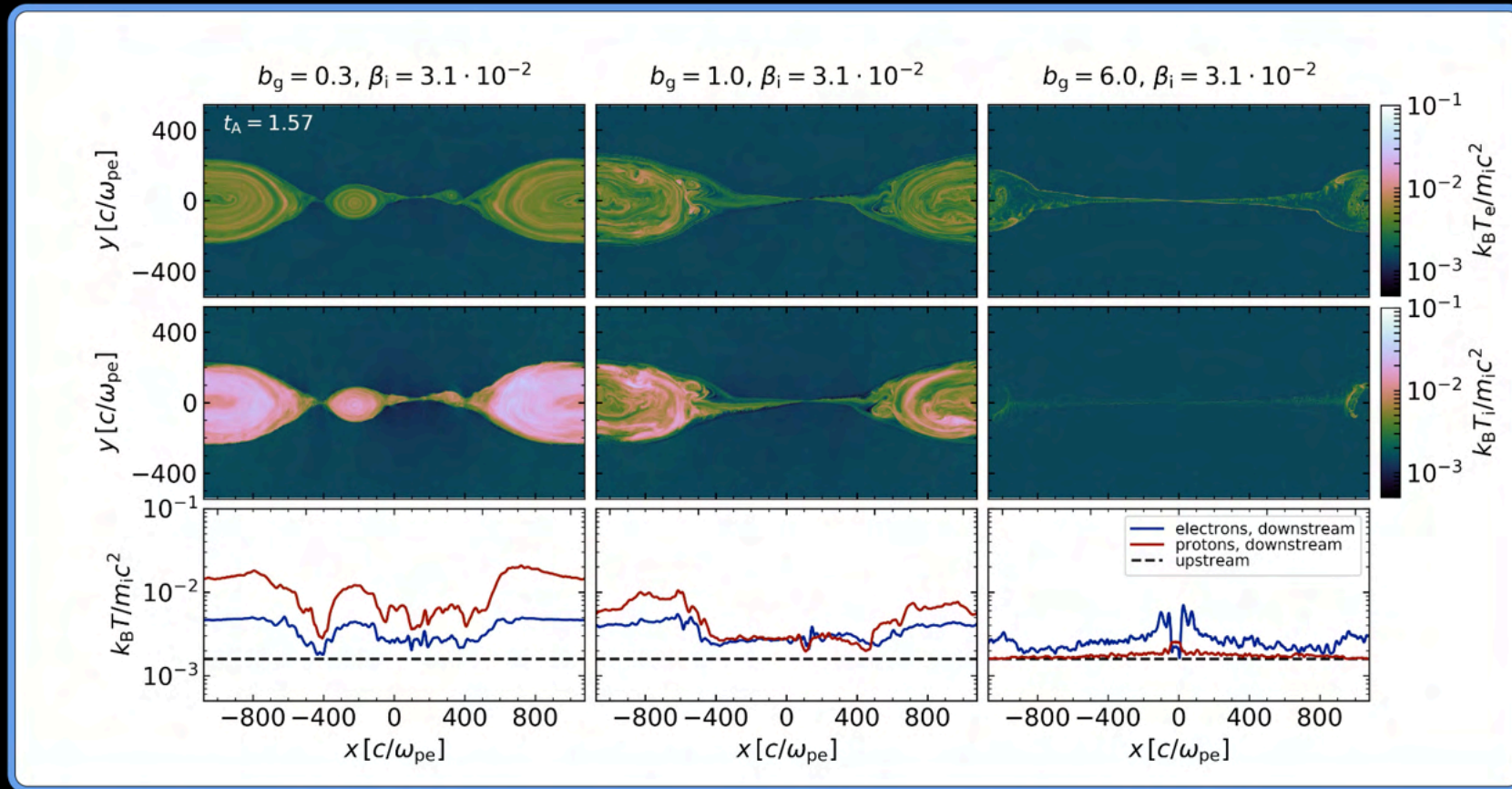
Simulation parameters: $\beta_i = 0.03$, $\sigma_w = 0.1$, $b_g = 0.3, 1, 6$



Guide field radically shifts energy partition between electrons and protons; electrons heated more than protons at high- b_g

Low- β_i , guide field dependence

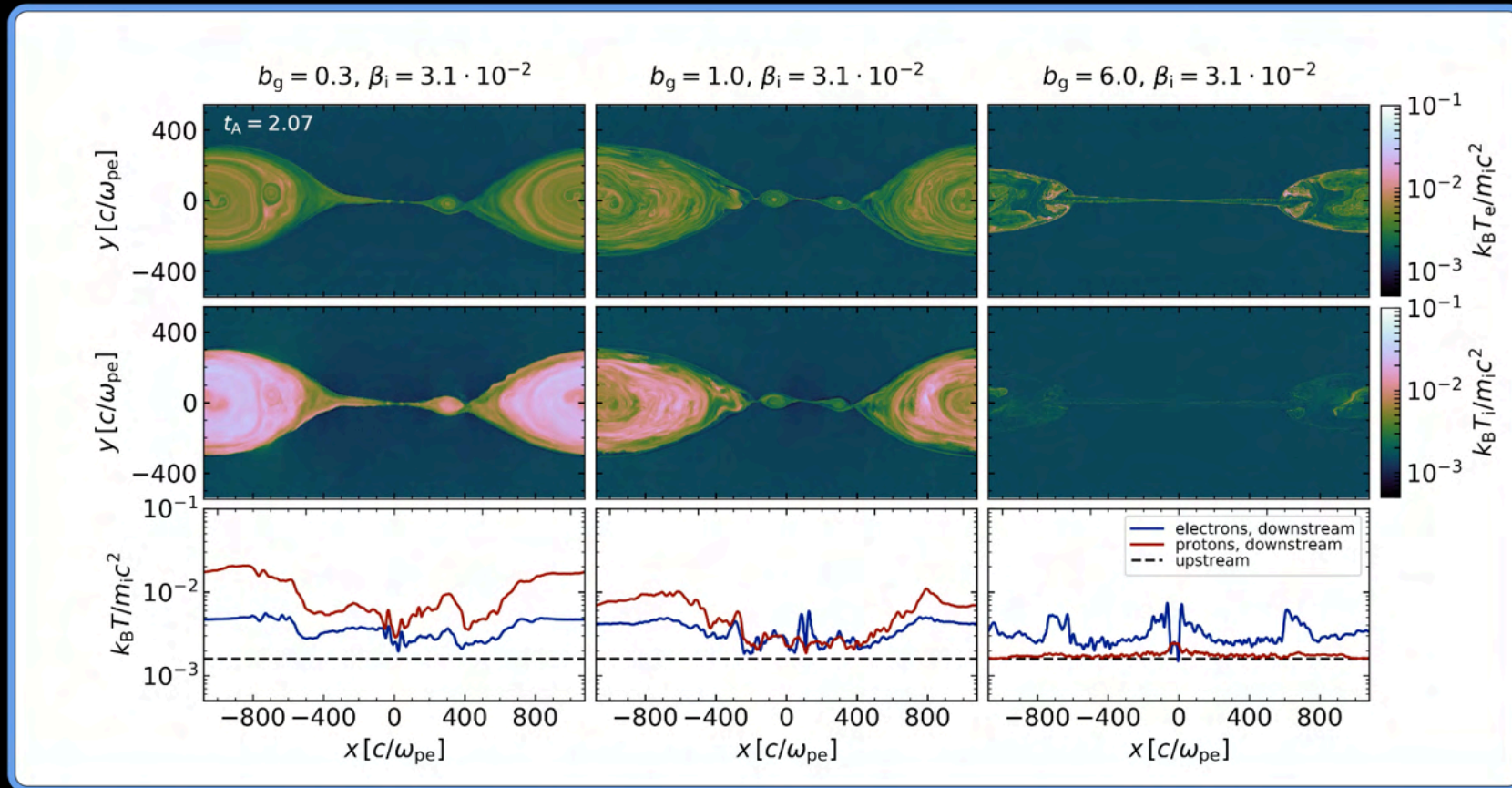
Simulation parameters: $\beta_i = 0.03$, $\sigma_w = 0.1$, $b_g = 0.3, 1, 6$



Guide field radically shifts energy partition between electrons and protons; electrons heated more than protons at high- b_g

Low- β_i , guide field dependence

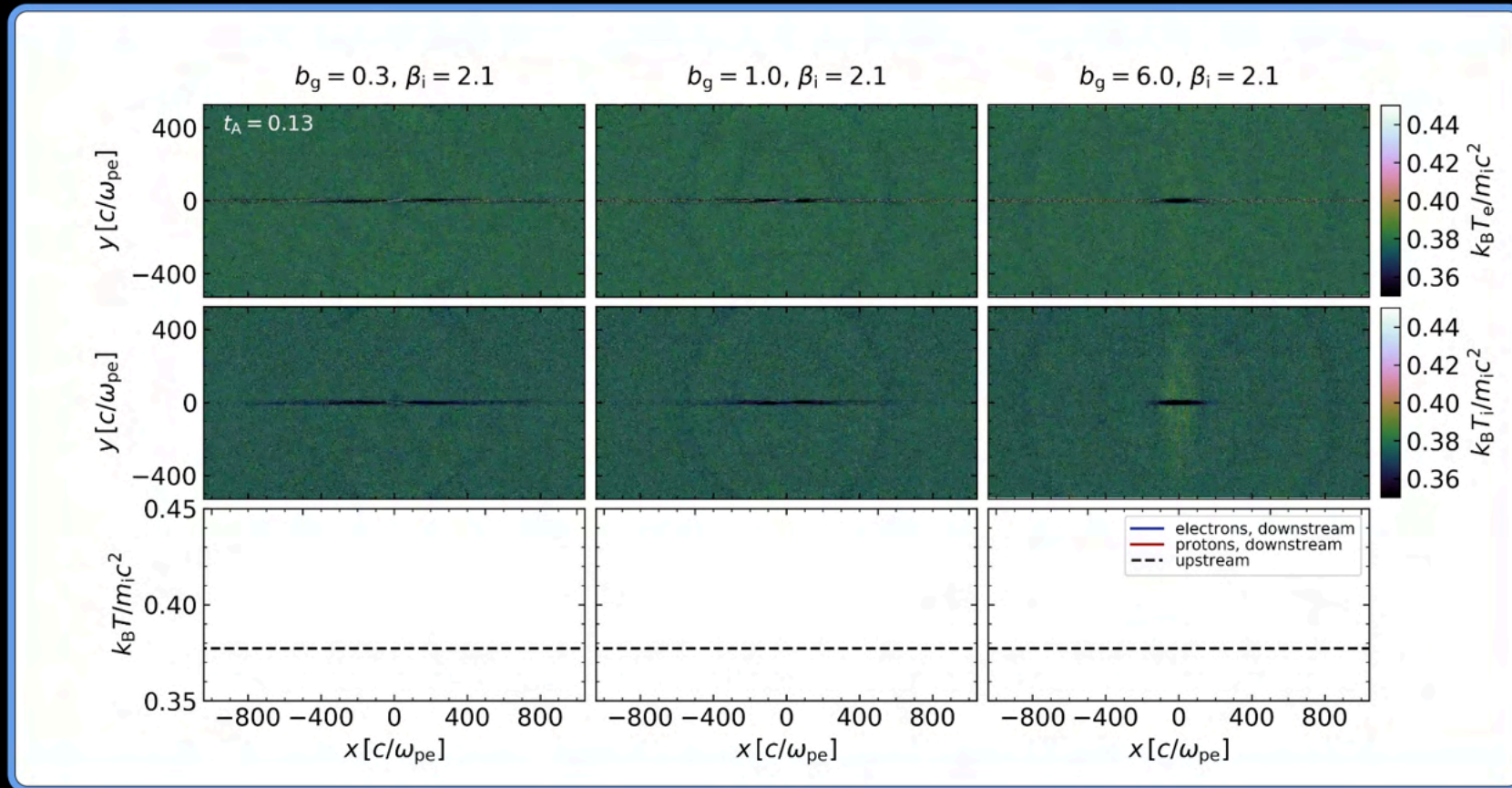
Simulation parameters: $\beta_i = 0.03$, $\sigma_w = 0.1$, $b_g = 0.3, 1, 6$



Guide field radically shifts energy partition between electrons and protons; electrons heated more than protons at high- b_g

High- β_i , guide field dependence

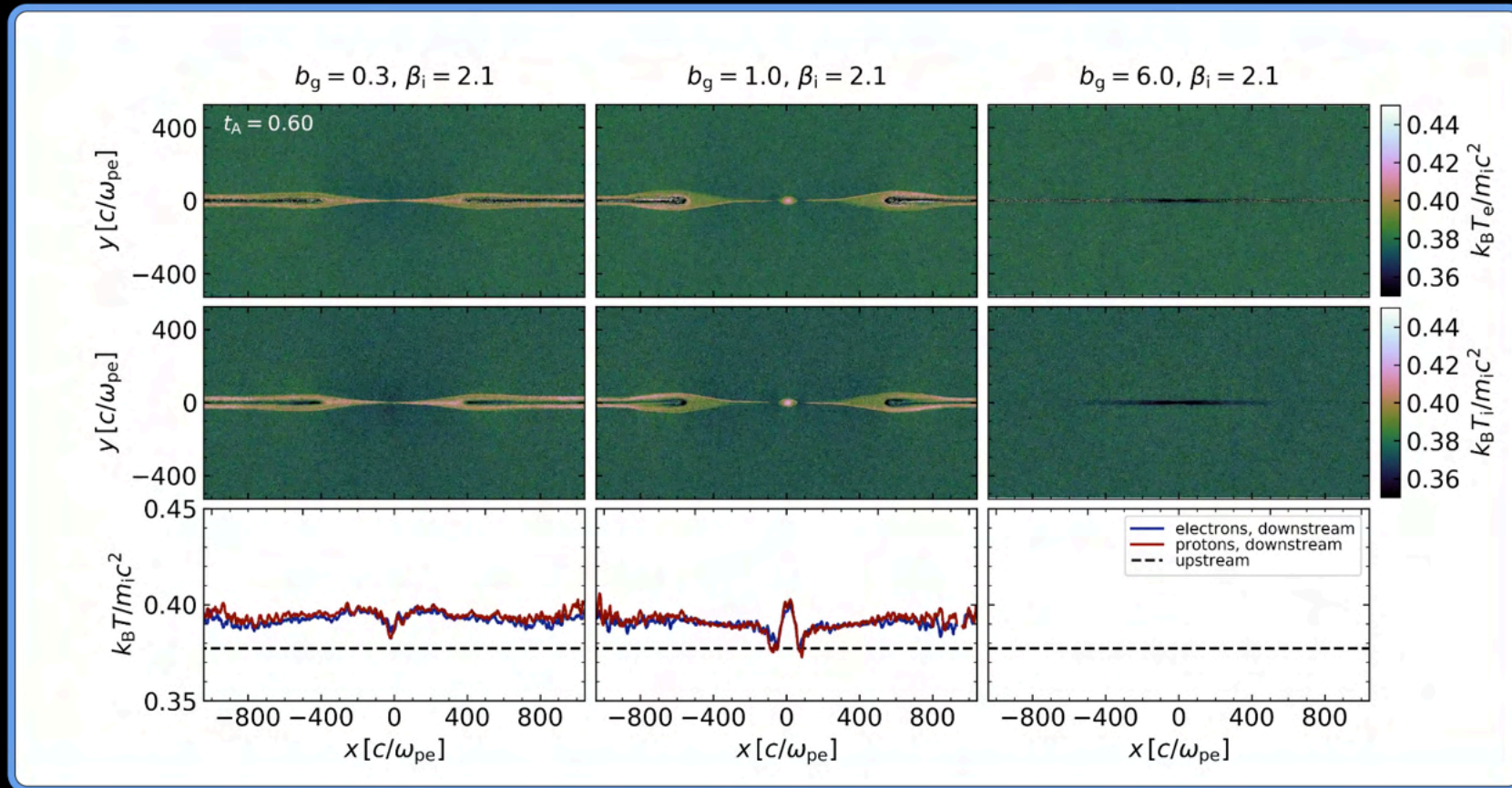
Simulation params: $\beta_i = 2$, $\sigma_w = 0.1$, $b_g = 0.3, 1, 6$, $N_{ppc} = 64$



At high- β_i , electrons and protons are generally in equipartition, but guide field tends to suppress overall amount of heating

High- β_i , guide field dependence

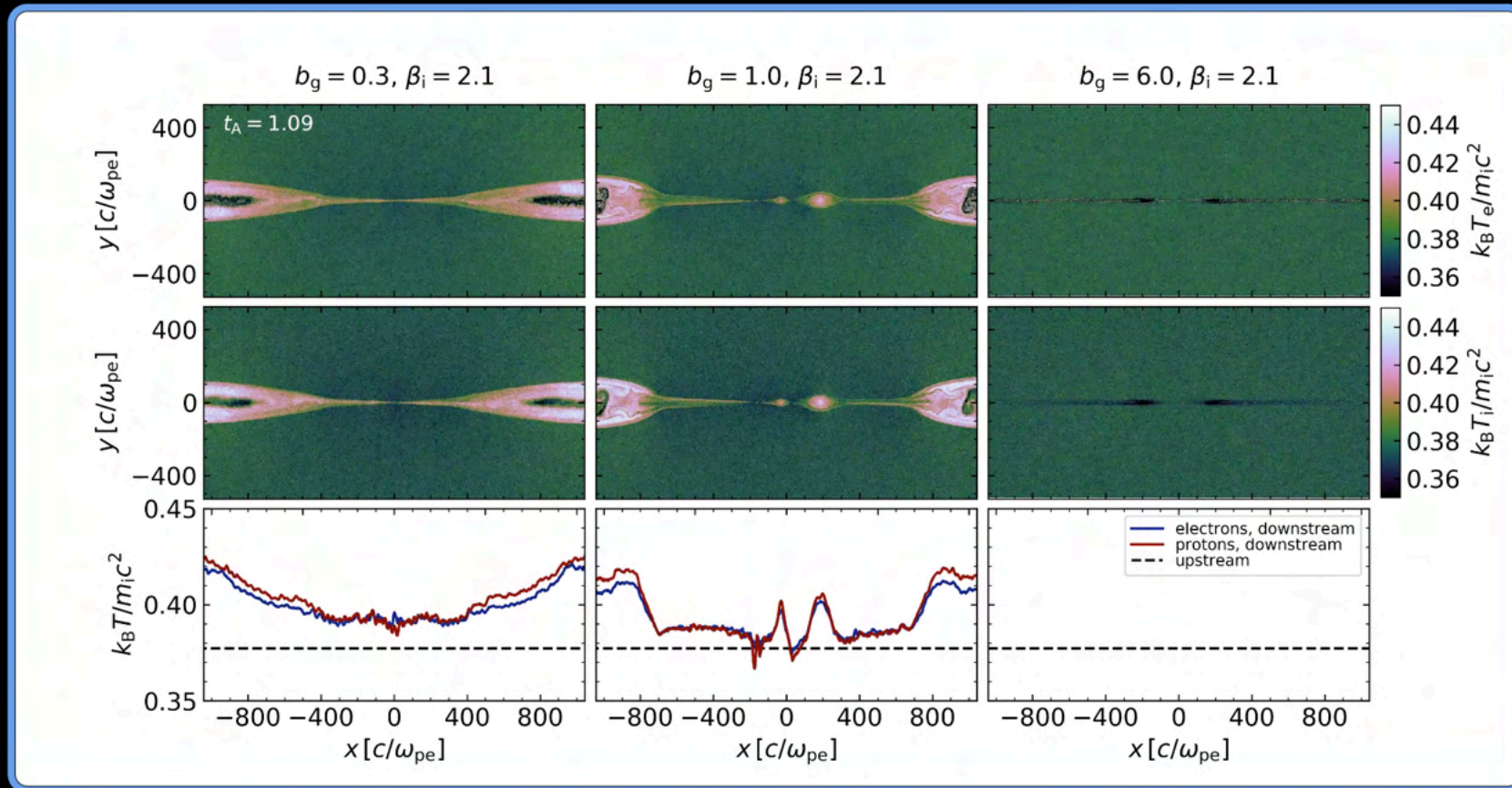
Simulation params: $\beta_i = 2$, $\sigma_w = 0.1$, $b_g = 0.3, 1, 6$, $N_{ppc} = 64$



At high- β_i , electrons and protons are generally in equipartition, but guide field tends to suppress overall amount of heating

High- β_i , guide field dependence

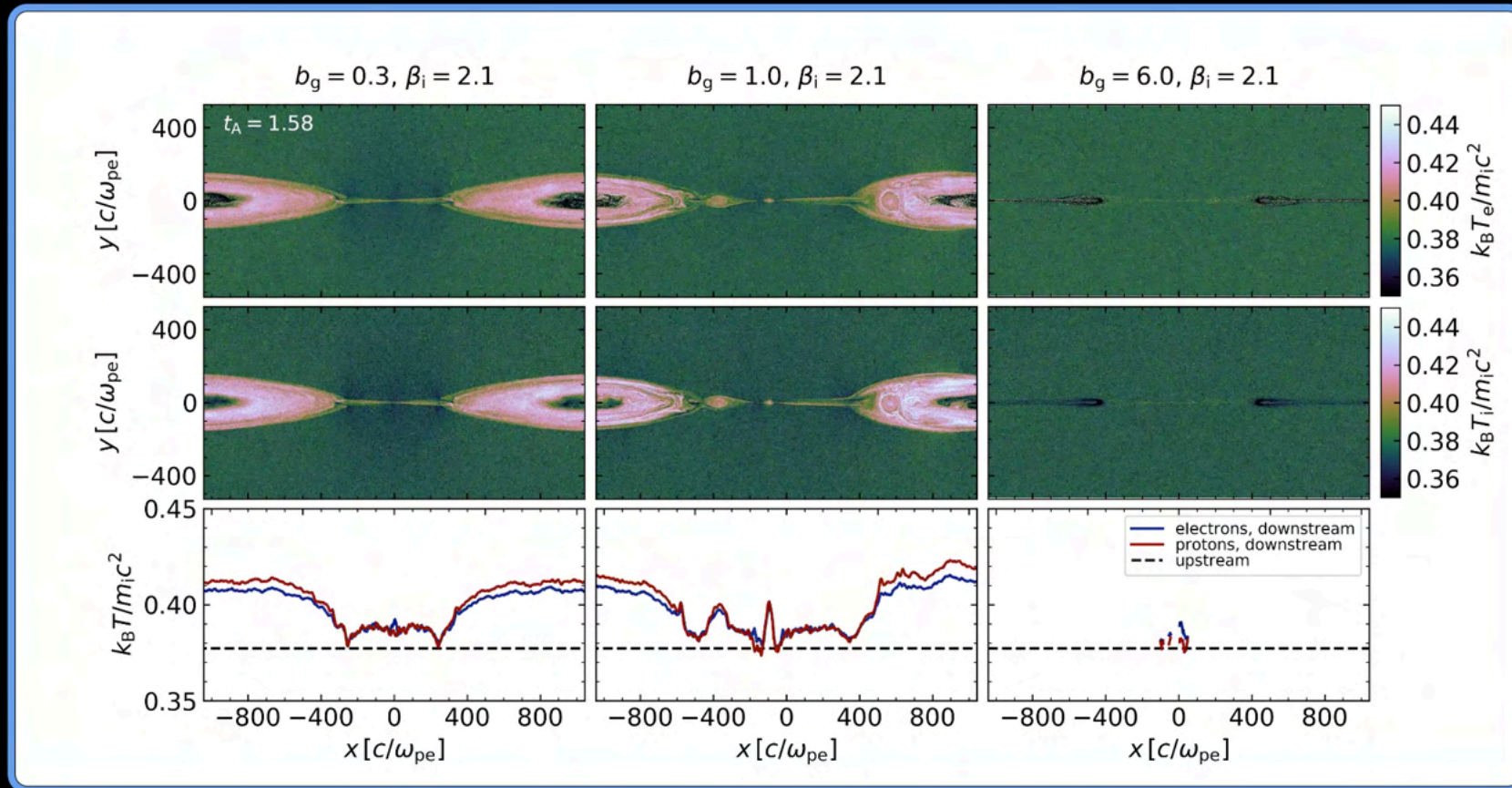
Simulation params: $\beta_i = 2$, $\sigma_w = 0.1$, $b_g = 0.3, 1, 6$, $N_{ppc} = 64$



At high- β_i , electrons and protons are generally in equipartition, but guide field tends to suppress overall amount of heating

High- β_i , guide field dependence

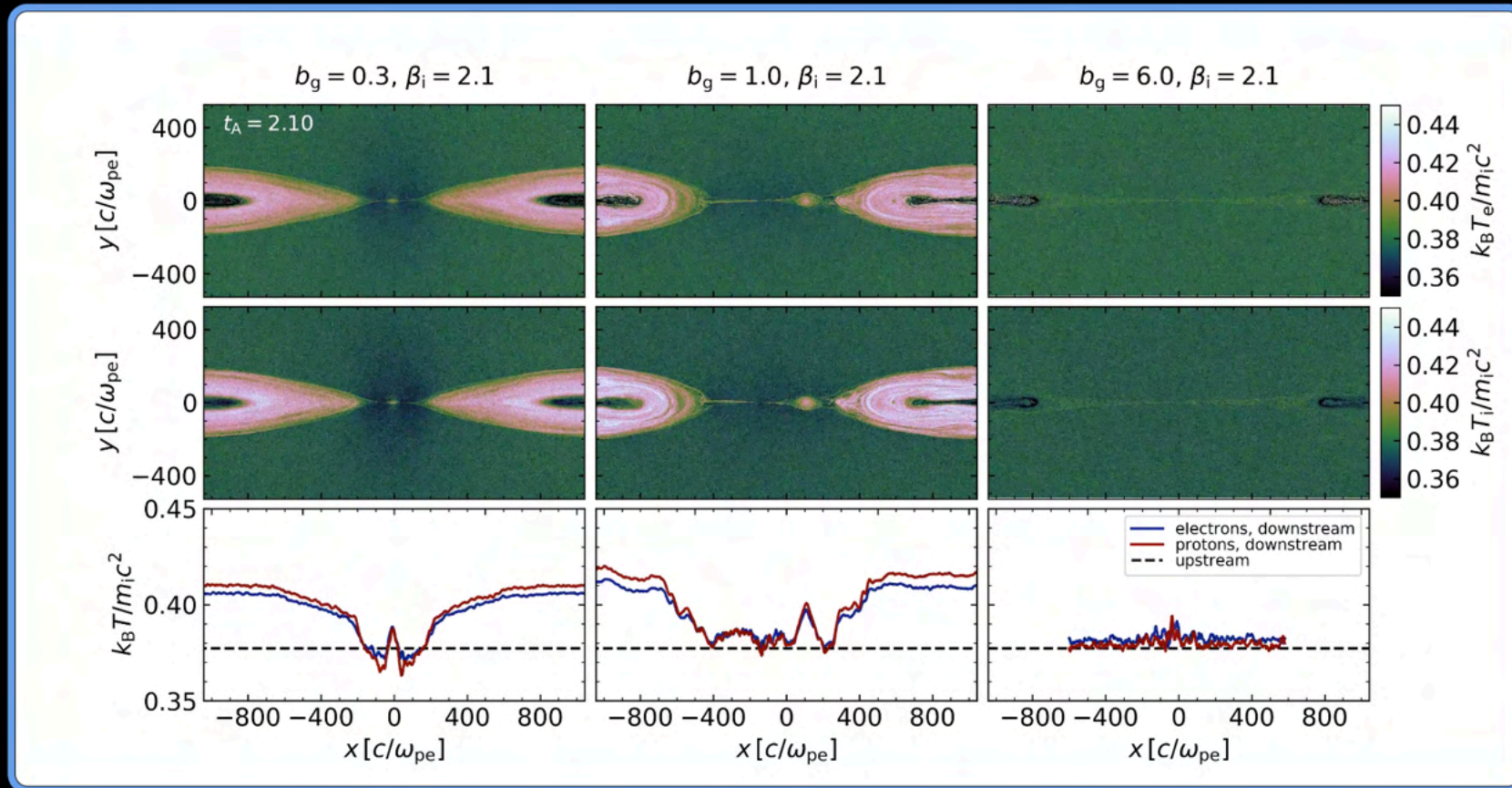
Simulation params: $\beta_i = 2$, $\sigma_w = 0.1$, $b_g = 0.3, 1, 6$, $N_{ppc} = 64$



At high- β_i , electrons and protons are generally in equipartition, but guide field tends to suppress overall amount of heating

High- β_i , guide field dependence

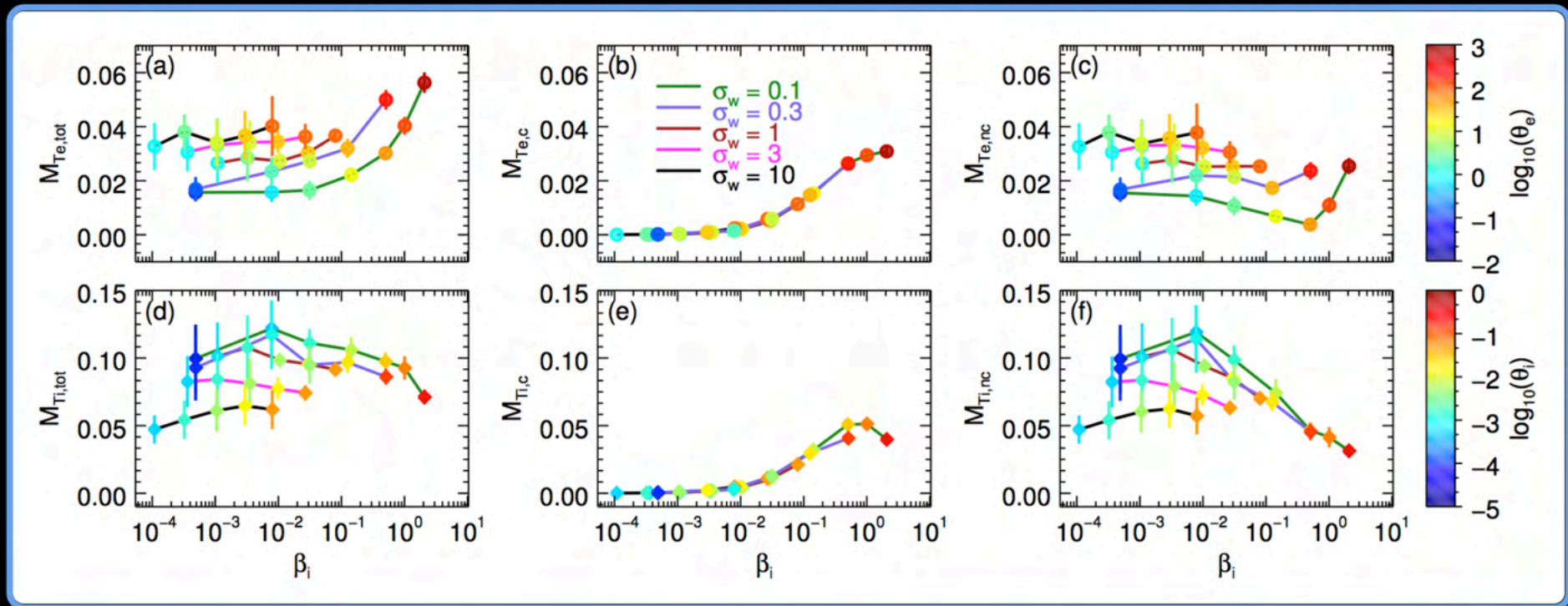
Simulation params: $\beta_i = 2$, $\sigma_w = 0.1$, $b_g = 0.3, 1, 6$, $N_{ppc} = 64$



At high- β_i , electrons and protons are generally in equipartition, but guide field tends to suppress overall amount of heating

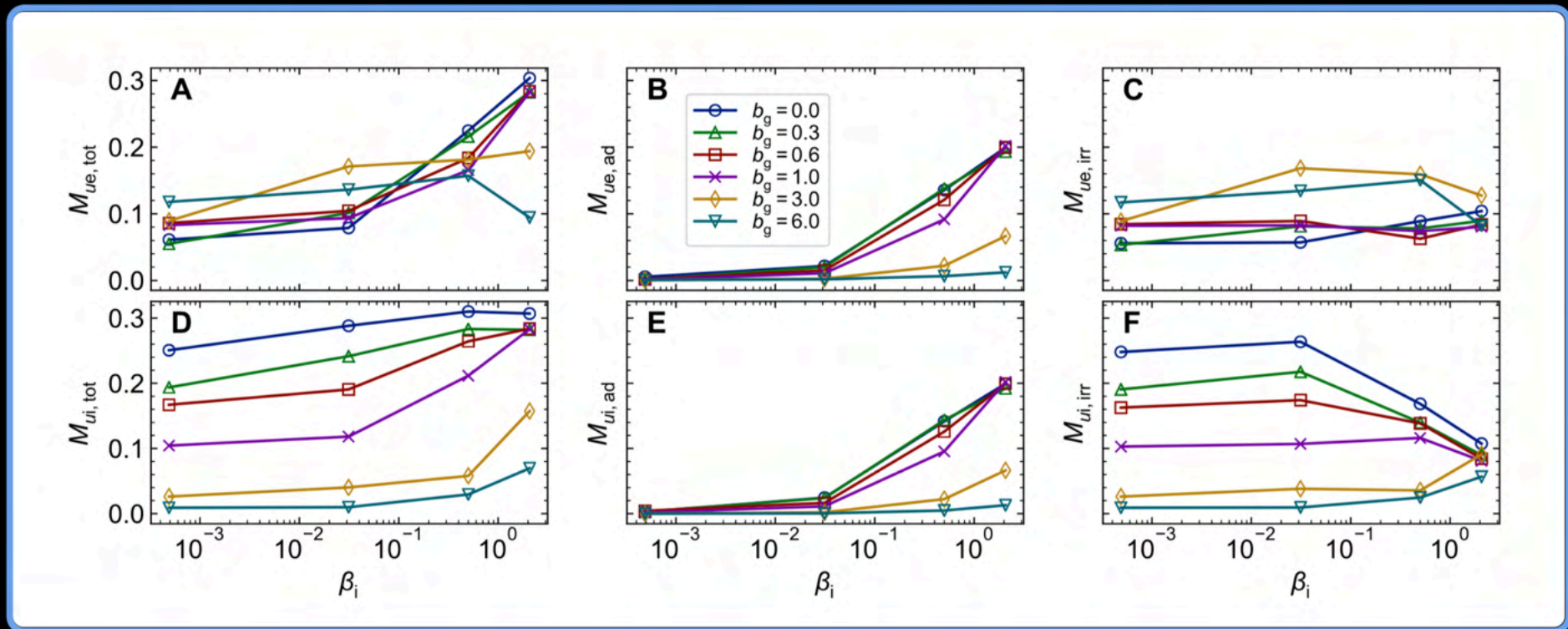
Results I(a): transrel. heating, no guide field

- Increasing magnetization at fixed β_i : plasma is more relativistic
- Seems to hasten onset of transition to rel. regime
- Decreasing elec., prot. scale-separation \Rightarrow energy equipartition



Results I(b): transrel. heating, guide field

- Electron irr. heating at low- β_i nearly independent of b_g
- For $\beta_i \sim \beta_{i,\max}$, both electron and proton irr. heating are nearly independent of b_g ; scale separation is about equal in this case



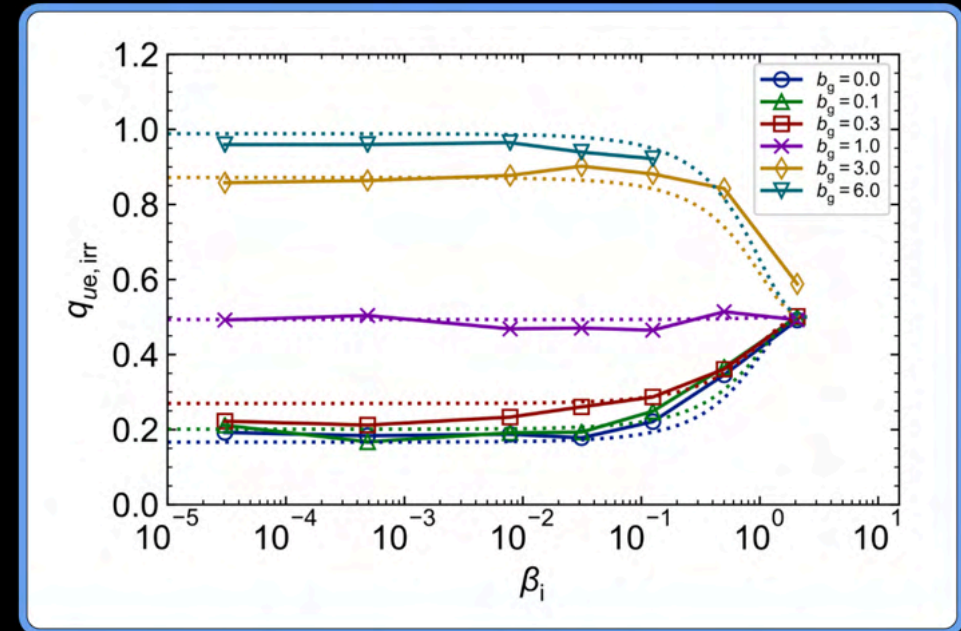
Results II(a): b_g -dependence of heating

Elec. irr. heating fraction:

$$q_{ue,irr} = \frac{M_{ue,irr}}{M_{ue,irr} + M_{ui,irr}}$$

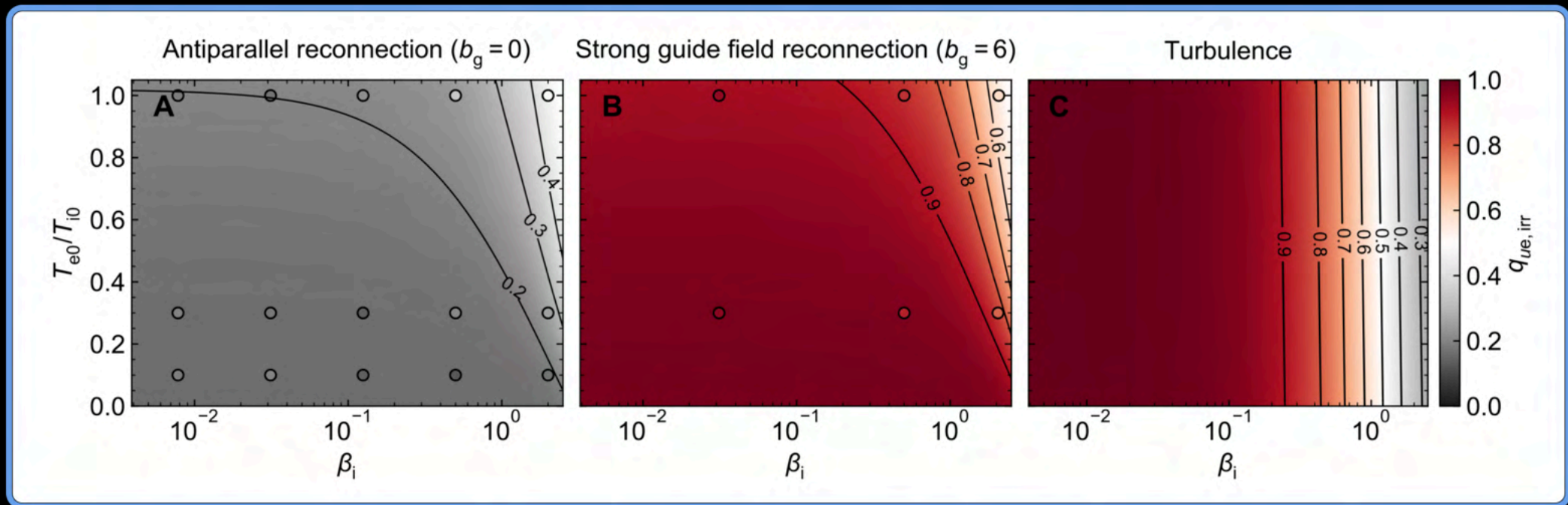
Fitting function provides dep. of elec. irr. heating on plasma parameters:

$$q_{ue,irr,fit}(\beta_i, b_g, T_e/T_i, \sigma_w) = \frac{1}{2}(\tanh(0.33b_g) - 0.4) \times 1.7 \tanh\left(\frac{(1 - \beta_i/\beta_{i,max})^{1.5}}{(0.42 + T_e/T_i)\sigma_w^{0.3}}\right) + \frac{1}{2}$$



Results II(b): b_g -dependence of heating

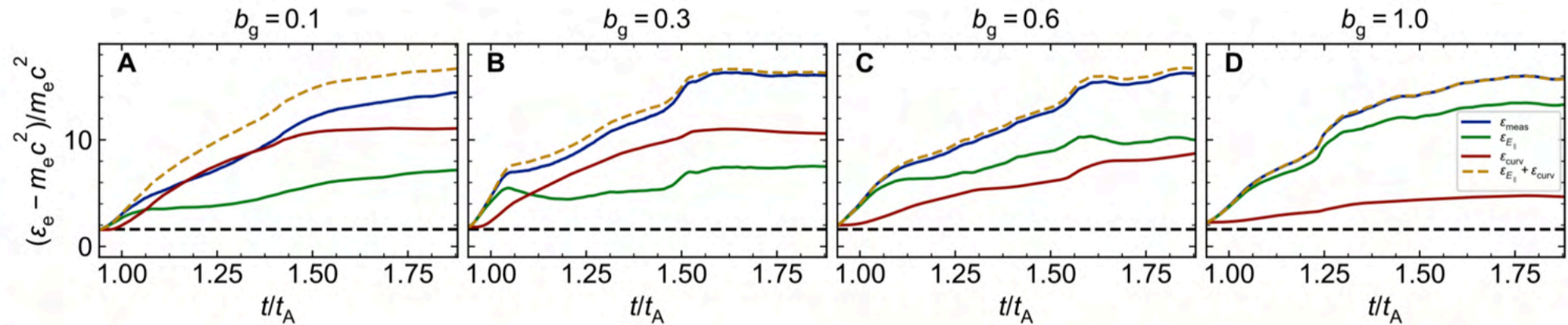
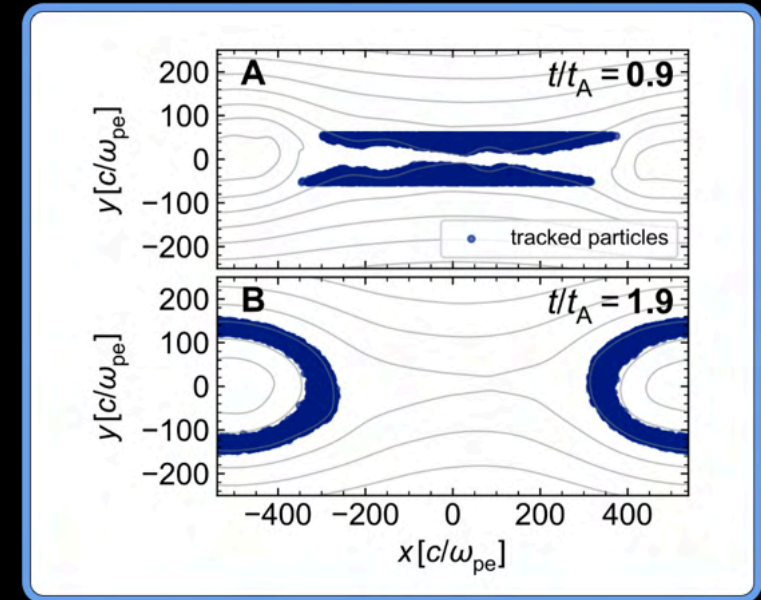
Particle heating in the presence of a guide field looks more similar to heating via turbulence; at small enough scales, turbulence is thought to be mediated by strong guide field reconnection



Results III(a): Guiding-center analysis

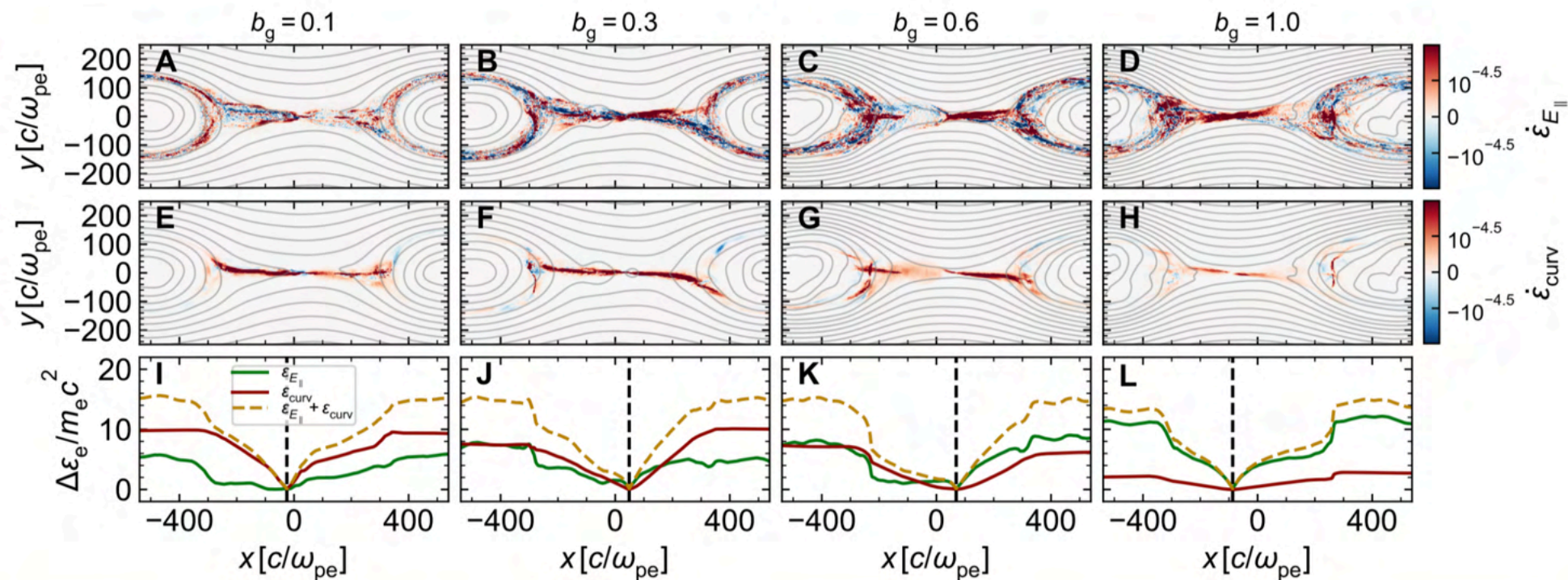
Track particles from upstream to downstream to assess relative importance of heating mechanisms

$$\frac{d\epsilon_e}{dt} = q\mathbf{E} \cdot (\mathbf{v}_{\parallel} + \mathbf{v}_c + \mathbf{v}_{\nabla B}) + \frac{\mu}{\gamma} \frac{\partial B}{\partial t}$$



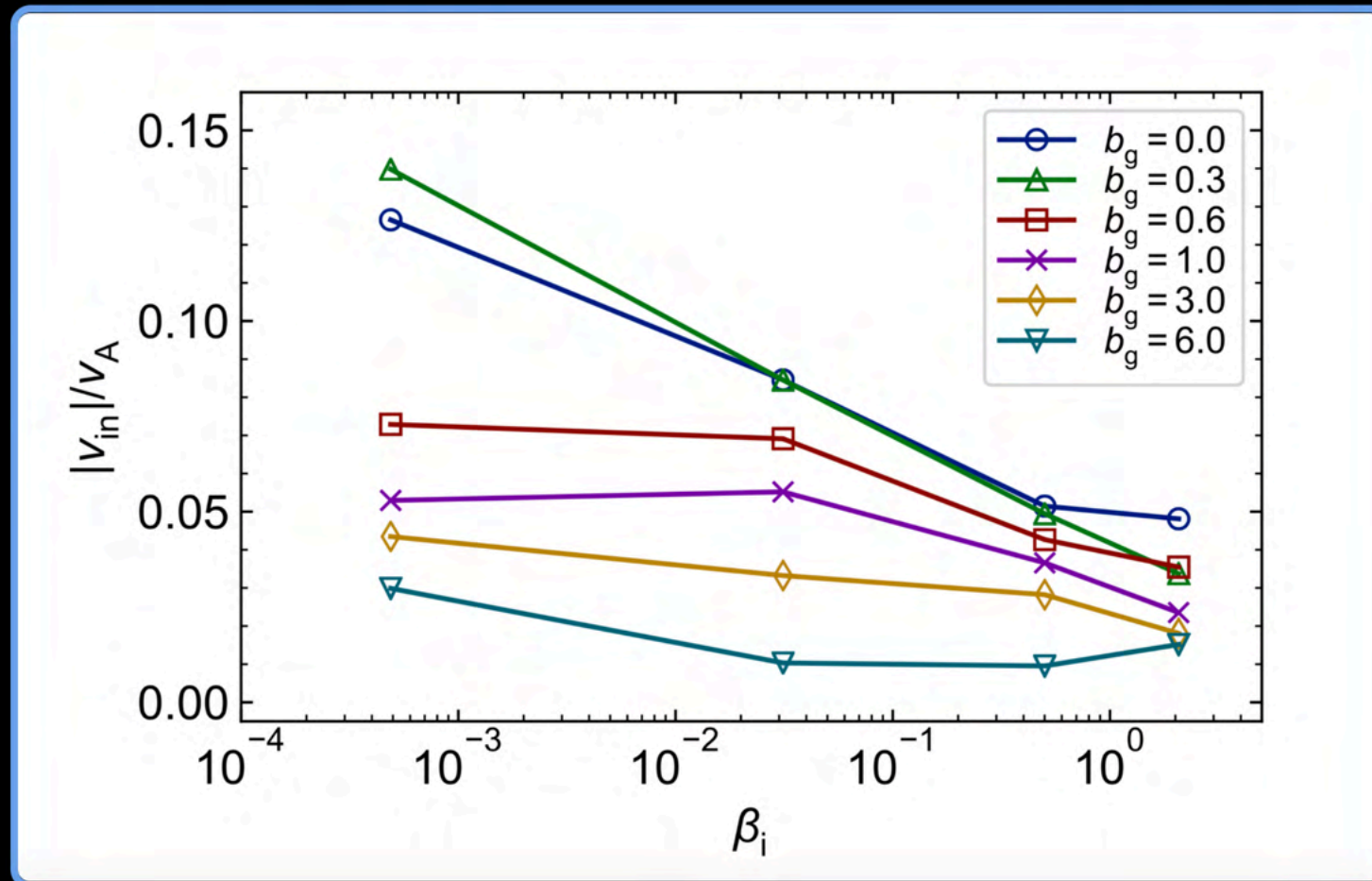
Results III(b): Guiding-center analysis

Curvature heating tends to dominate for weak guide field, whereas E -parallel dominates for strong guide field (in this case, the magnetic field is almost straight in the out-of-plane direction)



Results IV: b_g -dependence of rec. rate

Guide field suppresses reconnection rate, more variation at low- β_i



Outline

- Introduction
- Magnetic reconnection
- Kelvin-Helmholtz instability

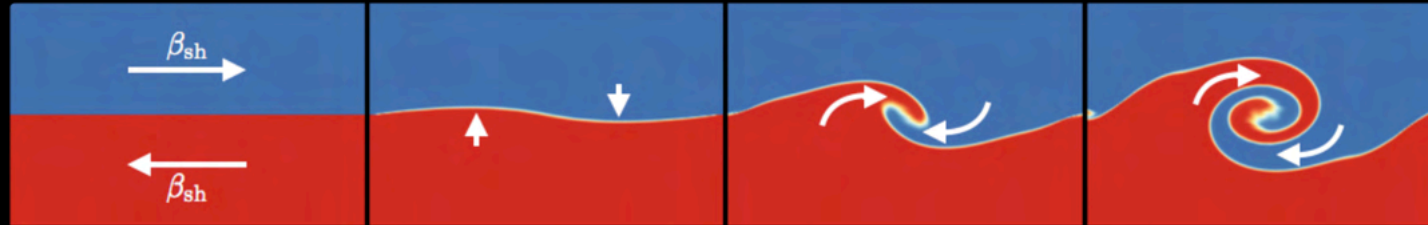
Kelvin-Helmholtz instability occurs all over

KH instability is ubiquitous in nature; here, KH forms in clouds:



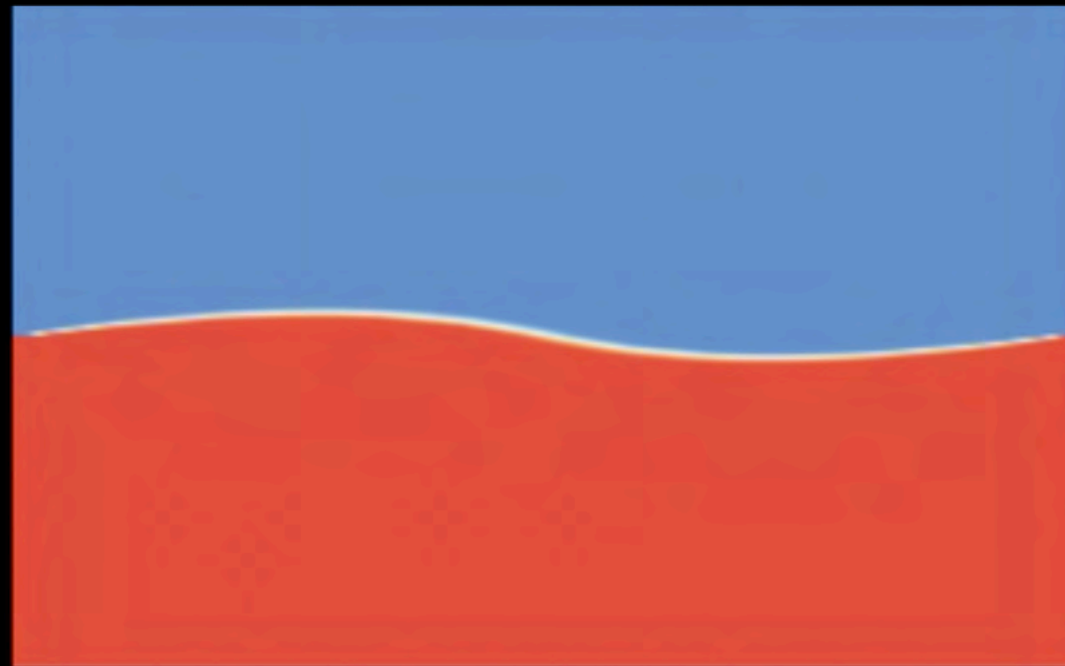
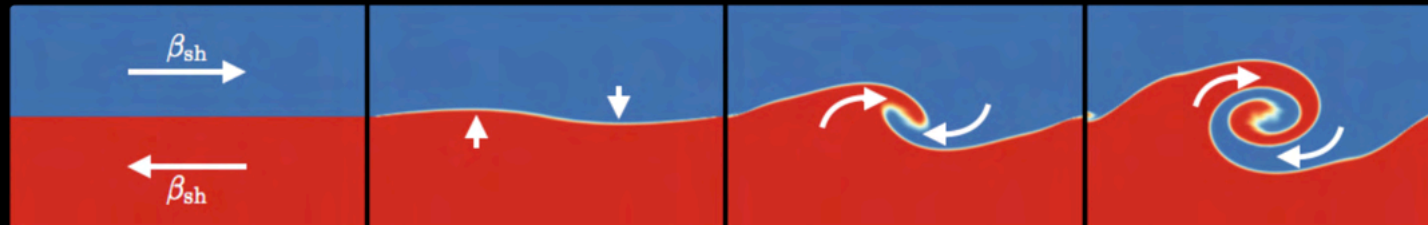
How does the KH instability grow?

Velocity perturbation \perp to shear velocity β_{sh} \rightarrow unstable growth



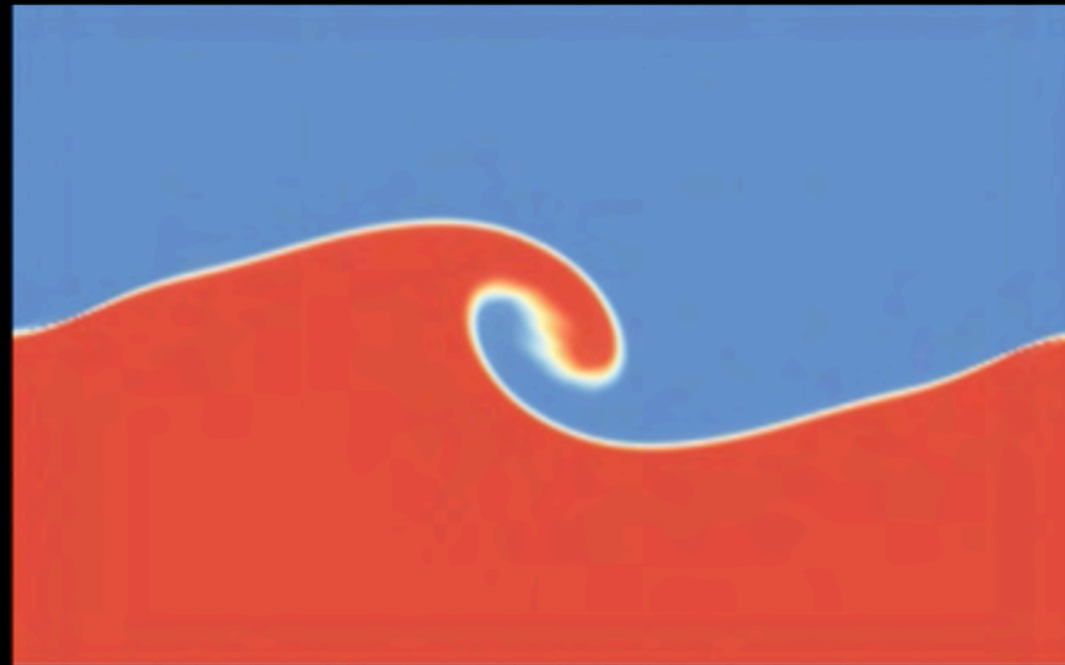
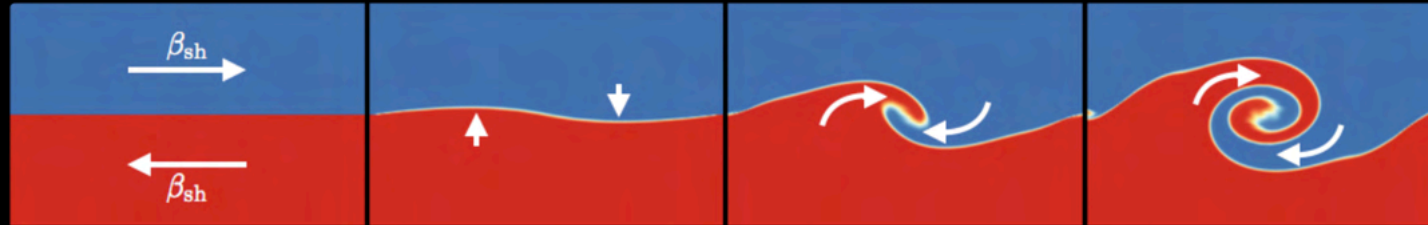
How does the KH instability grow?

Velocity perturbation \perp to shear velocity β_{sh} \rightarrow unstable growth



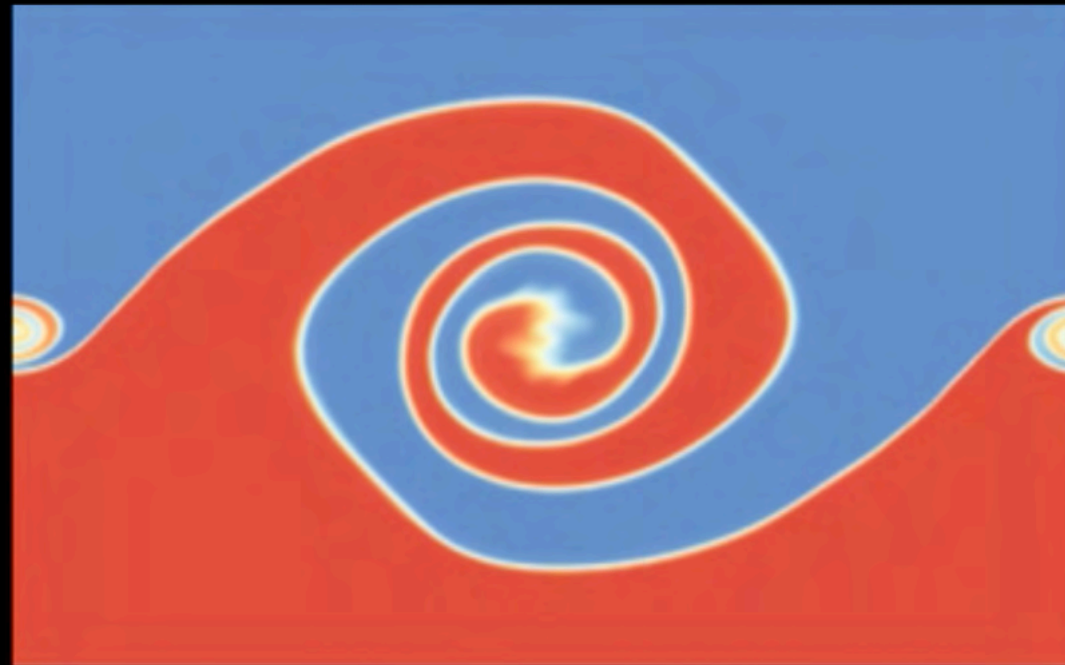
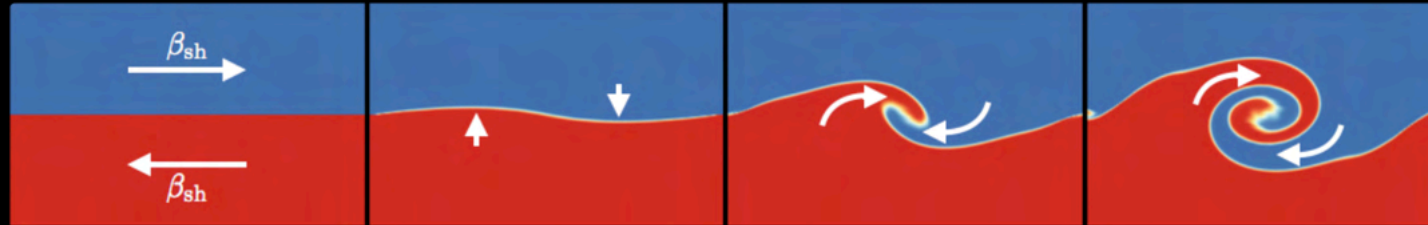
How does the KH instability grow?

Velocity perturbation \perp to shear velocity β_{sh} \rightarrow unstable growth



How does the KH instability grow?

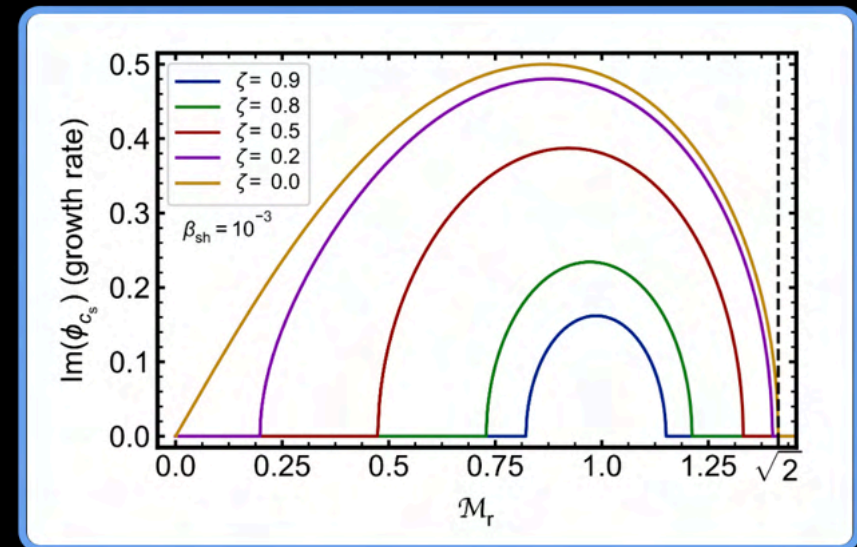
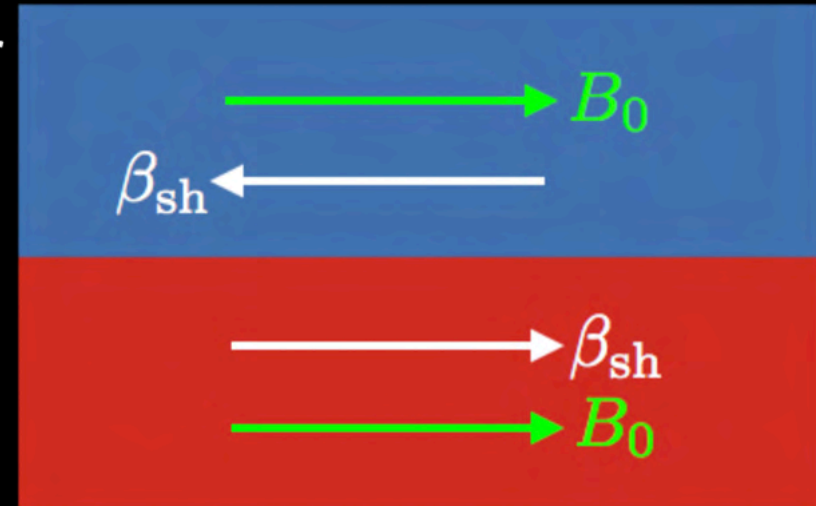
Velocity perturbation \perp to shear velocity β_{sh} \rightarrow unstable growth



Physics of the KH instability

In addition to shear velocity β_{sh} , consider a magnetic field B_0 that permeates the plasma

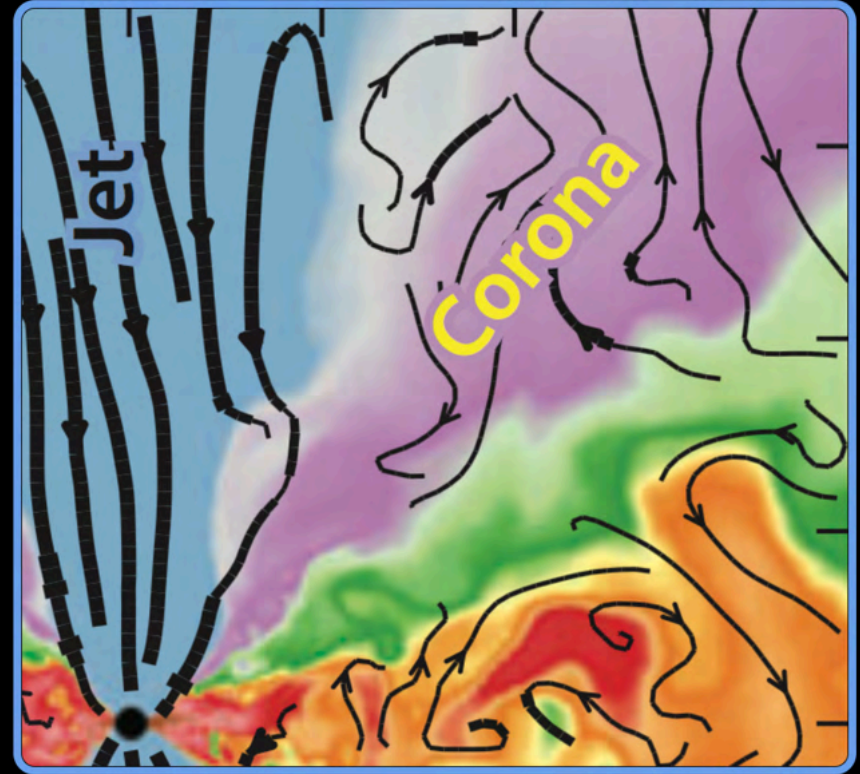
- If the magnetic field is too strong, magnetic tension inhibits KH
- Parametrize relative strength of field by Alfvénic Mach number, $\zeta \equiv v_A/c_s$; $c_s = \sqrt{\Gamma_{\text{ad}}\theta/h}$ is the sound speed, h is specific enthalpy
- Instability must also respect the subsonic bound $\mathcal{M} \leq \sqrt{2}$
- $\mathcal{M} \equiv \beta_{\text{sh}}/c_s$ is the Mach number



KH instability in astrophysical jets

A number of simulations suggest evidence for KH instability at the interface of the jet and wind/corona, which motivates a KH setup with:

- Strongly magnetized jet
- Weakly magnetized wind
- Somewhat relativistic shear flow
- KH-induced reconnection?



Addressing the question of magnetic dissipation via magnetic reconnection requires fully-kinetic PIC simulation

Predicted growth rate of KH instability

Three-pronged attack to studying KH-induced reconnection:

- What physical parameters lead to KH unstable growth?
- Does PIC capture the predicted growth rate?
- Does PIC show evidence of magnetic dissipation?

To answer the first point, solve relativistic magnetohydrodynamic (RMHD) dispersion relation (i.e., polynomial in ϕ_{v_A}) of the form:

$$F(\phi_{v_A}, \text{params}) = 0$$

$\phi_{v_A} \equiv \omega/(k_0 v_A)$ is the dimensionless growth rate of the mode

$$\text{Im}(\phi_{v_A}) > 0 \rightarrow \text{unstable growth}$$

Predicted growth rate of KH instability

Three-pronged attack to studying KH-induced reconnection:

- What physical parameters lead to KH unstable growth?
- Does PIC capture the predicted growth rate?
- Does PIC show evidence of magnetic dissipation?

To answer the first point, solve relativistic magnetohydrodynamic (RMHD) dispersion relation (i.e., polynomial in ϕ_{v_A}) of the form:

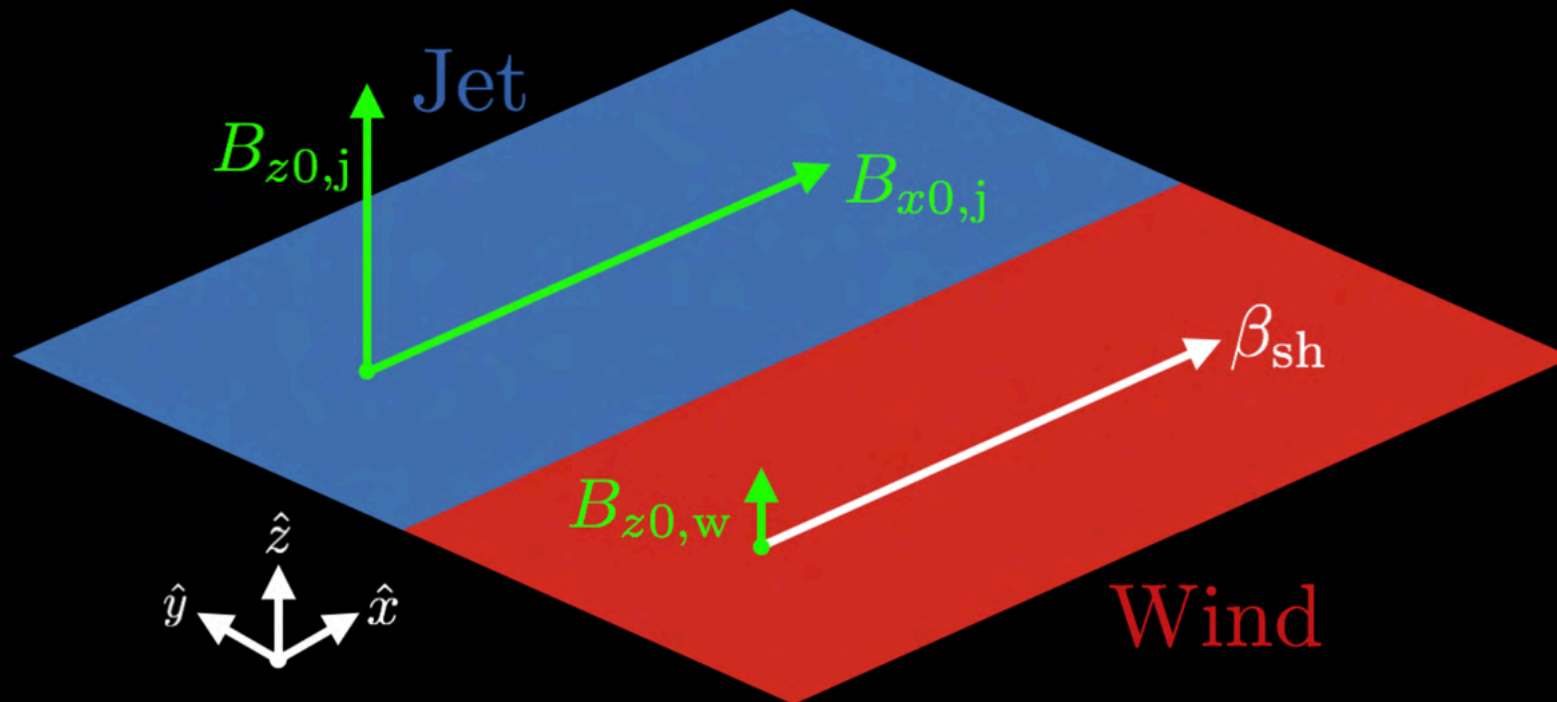
$$F(\phi_{v_A}, \text{params}) = 0$$

$\phi_{v_A} \equiv \omega/(k_0 v_A)$ is the dimensionless growth rate of the mode

$$\text{Im}(\phi_{v_A}) > 0 \rightarrow \text{unstable growth}$$

Simulation setup

- 'Sit' in rest frame of the jet; wind moves with velocity β_{sh}
- Jet is strongly magnetized with in-plane magnetic field $B_{x0,j}$ and out-of-plane (guide-field) component $B_{z0,j}$
- Wind is weakly magnetized with out-of-plane mag. field $B_{z0,w}$



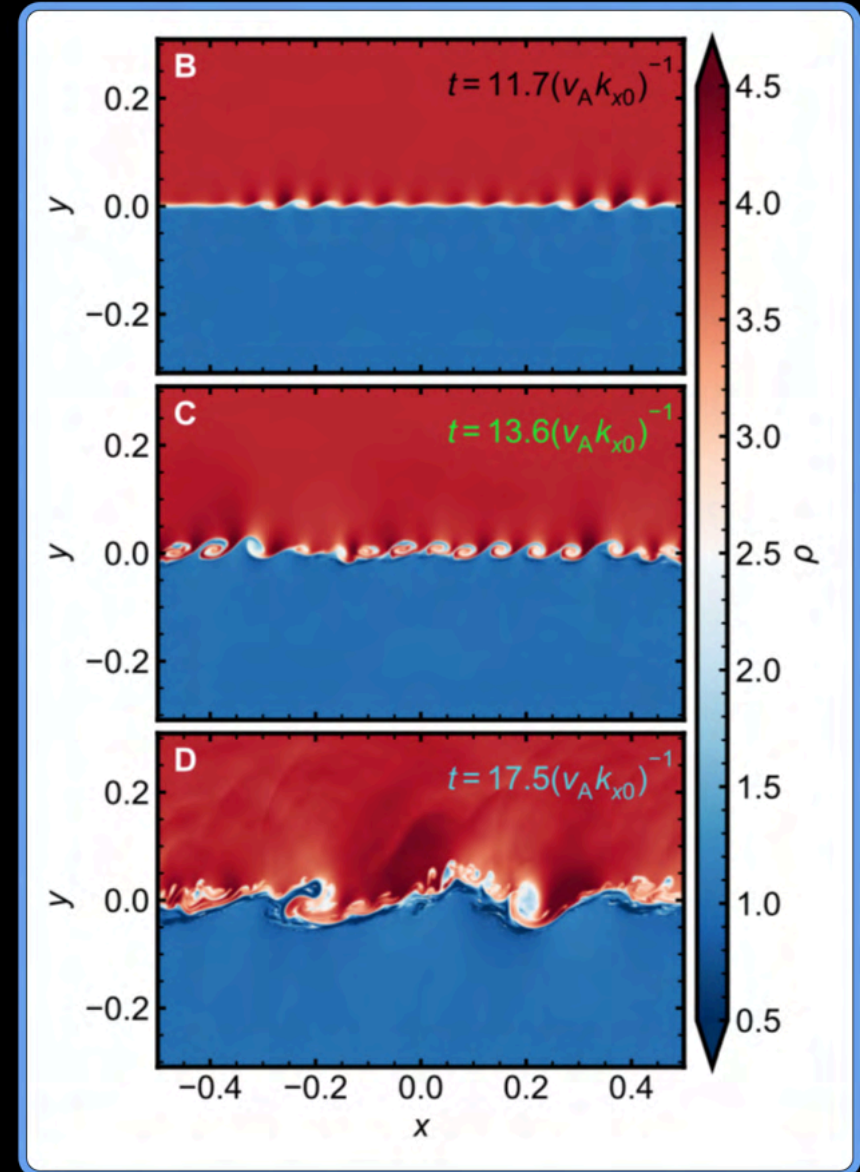
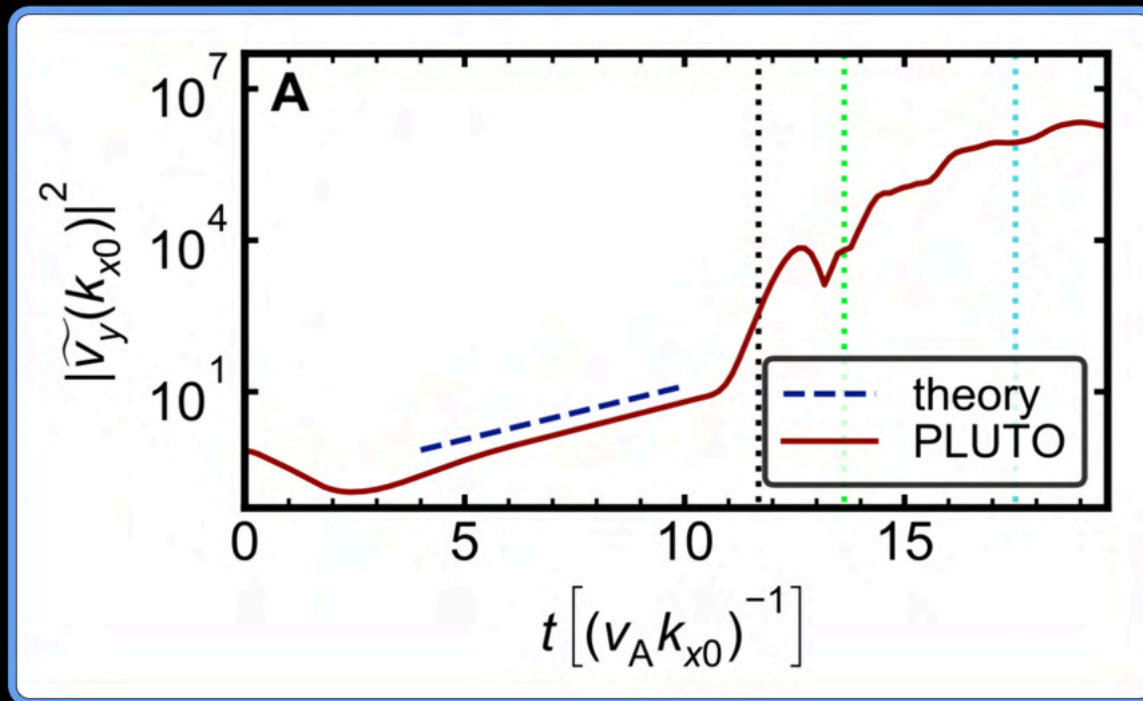
Simulation parameters

Parameter	Description
β_{ix}	Plasma-beta in jet, computed with in-plane $B_{x0, j}$
σ_{wx}	Magnetization in jet, computed with in-plane $B_{x0, j}$
β_{sh}	Speed of wind relative to jet
b_j	$B_{z0, j}/B_{x0, j}$; jet guide field strength
b_w	$B_{z0, w}/B_{x0, j}$; wind guide field strength
ρ_{0j}	Mass density in jet
ρ_{0w}	Mass density in wind
f	k_z/k_x ; controls ang. of propagation of perturbation

Sample simulation: RMHD

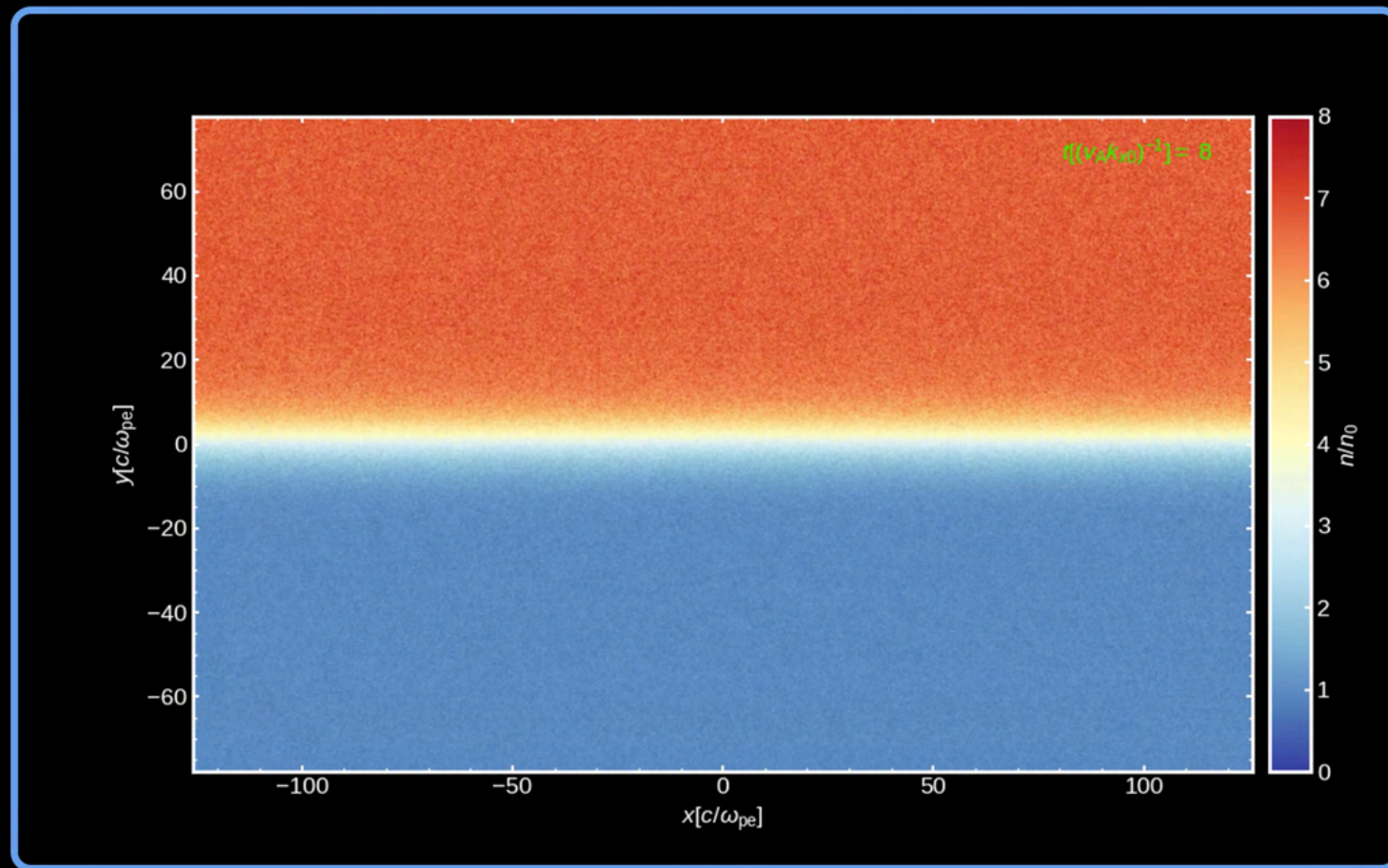
Time evolution of Fourier power (left)
for RMHD simulation; parameters:

$$\beta_{\text{sh}} = 0.8, \sigma_{wx} = 1, \beta_{\text{ix}} = 0.078, \\ b_j = 3, b_w = 0.3, \rho_{0w}/\rho_{0j} = 6.7$$



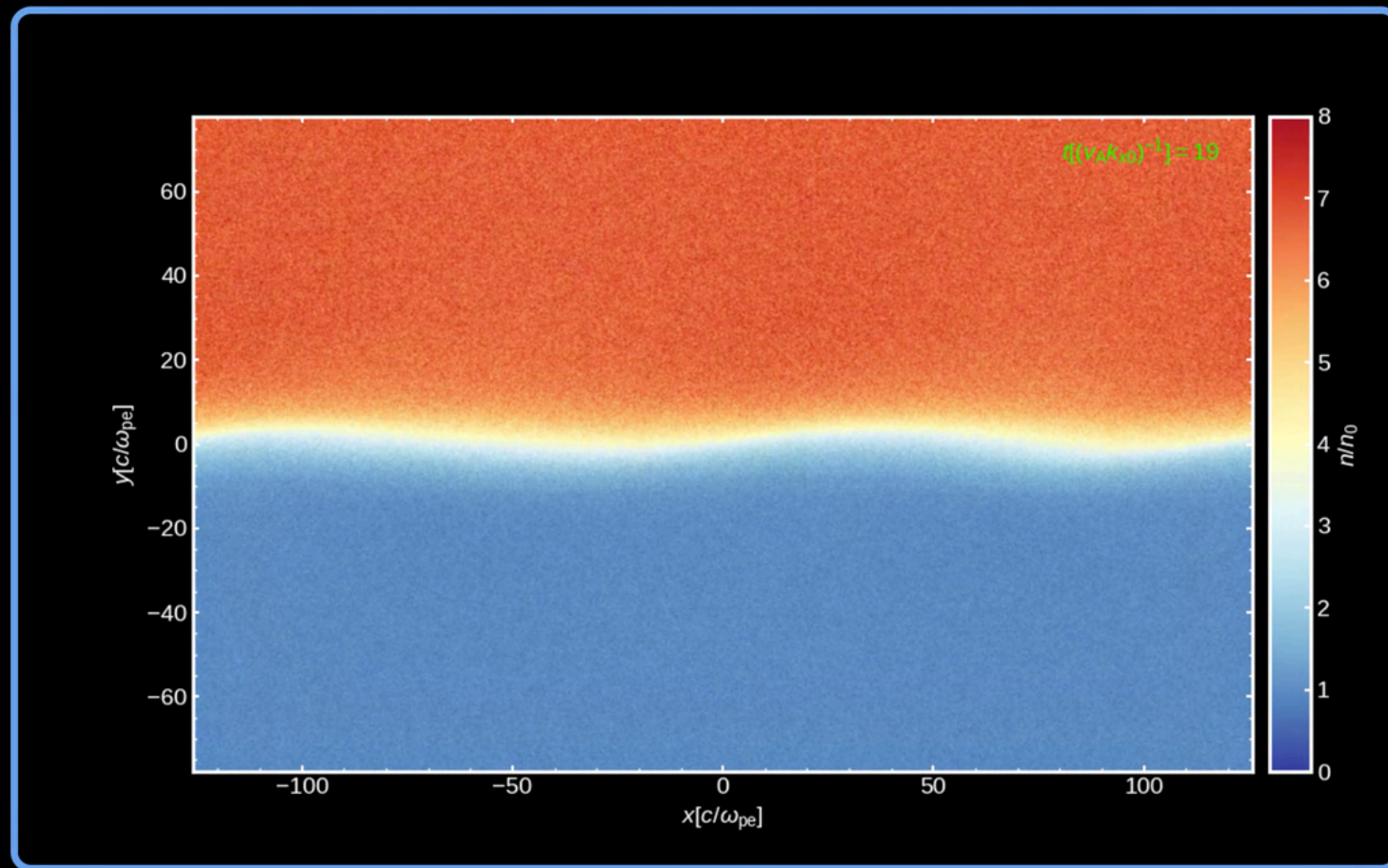
Sample simulation: PIC

Time evolution of density for PIC run; parameters: $\beta_{sh} = 0.8$,
 $\sigma_{wx} = 1$, $\beta_{ix} = 0.078$, $b_j = 3$, $b_w = 0.3$, $\rho_{0w}/\rho_{0j} = 6.7$



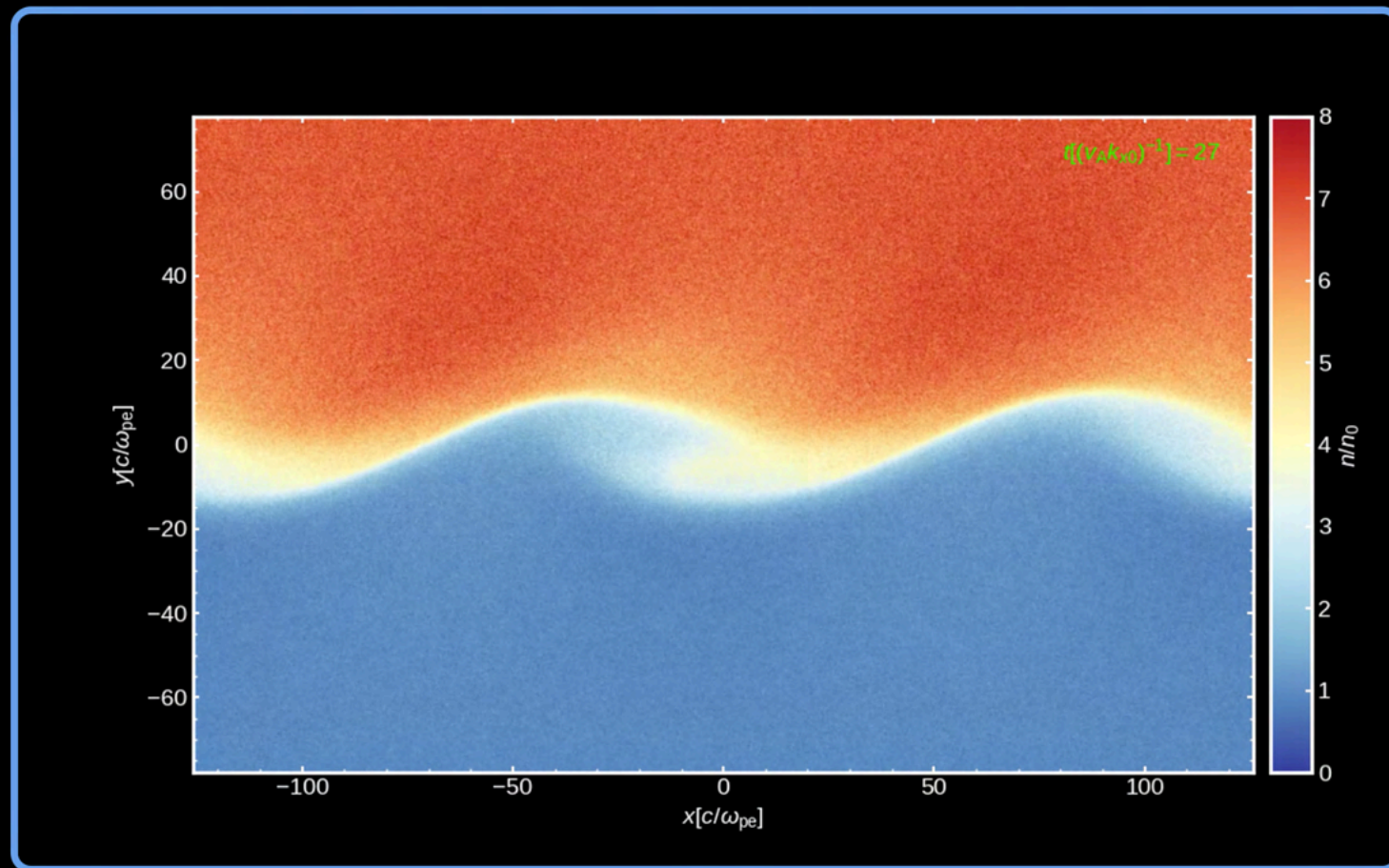
Sample simulation: PIC

Time evolution of density for PIC run; parameters: $\beta_{sh} = 0.8$,
 $\sigma_{wx} = 1$, $\beta_{ix} = 0.078$, $b_j = 3$, $b_w = 0.3$, $\rho_{0w}/\rho_{0j} = 6.7$



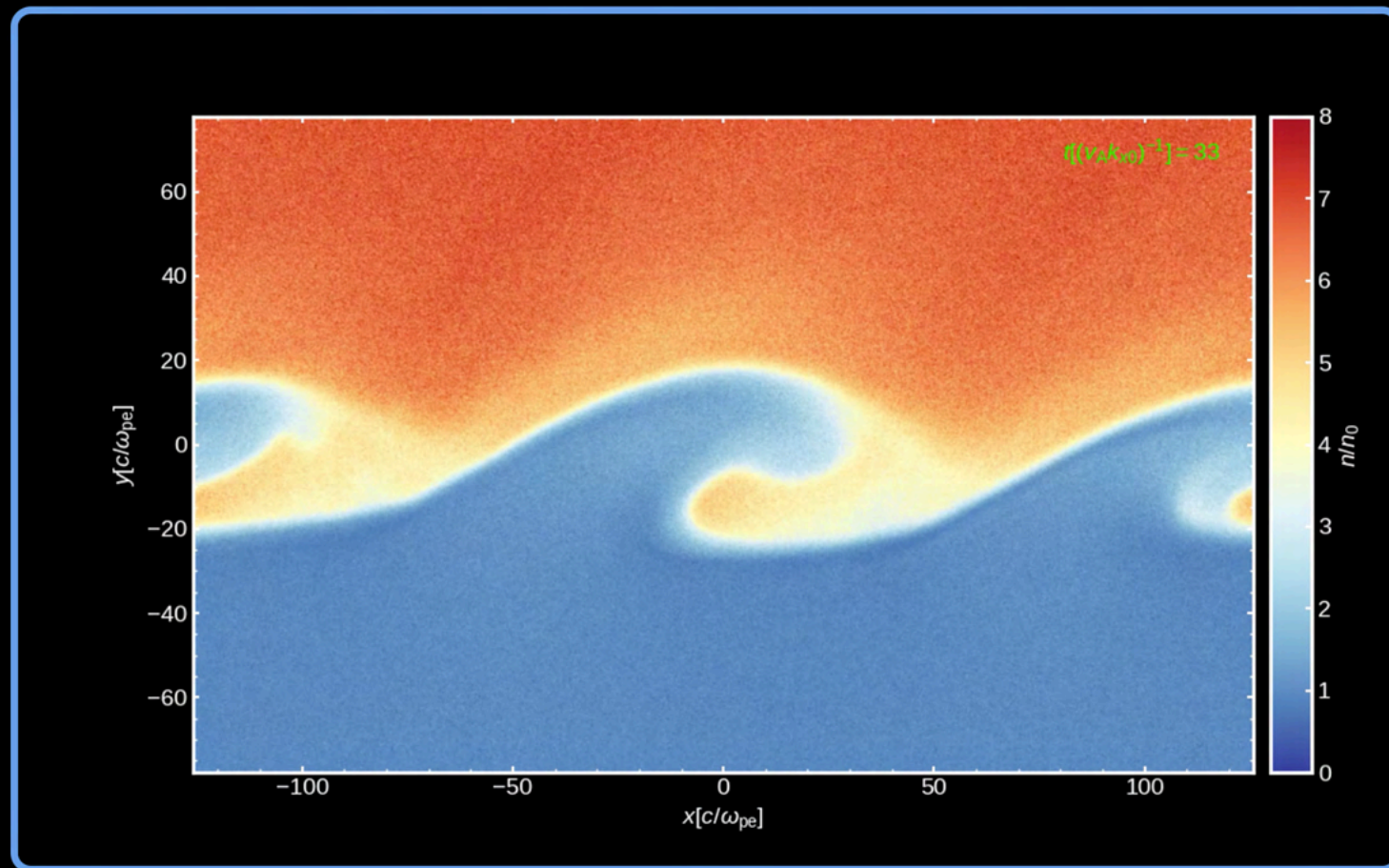
Sample simulation: PIC

Time evolution of density for PIC run; parameters: $\beta_{sh} = 0.8$,
 $\sigma_{wx} = 1$, $\beta_{ix} = 0.078$, $b_j = 3$, $b_w = 0.3$, $\rho_{0w}/\rho_{0j} = 6.7$



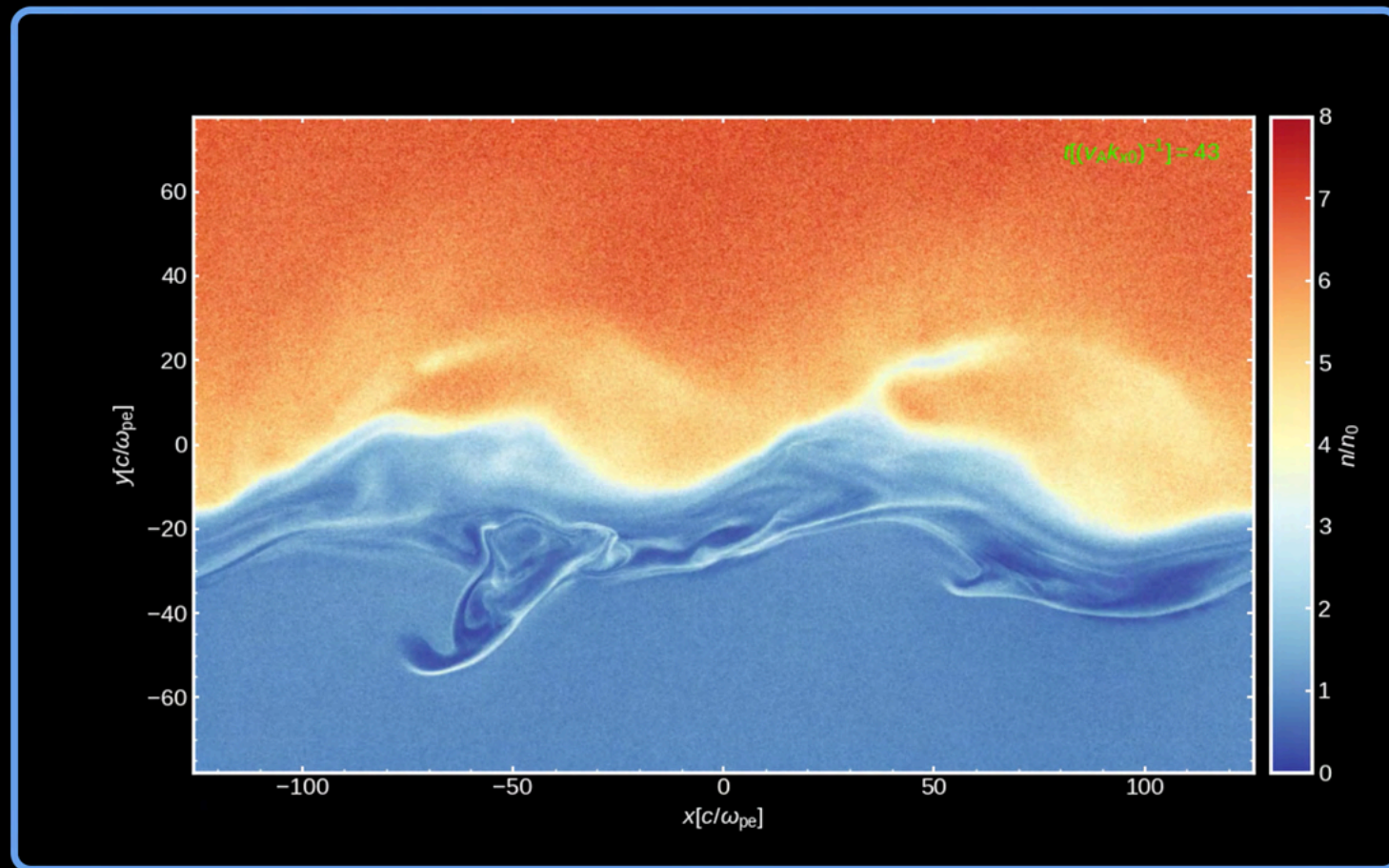
Sample simulation: PIC

Time evolution of density for PIC run; parameters: $\beta_{sh} = 0.8$,
 $\sigma_{wx} = 1$, $\beta_{ix} = 0.078$, $b_j = 3$, $b_w = 0.3$, $\rho_{0w}/\rho_{0j} = 6.7$



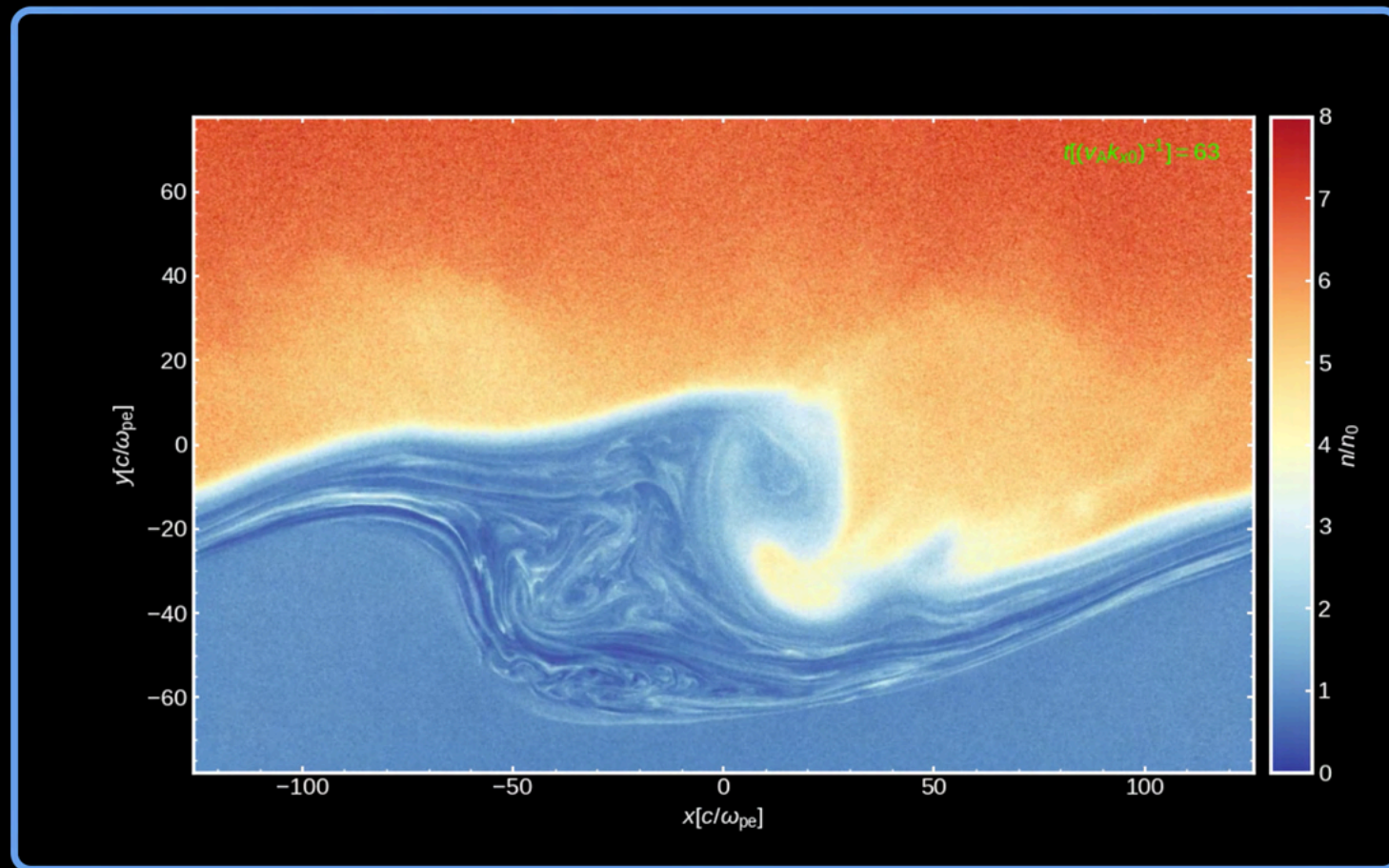
Sample simulation: PIC

Time evolution of density for PIC run; parameters: $\beta_{sh} = 0.8$,
 $\sigma_{wx} = 1$, $\beta_{ix} = 0.078$, $b_j = 3$, $b_w = 0.3$, $\rho_{0w}/\rho_{0j} = 6.7$



Sample simulation: PIC

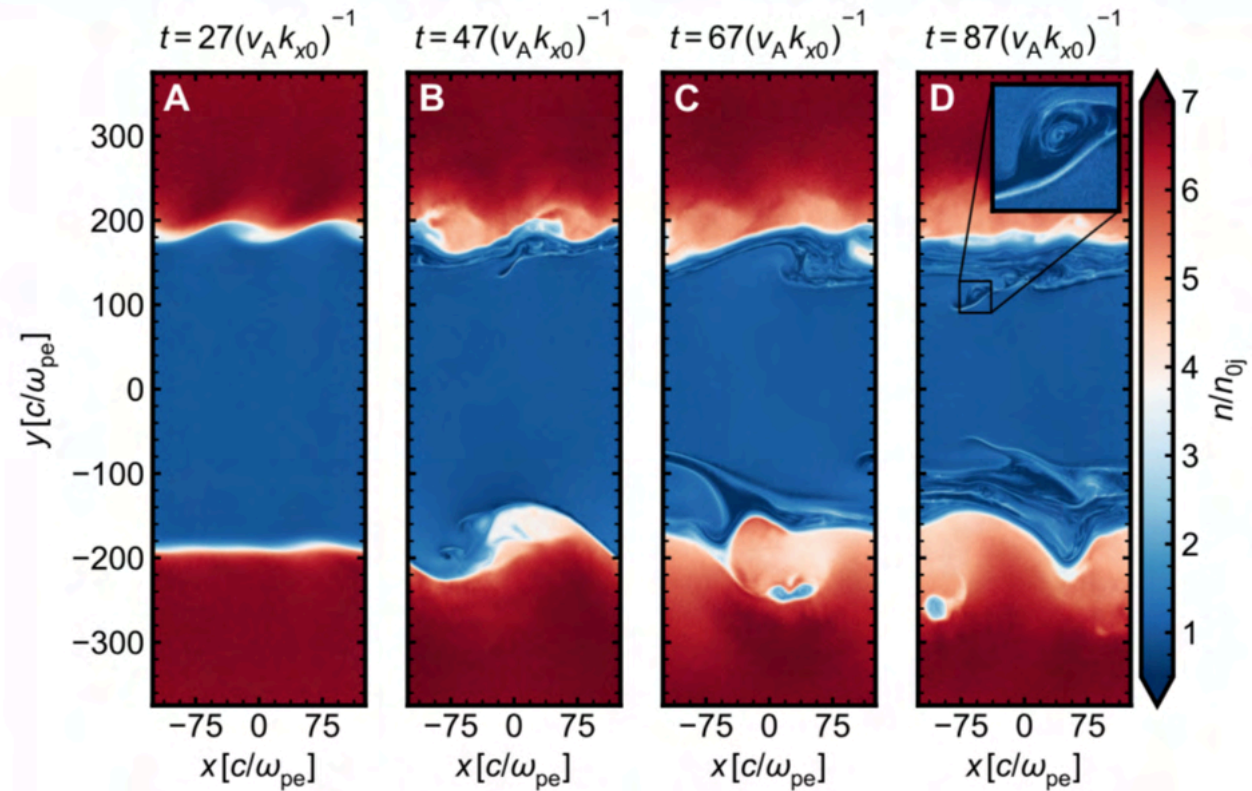
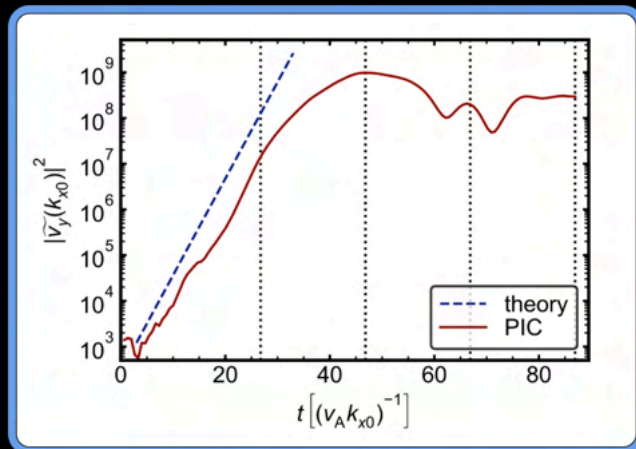
Time evolution of density for PIC run; parameters: $\beta_{sh} = 0.8$,
 $\sigma_{wx} = 1$, $\beta_{ix} = 0.078$, $b_j = 3$, $b_w = 0.3$, $\rho_{0w}/\rho_{0j} = 6.7$



Sample simulation: PIC

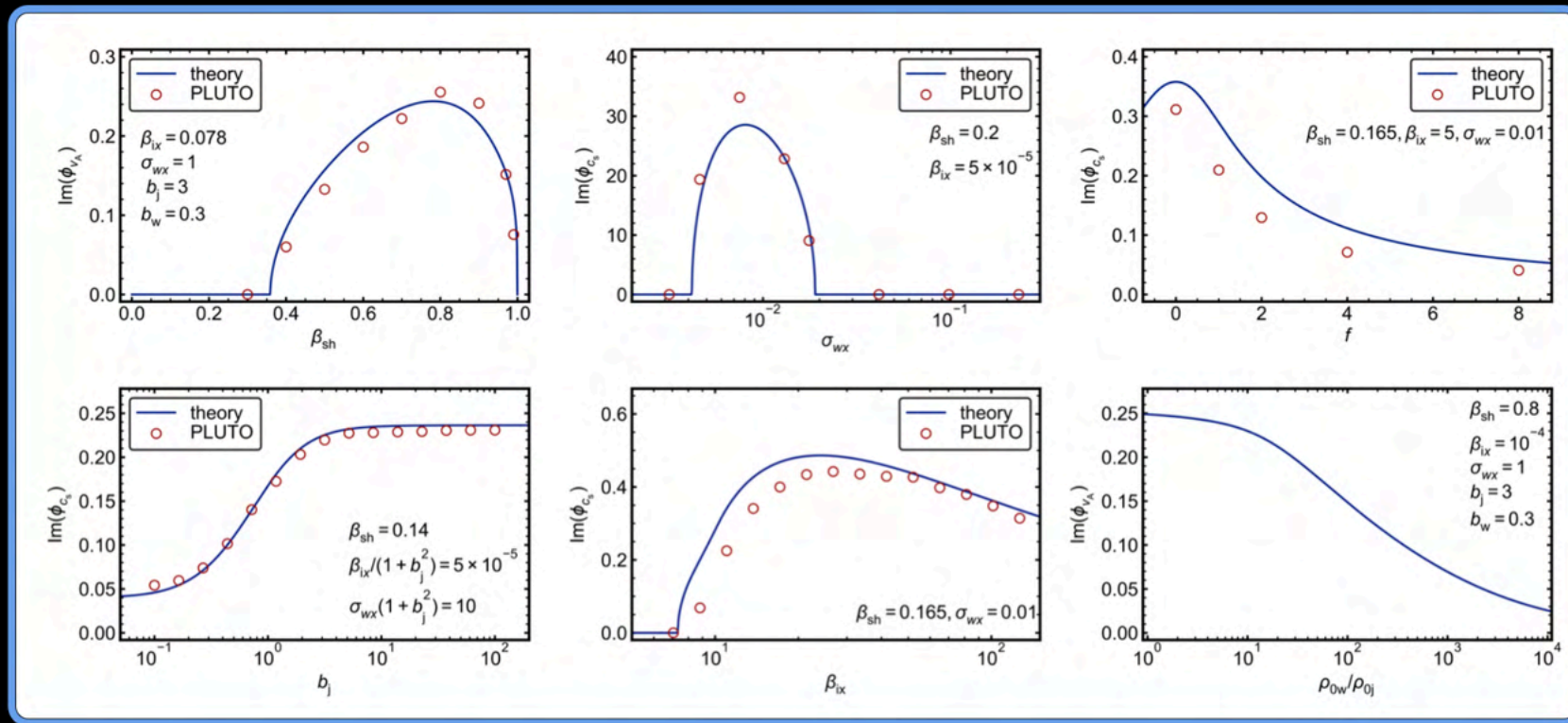
Time evolution of Fourier power (left) for PIC run; parameters:
 $\beta_{\text{sh}} = 0.8$, $\sigma_{wx} = 1$, $\beta_{\text{ix}} = 0.078$, $b_j = 3$, $b_w = 0.3$, $\rho_{0w}/\rho_{0j} = 6.7$

Dashed lines below
correspond to 2D
density profiles \rightarrow



Measured growth rate of KH: RMHD

Relativistic MHD simulations show good agreement with prediction:



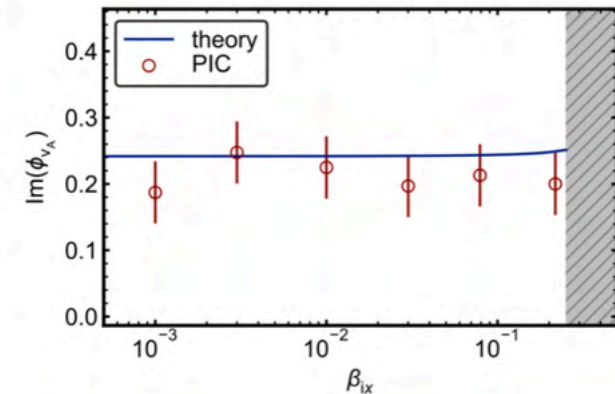
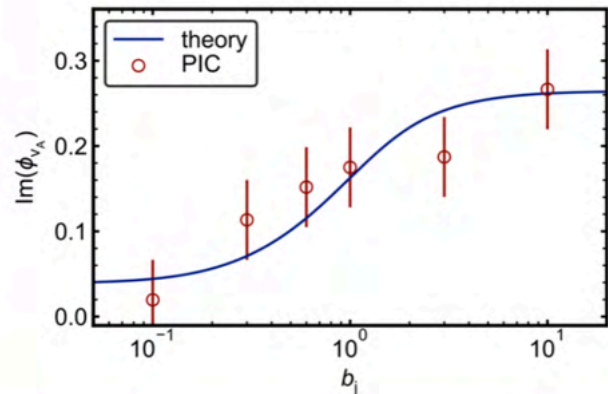
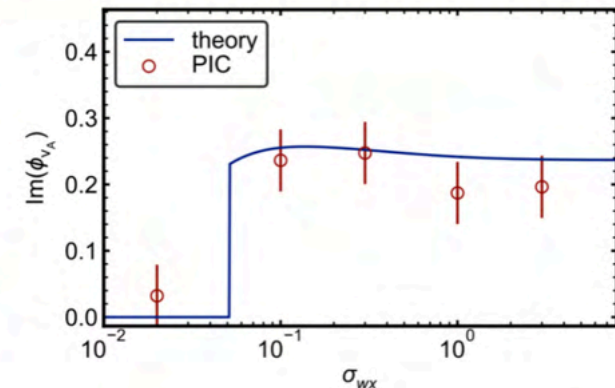
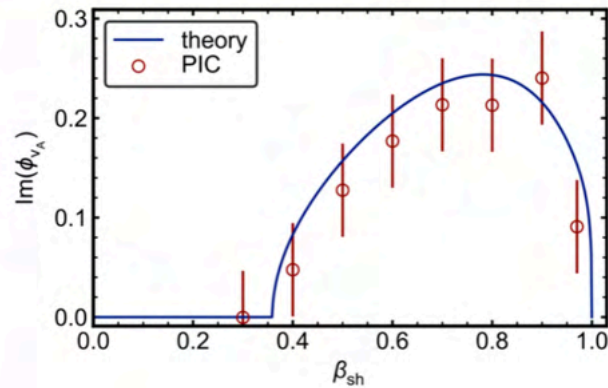
Growth rate dependence on density ratio ρ_{0w}/ρ_{0j} shows that even for $\rho_{0w}/\rho_{0j} \approx 10^3$, growth is reduced by only a factor of 3–4

Measured growth rate of KH: PIC

- What physical parameters lead to KH unstable growth?
- Does PIC capture the predicted growth rate?
- Does PIC show evidence of magnetic dissipation?

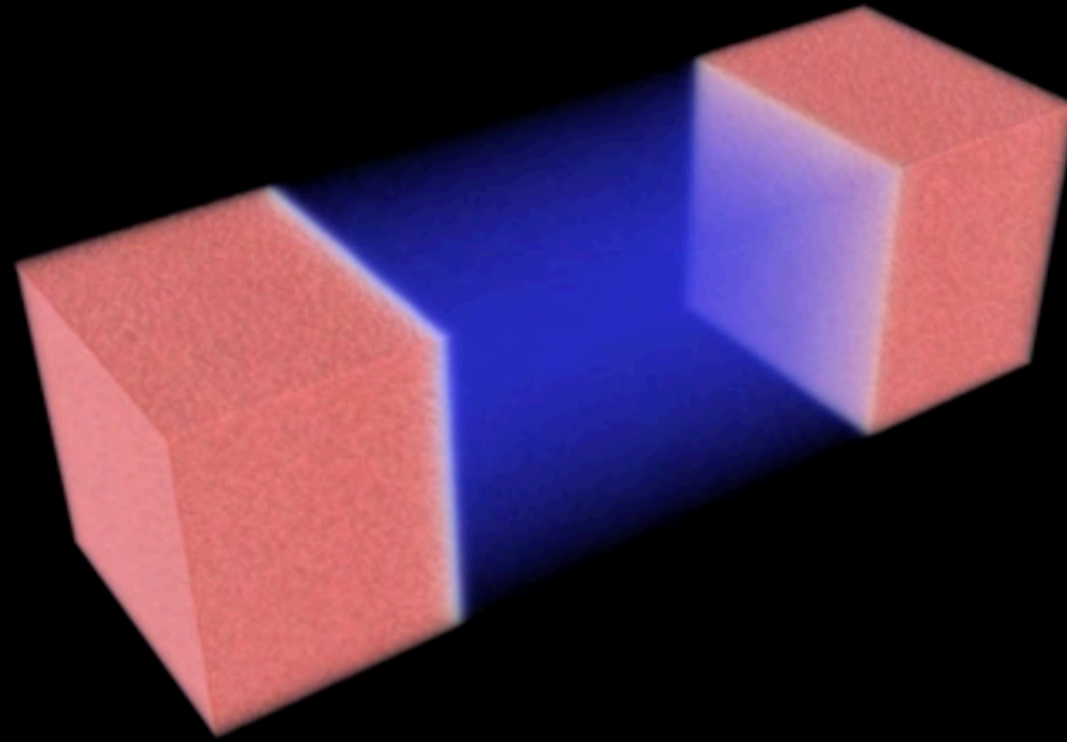
PIC simulations and analytical predictions show good agreement

Errorbars computed as standard deviation of measured slopes from five simulations with different random initial conditions



Measured growth rate of KH in 3D: PIC

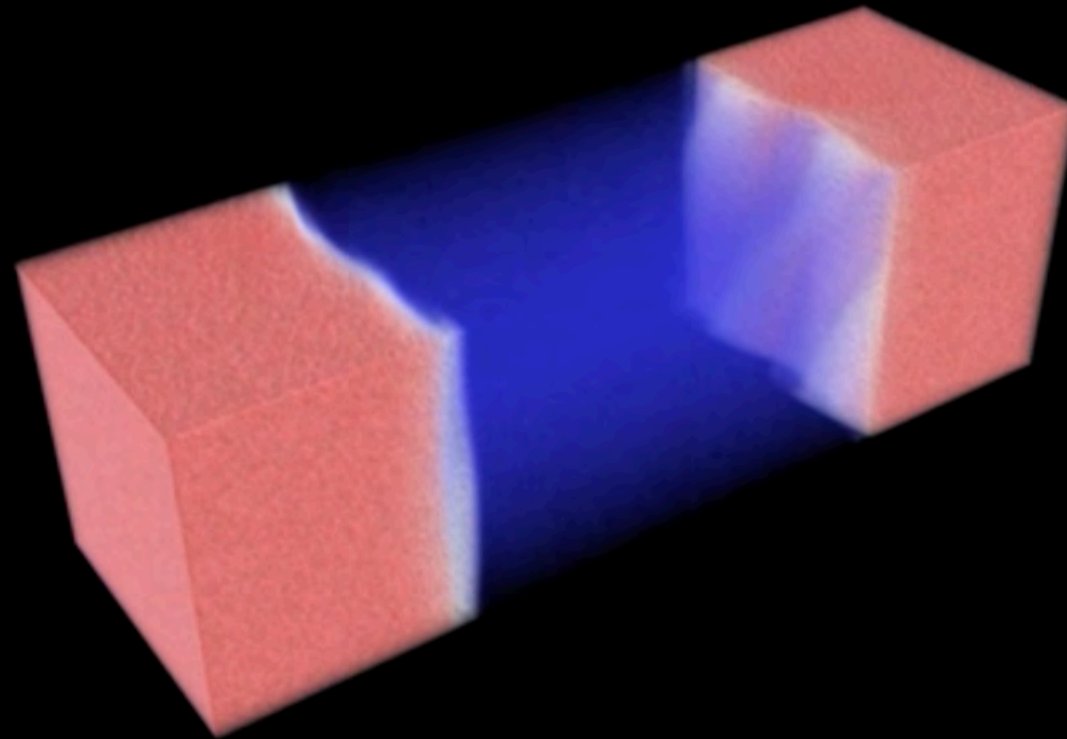
Time evolution of density for 3D simulation; blue is jet, red is wind



parameters: $\beta_{sh} = 0.8$, $\sigma_{wx} = 1$, $\beta_{ix} = 0.001$, $b_j = 3$, $b_w = 0.3$,
 $\rho_{0w}/\rho_{0j} = 6.7$; box size is $250 \times 750 \times 250 c/\omega_{pe}$ (jet skin depths)

Measured growth rate of KH in 3D: PIC

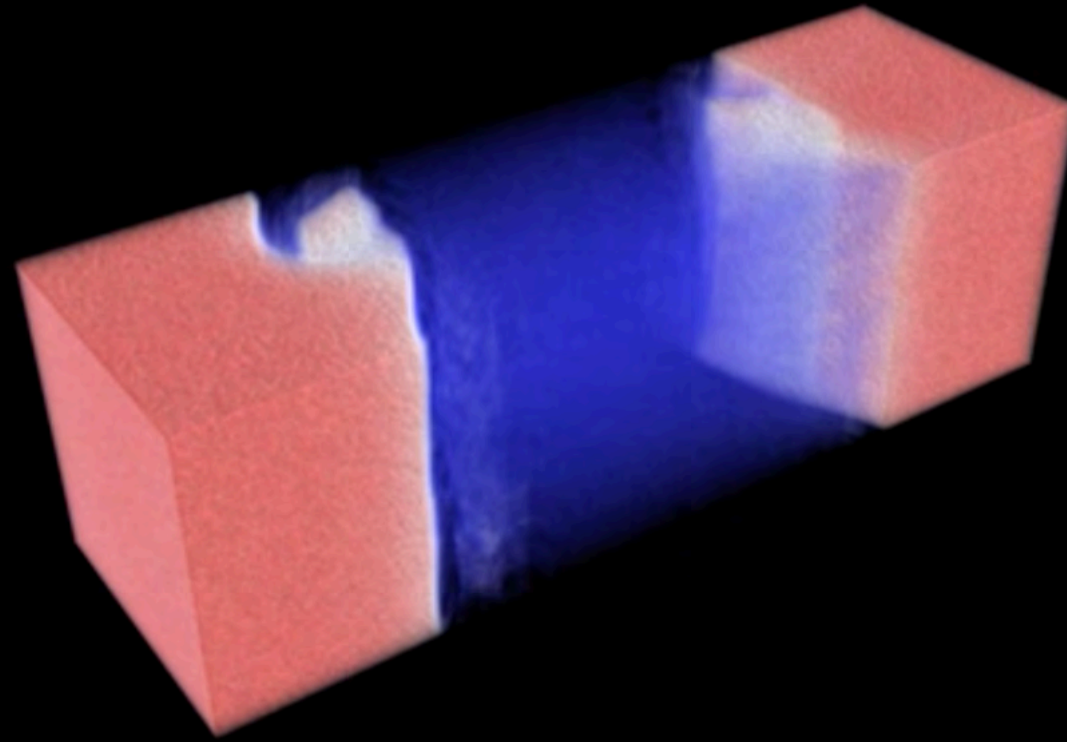
Time evolution of density for 3D simulation; blue is jet, red is wind



parameters: $\beta_{sh} = 0.8$, $\sigma_{wx} = 1$, $\beta_{ix} = 0.001$, $b_j = 3$, $b_w = 0.3$,
 $\rho_{0w}/\rho_{0j} = 6.7$; box size is $250 \times 750 \times 250 c/\omega_{pe}$ (jet skin depths)

Measured growth rate of KH in 3D: PIC

Time evolution of density for 3D simulation; blue is jet, red is wind

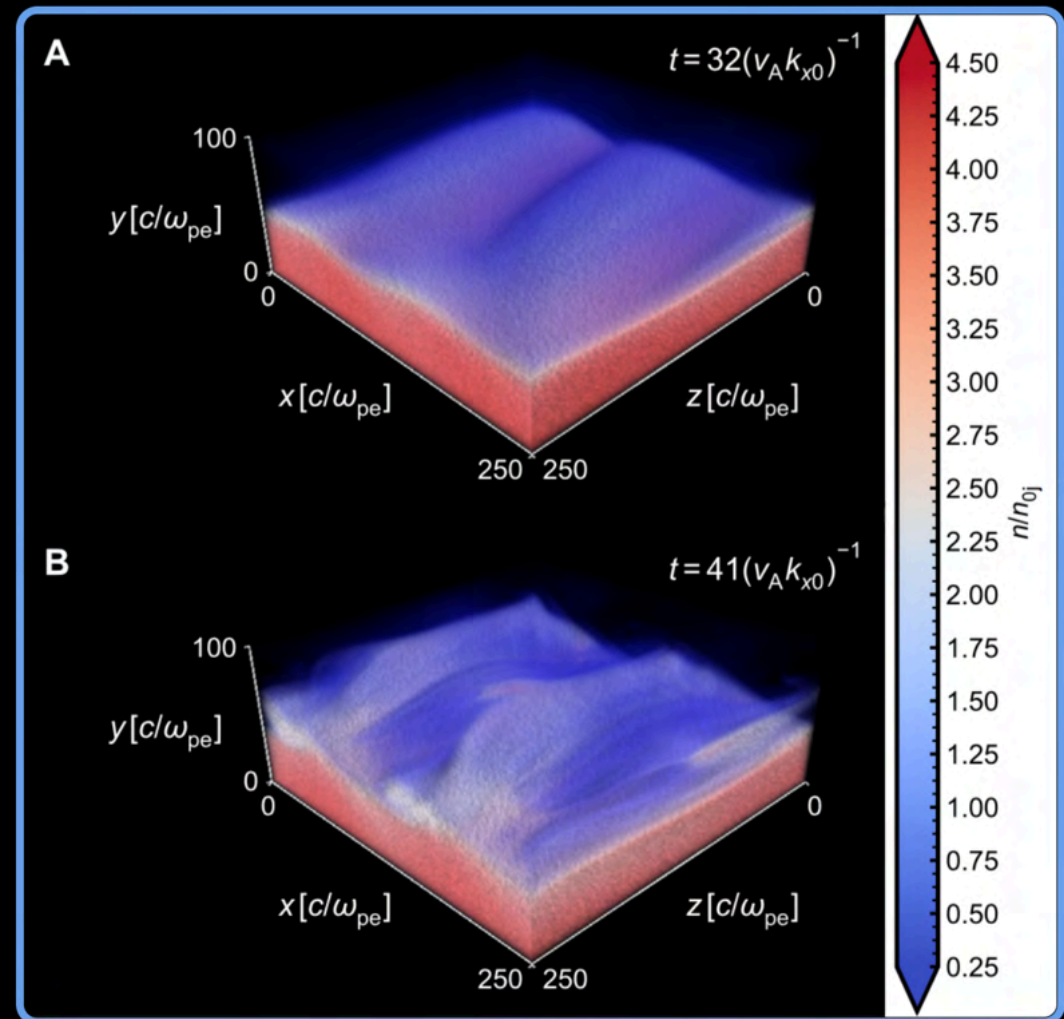
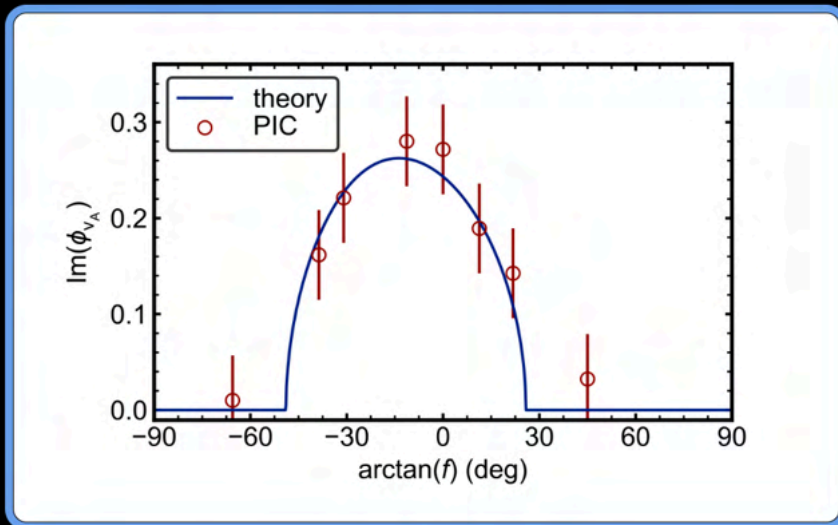


parameters: $\beta_{sh} = 0.8$, $\sigma_{wx} = 1$, $\beta_{ix} = 0.001$, $b_j = 3$, $b_w = 0.3$,
 $\rho_{0w}/\rho_{0j} = 6.7$; box size is $250 \times 750 \times 250 c/\omega_{pe}$ (jet skin depths)

Measured growth rate of KH in 3D: PIC

Comparison of predicted and measured growth rates from 3D run

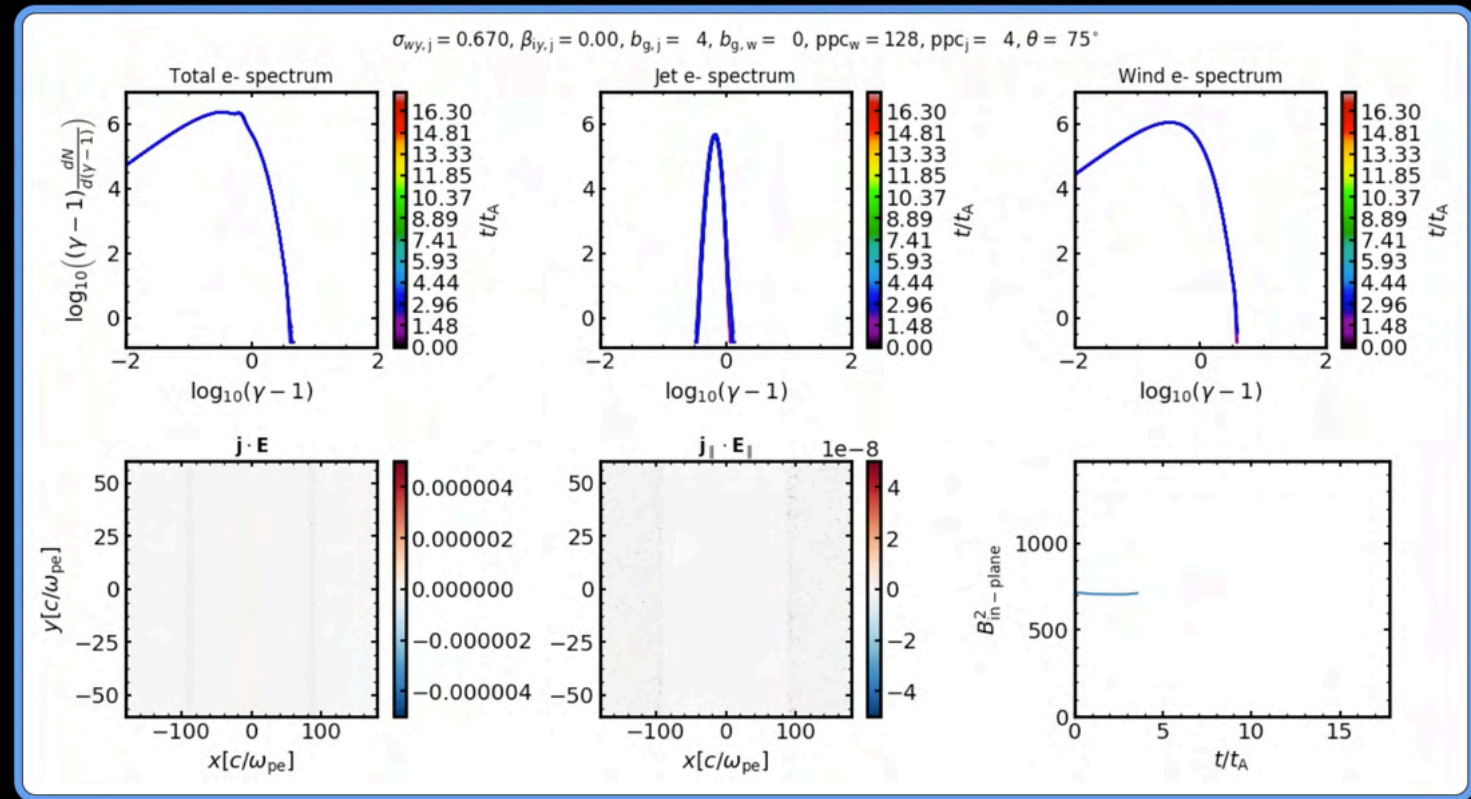
Note that growth rate is largest for an angle slightly out of xy plane; this angle in fact satisfies $k \cdot B_0 \approx 0$



Particle acceleration

- What physical parameters lead to KH unstable growth?
- Does PIC capture the predicted growth rate?
- Does PIC show evidence of magnetic dissipation?

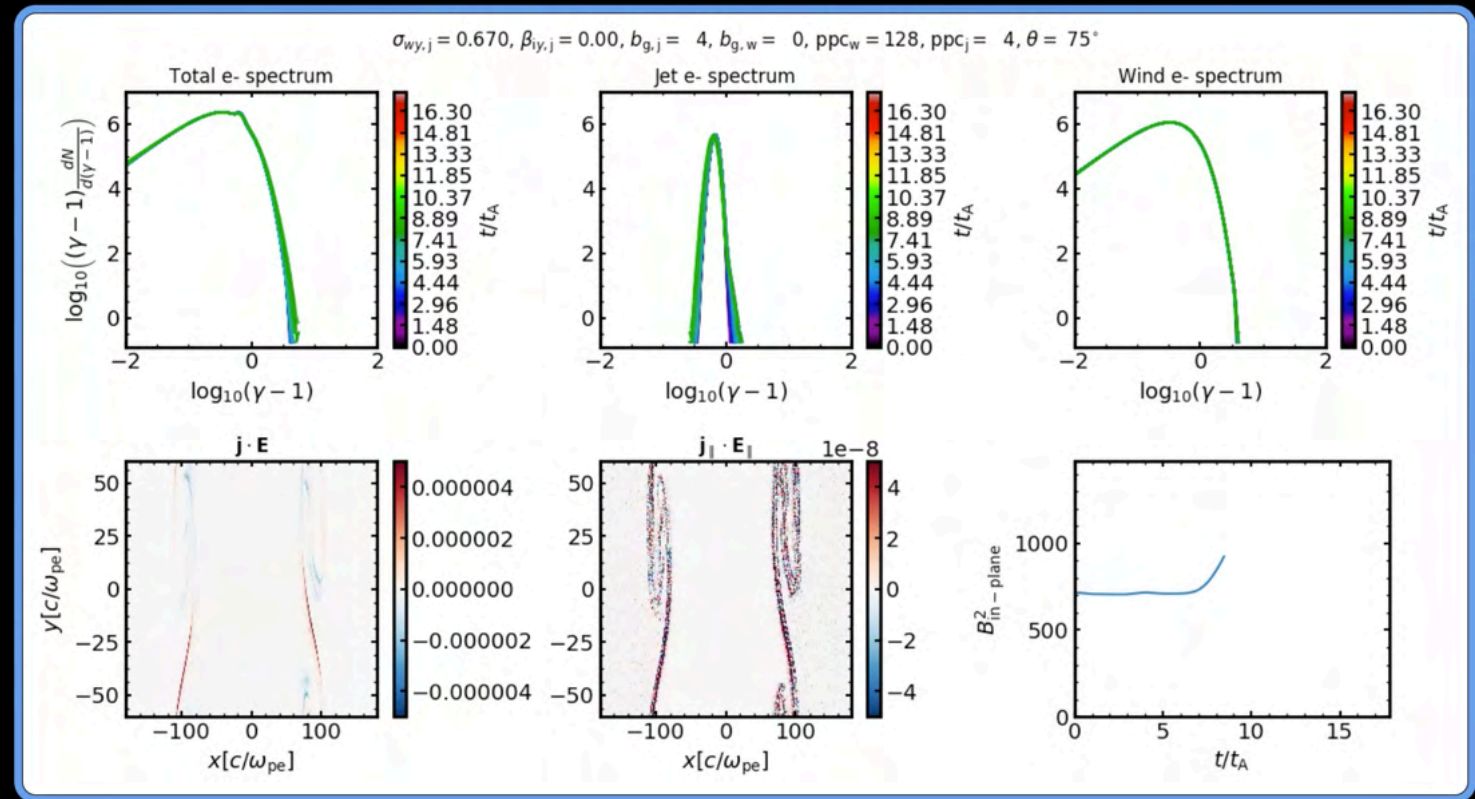
Time evolution
of electron
energy spectra
shows evidence
for particle
energization up
to Lorentz
factors $\gamma \approx 100$



Particle acceleration

- What physical parameters lead to KH unstable growth?
- Does PIC capture the predicted growth rate?
- Does PIC show evidence of magnetic dissipation?

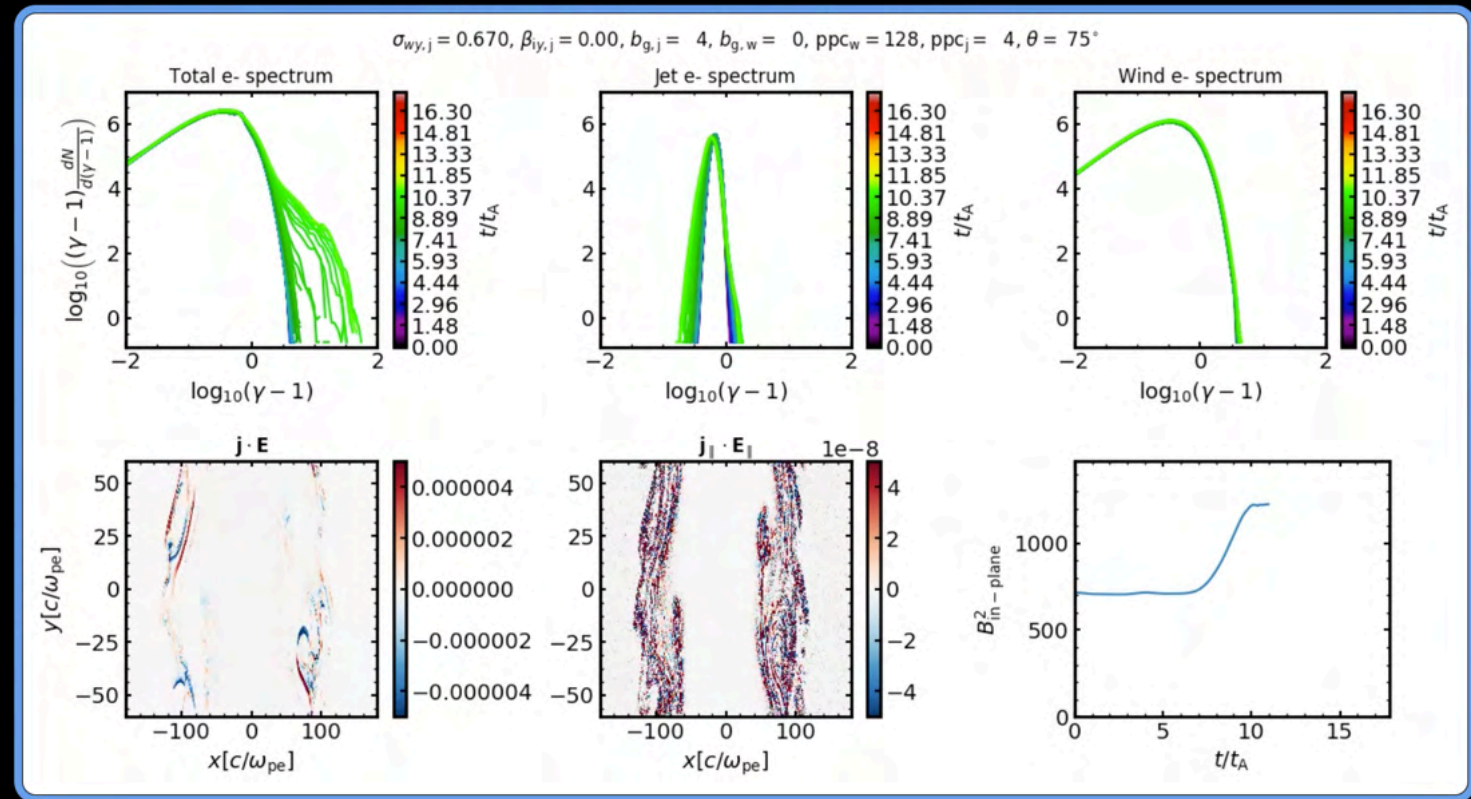
Time evolution
of electron
energy spectra
shows evidence
for particle
energization up
to Lorentz
factors $\gamma \approx 100$



Particle acceleration

- What physical parameters lead to KH unstable growth?
- Does PIC capture the predicted growth rate?
- Does PIC show evidence of magnetic dissipation?

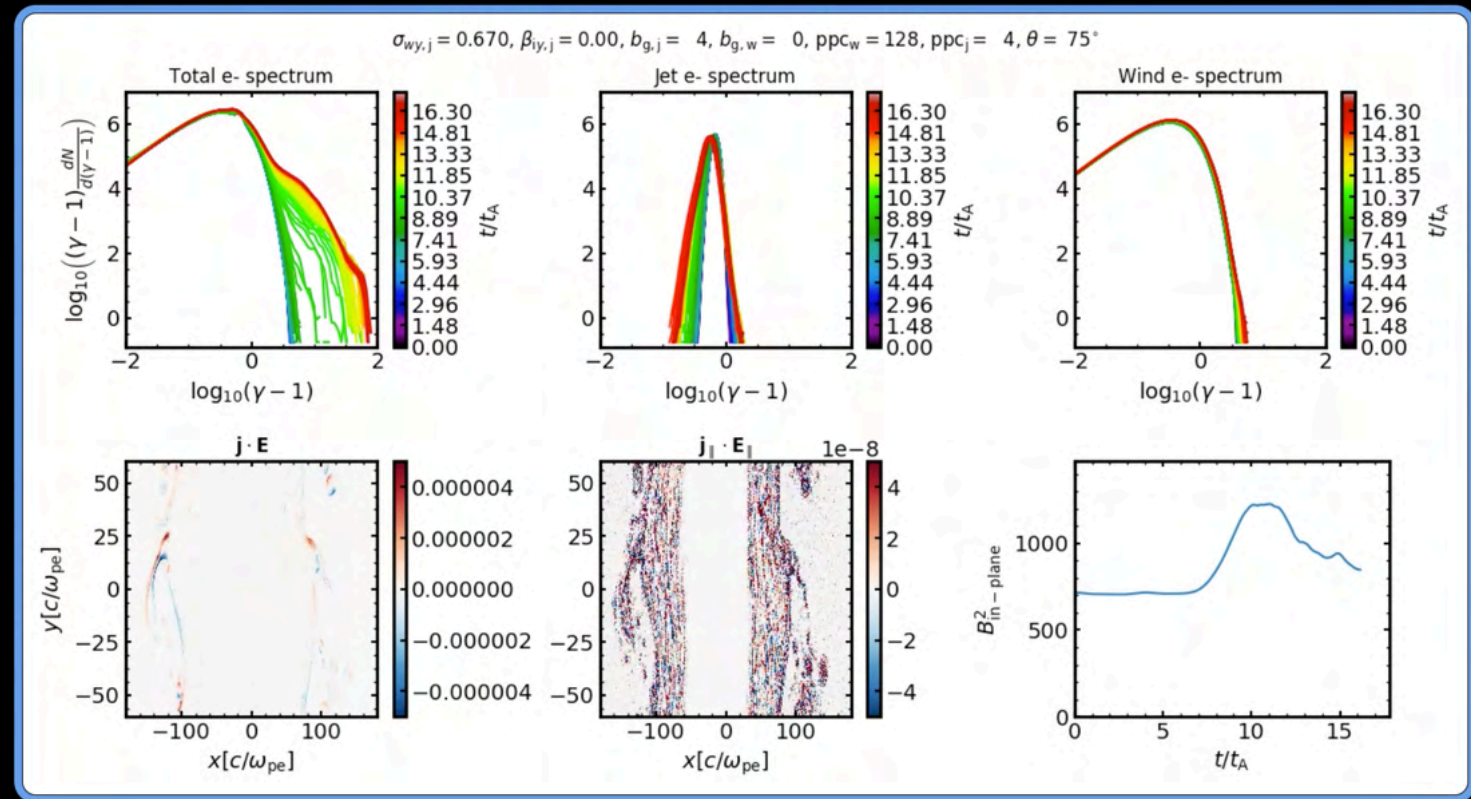
Time evolution of electron energy spectra shows evidence for particle energization up to Lorentz factors $\gamma \approx 100$



Particle acceleration

- What physical parameters lead to KH unstable growth?
- Does PIC capture the predicted growth rate?
- Does PIC show evidence of magnetic dissipation?

Time evolution of electron energy spectra shows evidence for particle energization up to Lorentz factors $\gamma \approx 100$



Summary

Exploration of guide field reconnection (see arXiv:1901.05438):

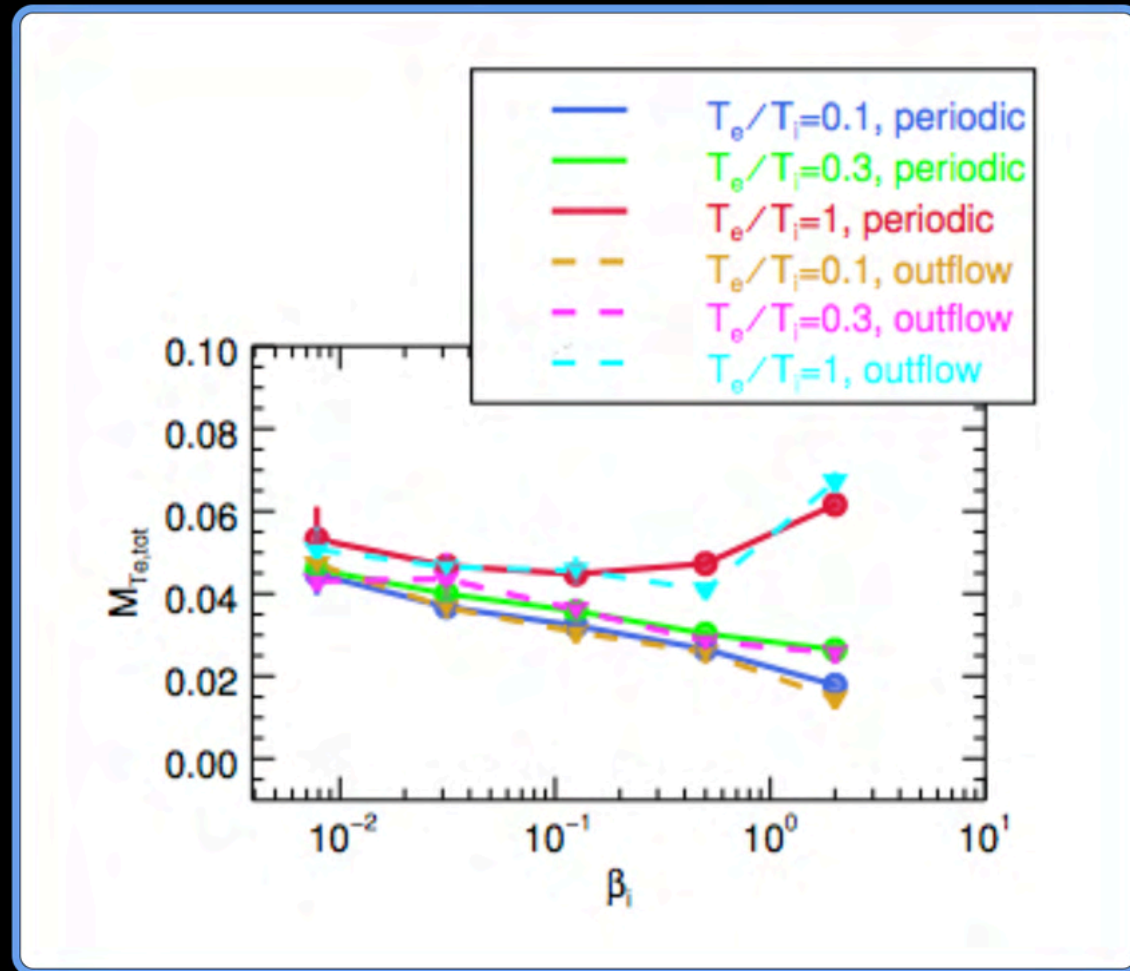
- low- β_i : irr. elec. heating nearly independent of b_g
- Protons get heated much less with increasing b_g
- As a result, for large b_g , elec. receive the overwhelming majority of irreversible heating ($\sim 93\%$ for $b_g = 6$)
- Differs significantly from antiparallel case ($\sim 18\%$ vs. $\sim 93\%$)

Studied KH instability analytically, in RMHD, and in PIC:

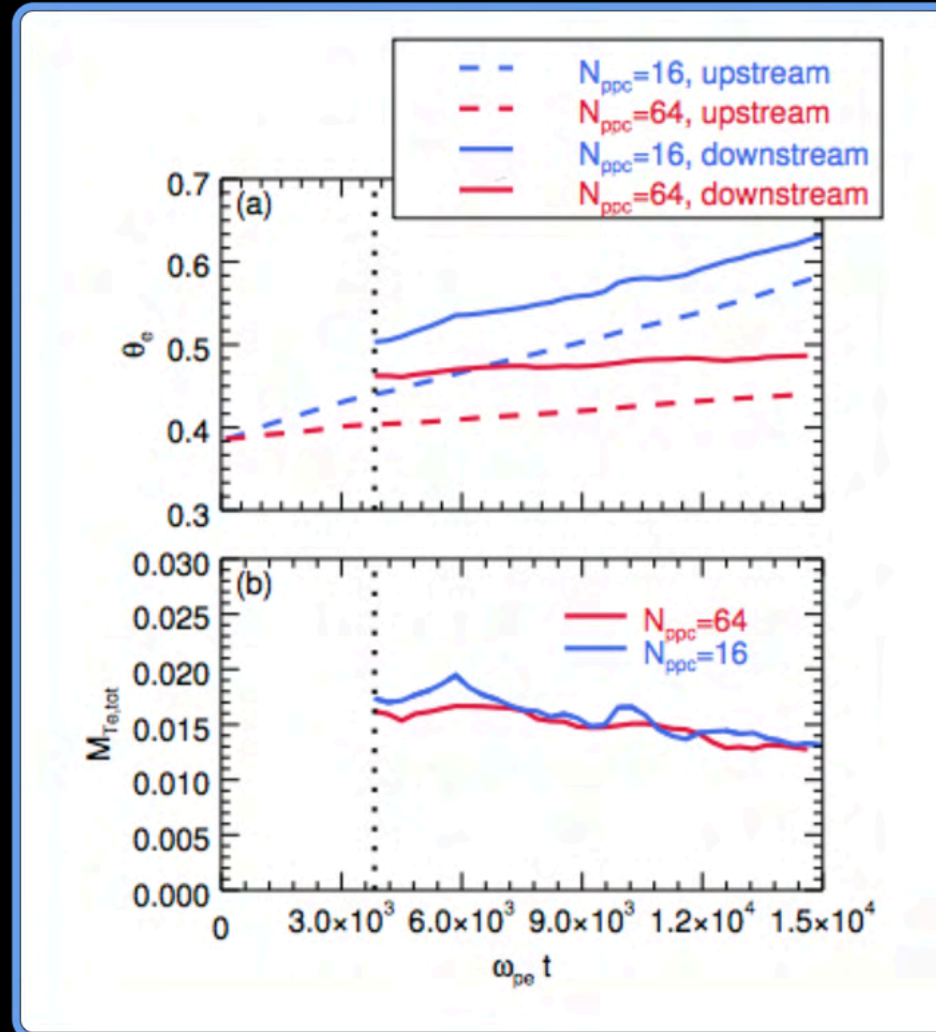
- RMHD simulations show good agreement with prediction, validating our dispersion relation calculation
- PIC also shows agreement with dispersion relation
- PIC simulations of KH in jets show particle acceleration

Design credits: [Hakim El Hattab](#) (black.css theme), [Peter K. G. Williams](#) (pkgwtheme.css)

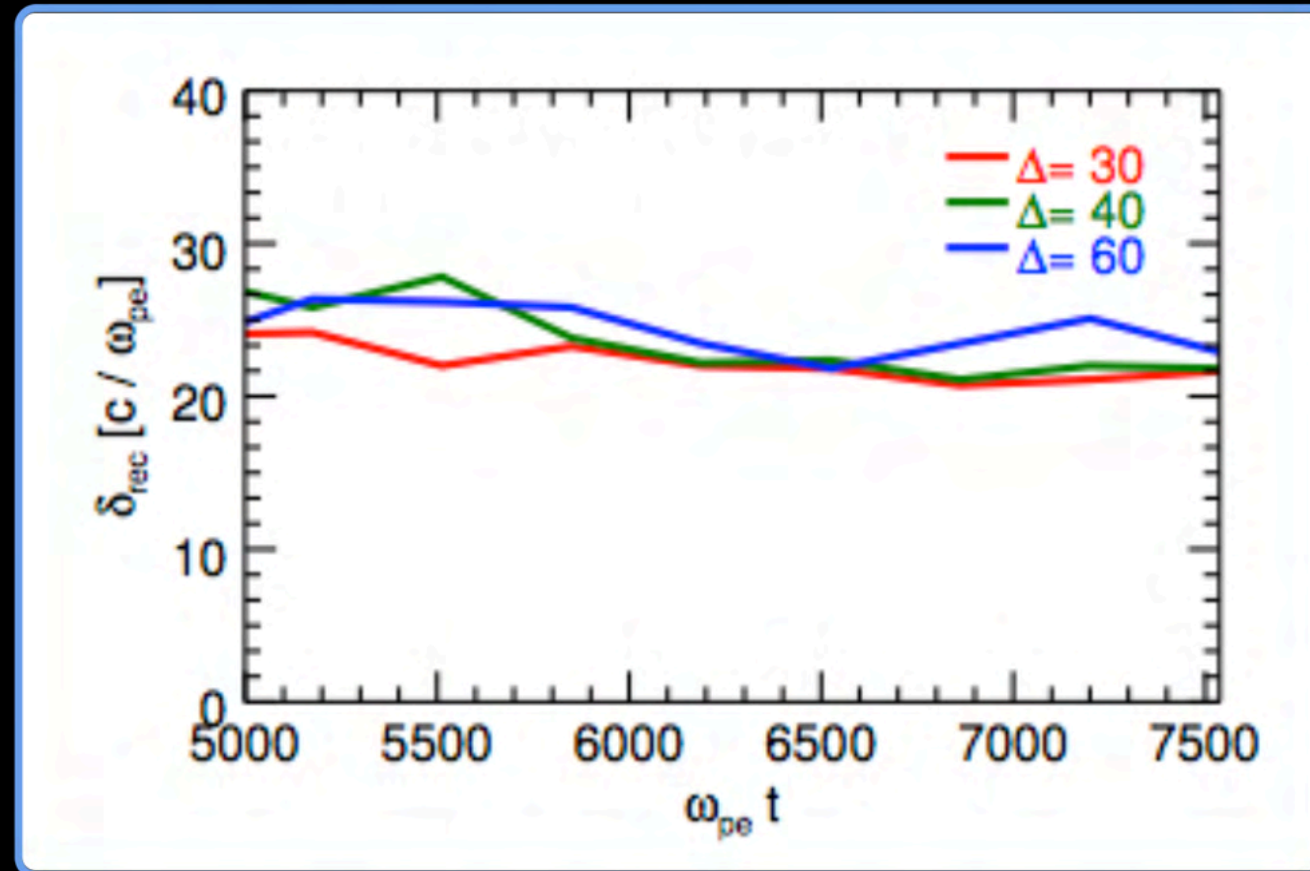
Convergence tests



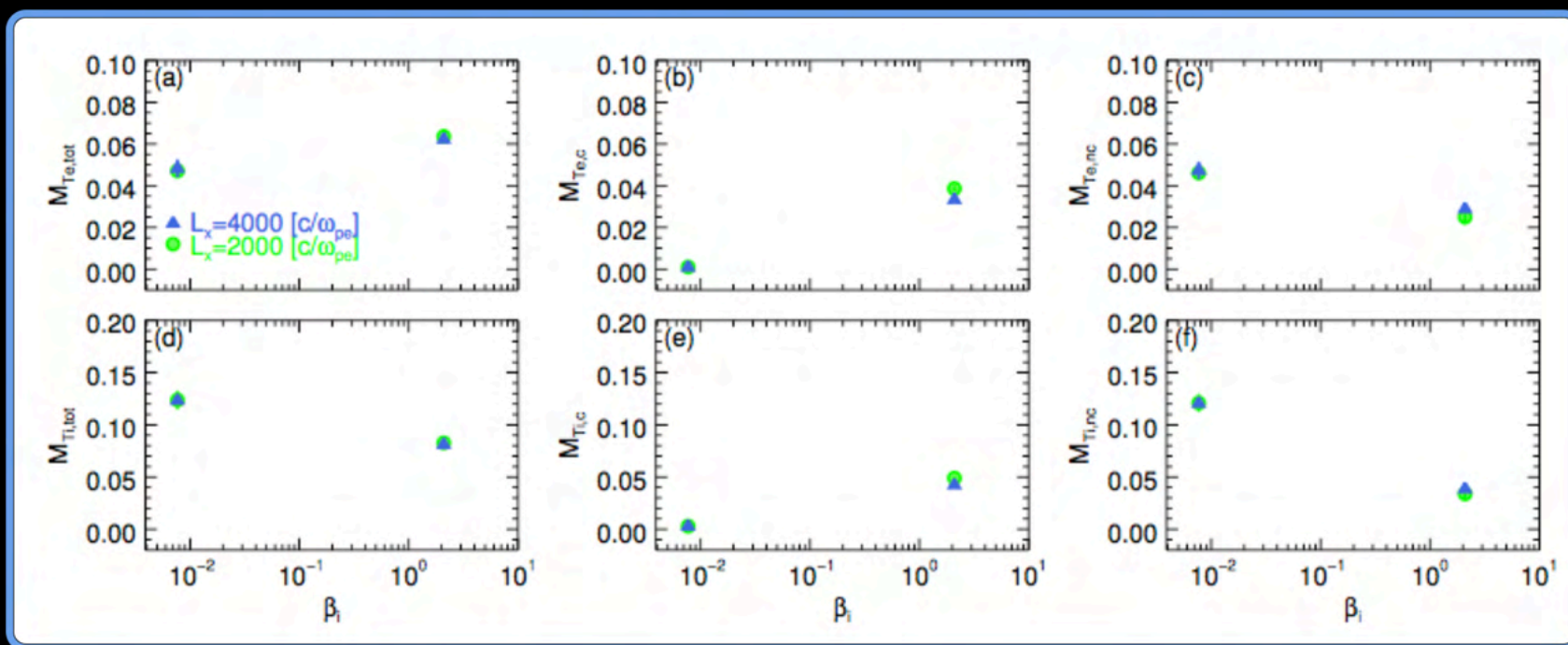
Convergence tests



Convergence tests



Convergence tests



Convergence tests

